Journal of Information Technology and Education Science

University of Computer Studies (Taungoo)

JITES 2019

Journal of Information Technology and Education Science

Vol-1
No-1
Dec
2019

ISBN: 978-99971-0-759-6
Volume-1, No-1 December, 2019

JOURNAL OF

INFORMATION TECHNOLOGY AND EDUCATION SCIENCE

JITES$_{2019}$ VOL. 01, NO.1, 2019

UNIVERSITY OF COMPUTER STUDIES (TAUNGOO)

Journal of Information Technology and Education Science
Vol. 01, No. 1, 2019

Contents

Natural Science

Calculation the Electrical Network by Using Matrices

Khin Moh Moh Thin[1], Hla Yin Moe[2], Linn Linn Aye[3]
Assistant Lecturer, Associate Professor, Assistant Lecturer
dawmohmoh1987@gmail.com, hlayinmoe5049663@gmail.com, linlinaye3288@gmail.com

ABSTRACT: *Matrices have a lot of application in all areas of human endeavor. In fact the use of matrices in modeling engineering networks has made matrices as essential part of research in the fields of science and engineering. In this paper, we used nodal incident matrices to construct electrical networks and Kirchhoff's law to construct the electrical networks with the currents. Also we will find the current of such electrical networks by using Gauss-elimination method.*

Keywords: Nodal incidence matrix; Kirchhoff 's Laws; Electrical Networks; Gauss-Elimination.

1. INTRODUCTION

A matrix is a rectangular array of real complex numbers (or elements), Ajayi and Joseph (2009) [1], Riley et al.(2002) and Stroud (1995). An incident matrix is a matrix that describes the topology of a network, Dass and Verma (2011) [4] and Oke (2008). It shows the relationship between two classes of objects in the network. If the first class is X and the second is Y, the matrix has one row for each element of X and one column for each element of Y. The entry in row i and column j is 1 or -1 if i and j are related or incident and 0 if they are not, Dada (2010)[3], Kreyszig (1987) and Oke (2012)[11].

Incidence matrices are mostly used in graph theory. In graph theory, an undirected graph has two kinds of incidence matrices, These are oriented (or directed) and unoriented (or undirected) incidence matrices, Gross and Yellen (2006)[7] and Diestel(2005)[5].

The incidence matrix of an oriented (or directed) graph is an m x n matrix A_ij where

$$A_{ij} = \begin{cases} +1 \; if \; edge \; j \; leaves \; vertex \; i \\ -1 \; if \; edge \; j \; enters \; vertex \; i \\ 0 \qquad\qquad otherwise \end{cases}$$

m and n are the number of vertices and edges respectively, Kreyszig (1987) and Binoy (2009)[2]. It is to be noted that opposite sign convention may also be used for this purpose depending on that we want to achieve in the design and construction, Dada (2010)[3] and Kreyszig (1987).

The Gauss elimination method can be motivated. Consider a linear system that is in triangular form (in full, upper triangular form) by row operation. Triangular means that all the non-zero entries of the corresponding coefficient matrix lie above the diagonal and form an upside-down 90 triangle). Then we can solve the system by back substation.

1.1 Material and methods

1.1.1. Nodal incidence matrices

In this paper, we would form nodal incidence matrices from electrical networks by defining our nodal incidence matrix as

$$a_{ij} = \begin{cases} +1 \; if \; branch \; k \;\; leaves \; node \; j \\ -1 \; if \; branch \; k \; enters \; node \; j \\ 0 \; if \; branch \; k \; does \; not \; touch \; node \; j \end{cases}$$

opposite sign convention may also be used for this purpose depending on that we want to achieve in the design and construction, Dada (2010) and Kreyszig (1987).

1.2 Kirchhoff's Law

The Kirchhoff's law says if the current will come out negative, this will simply mean that the current flows against the direction of our arrow. The current entring each battery will be the same as the current leaving it.[11]

1.2.1 Kirchhoff's Current Law (KCL)

At any point of a circuit, the sum of the inflowing currents equals the sum of the outflowing currents.[10]

1.2.2 Kirchhoff's Voltage Law (KVL)

In any closed loop, the sum of all voltage drops equals the impressed electromotive force.[10]

2. RESULT AND DISCUSSIONS

2.1 Example

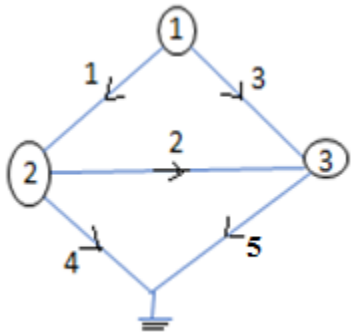

Figure 1 Electric Networks

Figure 1 represents an electrical network having five branches and three nodes. One of the node is reference node. All the nodes are numbered except the reference node. We also number and direct the branches.

We can now use 1.1 to form the nodal incidence matrix, we will need a computation table to relate the nodes.[10]

Table 1 Computation table for Electrical Network in Figure 1

	Branch 1	Branch 2	Branch 3	Branch 4	Branch 5
Node 1	1	0	1	0	0
Node 2	-1	1	0	1	0
Node 3	0	-1	-1	0	1

The nodal incidence matrix is now a 3×5 matrix given by

$$A = \begin{bmatrix} 1 & 0 & 1 & 0 & 0 \\ -1 & 1 & 0 & 1 & 0 \\ 0 & -1 & -1 & 0 & 1 \end{bmatrix}$$

To construct the electrical network in figure 1 from the nodal incidence matrix above, we will follow the reverse operation of the step above,

From the nodal incidence matrix, we will construct table 1 to show us clearly now the nodes and branches are related.

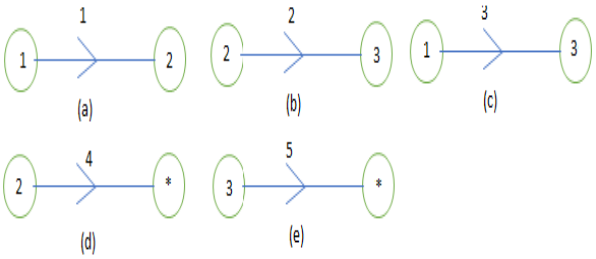

Figure 2 Sketches of connecting between Nodes and Branches for the construction of an Electrical network.

From table 1, we can see that branch 1 leave node (1) and enters node 2. The sketch is as shown in fig 2(a). Branch 2 leave node (2) and enters node (3). The sketch is as shown in figure 2(b). Branch 3 leave node (1) and enters node (3). The sketch is as shown in figure 2(c). Branch (4) leave node (2) to the reference node (which is marked as x).

The sketch is as shown in figure 2(d). Branch 5 leaves node (3) to the reference node. The sketch is as shown in figure 2(e) node. The sketch is as shown in figure 2(e).

Putting the sketches in figure 2 together, we have the electrical network in figure 1.

2.2 Example [11]

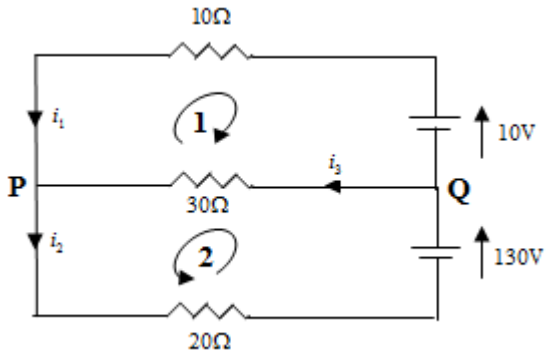

Figure 3 Network and relating the current

Figure 3 represents an electrical network with the currents. We label the currents as shown, choosing direction arbitrary. (i.e., the unknown different current are i_1, i_2 *and* i_3) We can now define as

Nope p gives the first equation, node Q the second, the upper loop the third and the lower loop the fourth as

$$\begin{aligned} &Node\ P: && i_1 - i_2 + i_3 = 0 \\ &Node\ Q: && -i_1 + i_2 - i_3 = 0 \\ &Upper\ Loop, && 10i_1 - 30i_3 = 10 \\ &Lower\ Loop, && 20i_2 + 30i_3 = 130 \end{aligned}$$

For node p is indicated, at which may apply KCL, current i_1 and i_3 come in and i_2 come out. So, $i_1 - i_2 + i_3 = 0$ and

For node Q is indicated, at which may apply KCL, current i_1 come out and i_2 and i_3 come in.

therefore $-i_1 + i_2 - i_3 = 0$. The upper loop, at which may apply KVL, current i_1 passing through 10Ω. Resistor and current i_3 passing through 30Ω.

Resister but they are opposite direction. Therefore, we have $10i_1 - 30i_3 = 10$.

The lower loop, at which may apply KVL, current i_2 *and* i_3 passing through 20Ω and 30Ω resistors respectively. So, we have $20i_2 + 30i_3 = 130$.

Now, we will find the currents by using Gauss-Elimination. We have to change the unknown currents $x_1 = i_1, x_2 = i_2, x_3 = i_3$ in the electrical network in figure 3. Then we have the linear system

$$x_1 - x_2 + x_3 = 0$$
$$-x_1 + x_2 - x_3 = 0$$
$$10x_1 - 30x_3 = 10$$
$$20x_2 + 30x_3 = 130$$

The Argument matrix

$$\tilde{A} = \left[\begin{array}{ccc|c} 1 & -1 & 1 & 0 \\ -1 & 1 & -1 & 0 \\ 10 & 0 & -30 & 10 \\ 0 & 20 & 30 & 130 \end{array}\right]$$

Step 1, *Elimination of* x_1

Call the first row of $\tilde{A}$ the pivot row and the first equation the pivot equation.

Add 1 times the pivot equation to the second equation.

$$\tilde{A} = \left[\begin{array}{ccc|c} 1 & -1 & 1 & 0 \\ 0 & 0 & 0 & 0 \\ 10 & 0 & -30 & 10 \\ 0 & 20 & 30 & 130 \end{array}\right] Row\ 2 + Row\ 1$$

Add -10 times the pivot equation to the third equation.

$$\tilde{A} = \left[\begin{array}{ccc|c} 1 & -1 & 1 & 0 \\ 0 & 0 & 0 & 0 \\ 0 & 10 & -40 & 10 \\ 0 & 20 & 30 & 130 \end{array}\right] Row\ 3 - 10Row\ 1$$

Step 2, *Elimination of* x_2

The first equation remains as it is. We want to new second equation to serve as the next pivot equation. But since it has no x_2-terms (in fact, it is 0=0), we must first change the order of the equation and the corresponding rows of the new matrix. We put 0=0 at the end and move the third equation one place up.

$$\tilde{A} = \left[\begin{array}{ccc|c} 1 & -1 & 1 & 0 \\ 0 & 10 & -40 & 10 \\ 0 & 0 & 0 & 0 \\ 0 & 20 & 30 & 130 \end{array}\right] Row\ 2 \leftrightarrow Row\ 3$$

To eliminate x_2, do: Add -2 times the pivot equation to the second equation. The result is

$$\tilde{A} = \left[\begin{array}{ccc|c} 1 & -1 & 1 & 0 \\ 0 & 10 & -40 & 10 \\ 0 & 0 & 0 & 0 \\ 0 & 0 & 110 & 110 \end{array}\right] Row\ 4 - 2\ Row\ 2$$

But since it has no x_3-terms (in fact, it is 0=0), we must first change the order of the equation and the corresponding rows of the new matrix. We put 0=0 at the end and move the fourth equation one place up. This is called partial pivoting.

$$\tilde{A} = \left[\begin{array}{ccc|c} 1 & -1 & 1 & 0 \\ 0 & 10 & -40 & 10 \\ 0 & 0 & 110 & 110 \\ 0 & 0 & 0 & 0 \end{array}\right] Row\ 3 \leftrightarrow Row\ 4$$

Back substitution. Determination of x_1, x_2, x_3

Working backward from the last to the first equation of this 'triangular' system, we can now readily find x_3, then x_2, and then x_1:

$$110x_3 = 110$$
$$10x_2 - 40x_3 = 10$$
$$x_1 - x_2 + x_3 = 0$$

Above the equations: We can get

$$110x_3 = 110$$
$$x_3 = 1$$
$$10x_2 - 40x_3 = 10$$
$$x_2 = 5$$
$$x_1 - x_2 + x_3 = 0$$
$$x_1 - 5 + 1 = 0$$
$$x_1 = 4$$

$Current\ I_1 = 4A, I_2 = 5A, I_3 = 1$

$$X = \begin{bmatrix} x_1 \\ x_2 \\ x_3 \end{bmatrix} = \begin{bmatrix} 4 \\ 5 \\ 1 \end{bmatrix}$$

3. CONCLUSION

In this paper, firstly we have considered how to derive nodal incidence matrices from electrical networks, conversely how to sketch electrical networks from nodal incidence matrices by 2.1 example.

In this study, we used the krichhoff 's law to derive linear system from electrical networks with currents. And then, we have calculated the current from linear system by using Gauss Elimination we show detail our works in 2.2 example.

The advantage of this paper is that it would be desirable to continuous the study of model engineering networks, networking in the computer studies and any other scientific field.

ACKNOWLEDGEMENTS

We would like to express my sincere gratitude, Dr. Ei Ei Hlaing, Rector, University of Computer Studies (Taungoo) and Dr. Aye Theingi, Professor, Head of Department of Computational Mathematics for their encouragement to carry out this paper and a critical reading the manuscript. We have grateful to all the teachers who are work in Department of Computational Mathematics.

I am gracefully thank to Associate Professor Daw Hla Yin Moe, Department of Computational Mathematics, for her encouragement, closed guidance, critical reading the manuscript, corrected various mistakes and help to finish this paper on time.

REFERENCES

[1] Ajayi,J.A.and K. Joseph, " Application of matrices to some selected engineering problems", Damson Journal of Science and Engineering , 2009, 3(2): 115-128.

[2] Binoy, B., "Mathematical Physics", New Delhi; New Central Book Agency(p) Ltd, 2009.

[3] Dada, J.O., "Using nodal and mesh incidence matrices in solving engineering problems". Journal of Engineering Applications, 2010, 2(1); 150-168.

[4] Dass, H.K. and R. Verma, "Mathematical physics", S. New Delhi; Chand and Company Ltd, 2011.

[5] Diestel, R., "Graph theory", Graduate texts in mathematics, United kingdom, Springer-Verlag, 2005.

[6] Dr.Len Trombetta, "Experimental Verification of Kirchoff's voltage law and Kirchoff's Current law", University of Houston Electrical and Computer Engineering Department, 2010.

[7] Gross, L. and J. Yellen, "Graph theory and its application", London: Macmillan Press Ltd, 2006.

[8] Gupta, B.D., "Mathematical physics", New Delhi; Vikas Publishing House PVT Ltd, 2009.

[9] Janes W. Nillson and Susan A. Riedel, "Electrical Circuits", 8 Edition, Person/ Prentice Hall, New Jersey, 2008, pp.36-41.

[10] Kreyszing, E., "Advanced Engineering Mathematics", 10 Edition, John Wiley & Sons, Inc, 2011.

[11]M.O.Oke,R.A.Raji.Y.O.Aderinto,"Modelling Engineering networks by using nodal and mesh incidence matrices" ,Journal of Asian scientific Research, 2013,3(3):328-336.

Optimization Problem Solving By Graphical and Simplex Method

Zin Nwe Khaing[1], Hla Yin Moe[2], San San Nwe[3]
Assistant Lecturer, Associate Professor, Lecturer
flowerlayfl1990@gmail.com, hlayinmoe5049663@gmail.com, panswaltaw26@gmail.com

ABSTRACT: *This paper demonstrates the use of linear programming methods as applicable of The Primo Insurance Company problem. A linear programming model for this problem is developed for profit optimization. This problem is solved by two methods. One is graphical method and the other one is algebraic method (simplex method). Then, this paper describes the linear programming model equations with adequate restraints taking into account manufacturing limitations are solved use Microsoft Excel Solver. We illustrate the use of spreadsheet modeling and Excel Solver in solving linear programming problems.*

Keyword; Linear programming; Linear programming model; Graphical method; Simplex method; MS Excel

1. INTRODUCTION

Linear programming is a mathematical programming technique that is used to determine the best possible outcome or solution from a given set of parameter or list of requirement. The term linear programming was first used by G.B. Dantzig in 1947 to refer to specific problems of optimization which assume that both constraints and objective function are linear. [3].

A graphical method is used to solve problem by finding the highest or lowest point of intersection between the objective function line and the feasible region on a graph. The simplex method is an efficient iterative method and is widely used in solving LP problem and containing several variables and constraints. Graphical method is used when the constraints contain two variables only. But simplex method can be used to solve constraints having more than two variables,[4].

The Microsoft Excel (Wikipedia, 2010) contains a built-in optimization tool know as solver. The Microsoft Excel Solver has become the most widely distributed and almost surely the most widely used general purpose optimization modeling system.

2. LINEAR PROGRAMMING

Linear problem involve the planning of activities to obtain an optimal results. Linear programming is a technique used to solve models with linear objective function and linear constraints,[3].

2.1. Linear programming model

If the model consists of a linear objective function and linear constraints in decision variables, it is called a linear programming model.

2.1.1. Basic component of a linear programming model

A linear programming usually is expressed in inequalities, below are the various component that make up on LP model. (a) decision variables (b) objective function (c) constraints /limitations (d) non – negativity constrain [2], [3].

2.1.2 Common terminologies used in linear programming

Let us define some terminologies used in linear programming:

Decision variables: that are mathematical symbols representing level of activity of an operation.

Objective function: that is a linear mathematical relationship describing on objection of the firm in terms of decision variables that is to be maximized or minimized.

Constraints: The constraints are the restrictions or limitations on the decision variables.

Non – negativity constraints: For all linear programs the decision variables should always take non-negativity values (greater than or equal to 0).

3. SOLVING A LINEAR PROGRAMMING PROBLEM

3.1 Modeling

The Primo Insurance Company is introducing two new product lines: special risk insurance and mortgages. The expected profit is $5 per unit on special risk insurance and $2 per unit on mortgage. Management wishes to establish sales quotas for the new product lines to maximize total expected profit. The work requirements are as follows [2].

Department	Hours Used per Unit produced		Hours Available
	Special Risk Insurance	Mortgage	
Underwriting	3	2	2400
Administration	0	1	800
Claim	2	0	1200
Unit profit ($ thousand)	5	2	

Let x_1= the total number of units on special risk insurance
Let x_2 = the total number of units on mortgages

Now, the total profit is represented by Z.

The total profit the company makes is given by the total number of units of special risk insurance and mortgages produced multiplied by its per unit profit $5 and $2 respectively.

Profit: Max Z (1)

As per above the table, each unit of special risk insurance and mortgages requires 3 hours and 2 hours of Underwriting. The total hours of underwriting available are 2400 hours. To represent this mathematically

(2)

Each unit of mortgage require 1 hour of Administration. The total hours of Administration available are 800 hours. To represent this mathematically

(3)

Also, each unit of special risk insurance requires 2 hours of claim. The total hours of claim are 1200 hours. To represent this mathematically

(4)

So, we have two more constraints $x_1 \geq 0, x_2 \geq 0$ for the company to make maximum profit, the above inequalities have to be satisfied.

3.2. Solve a LP problem through graphical method

. We will consider only the first quadrant. To plot for the graph for the above equation, first I will simplify all the equation. The first equation is in its simplified from

We consider only equality 3 which represents a straight line (800, 1200).

The horizontal line labeled is the limiting value of the inequality x 800.

The vertical line labeled is the limiting value of the inequality $2x$ 1200.

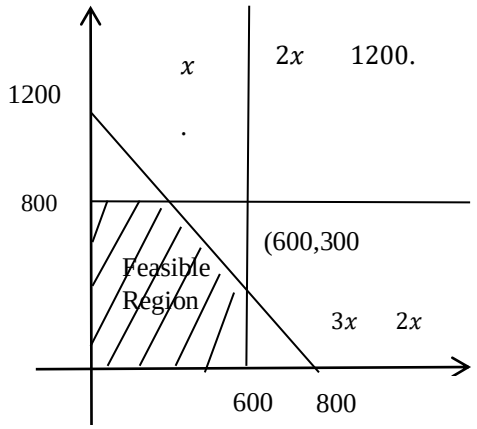

Figure 1. The Primo Insurance Company would have optimal solution

Plot the lines on a graph in first quadrant. It can be seen that the region satisfied the constraints. This shaded area is called as the feasible region. The feasible region is also called the solution space. Now, it is possible to choose any point in the solution space which would maximize the objective function. The value for and which gives the optimal solution is at (600,300).To maximize profit the management should produce special risk insurance in 600 units and mortgages 300 units respectively.

The optimal solution is $x_1 = 600$ and with Z=3600.

3. 3. The linear programming problem solving by Excel

Technology can be used to solve a system of equation once the constraints and objective function have been defined. Excel has an add-in called the Solver which can be used to solve systems of equation or inequalities. To add this facility to yours tools menu you need to carry out the following steps [2]

1. Select the menu option Tools / Add-In (this will take a few seconds to load the necessary file)
2. From the dialogue box presented check the box for Solver Add-in.
3. On clicking OK, you will then be able to access the Solver option from the new menu option Tools / Solver.

3.3.1. Display the Linear Programming Models on a Spreadsheet

Spreadsheet software, such as Excel, is a popular tool for analyzing and solving small linear programming problems. The main features of a linear programming model, including all its parameters, can be easily entered onto a spreadsheet.

	A	B	C	D	E	F	G
1	The Primo Insurance Company						
2							
3			Hours used per Unit produced				
4	Department		Special Risk Insurance	Mortgage	Total		Hours Available
5	Underwriting		3	2	0	<=	2400
6	Administration		0	1	0	<=	800
7	Claim		2	0	0	<=	1200
8	Unit profit ($ thousand)		5	2	0		
9	Solution		0	0			

	E
5	=SUMPRODUCT(C5:D5,C9:D9)
6	=SUMPRODUCT(C6:D6,C9:D9)
7	=SUMPRODUCT(C7:D7,C9:D9)
8	=SUMPRODUCT(C8:D8,C9:D9)

Figure 2. The spreadsheet for the Primo Insurance Company problem before using the Excel Solver

This equation involves the sum of two products. There is a function in Excel, called SUMPRODUCT that will sum up the product of each of the individual terms in two different ranges of cells. For instance, SUMPRODUCT (C7:D7, C9:D9) takes each of the individual terms in the range C7:D7, multiplies them by the corresponding term in the range C9:D9, and then sums up these individual products, just as shown in the above equation.

3.3.2 Calculation with Excel Solver

The Solver can be started by choosing “Solver” in the Tools menu. The Solver dialogue box is shown in Figure 3. The “Target Cell” is the cell containing the value of the objective function, while the “Changing Cells” are the cells containing the values of the decision variables. Since the goal is to maximize the objective function, “Max” also has been selected.

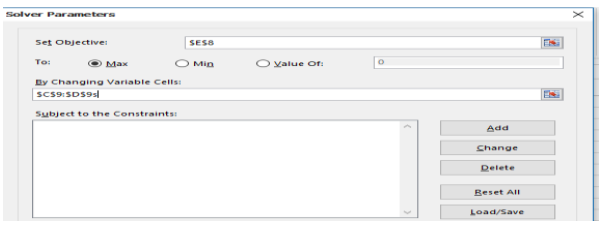

Figure 3. The solver dialogue box after specifying which cell

Next, the addresses for the functional constraints need to be added. This is done by clicking on the “Add . . .” button on the Solver dialogue box.

The cell reference is to the cell containing your constraint formula, so for the Underwriting constraint you enter E5. By default <= is selected but you can change this by clicking on the drop down arrow to reveal a list of other constraint types. In the right hand white box you enter the cell reference to the cell containing the RHS value. You then click 'Add' to add the rest of the constraints, remembering to include the non-negativity constraints.

You then click 'Add' to add the rest of the constraints, remembering to include the non-negativity constraints. Having added all the constraints, click 'OK' and the Solver dialogue box should look like that shown in Figure 4.

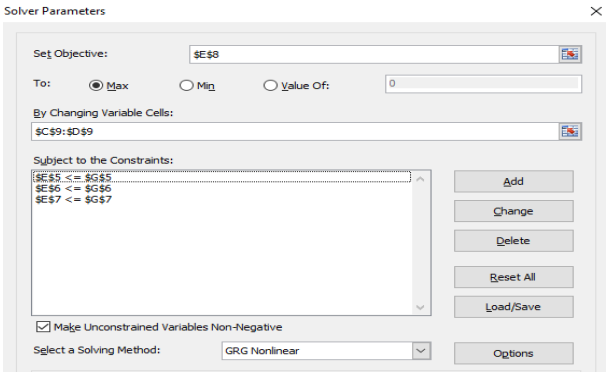

Figure 4. The completed Solver Dialogue Box

Before asking Solver to solve the model, one more step should be taken. Clicking on the Options . . . button brings up the dialogue box shown in Fig.5. This box allows you to specify a number of options about how the problem will be solved. The most important of these are the Assume Linear Model option and the Assume Non-Negative option. Be sure that both options are checked as shown in the figure. This tells Solver that the problem is a linear programming problem with no negativity constraints for all the decision variables. Then, clicking on the “OK” button.

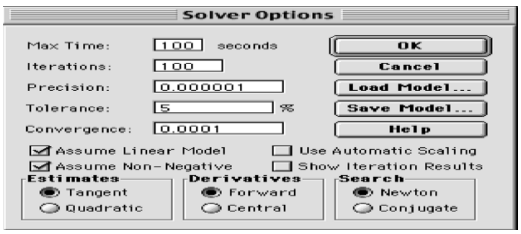

Figure 5. The Solver Options dialogue box

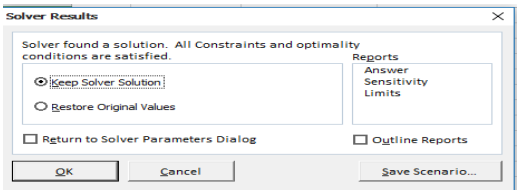

Figure 6. Solver Result

Clicking on the OK button then returns you to the Solver dialogue box. Now you are ready to click on Solver in the Solver dialogue box. After a few seconds, Solver will then indicate the results.

	A	B	C	D	E	F	G
1	The Primo Insurance Company						
2							
3			Hours Used per Unit produced				
4		Department	Special Risk Insurance	Mortgage	Total		Hours Available
5		Underwriting	3	2	2400	<=	2400
6		Administrstion	0	1	300	<=	800
7		Claim	2	0	$1,200	<=	1200
8		Unit profit ($ thousand)	5	2	3600		
9		Solution	600	300			

Figure 7. The spreadsheet obtained after solving the problem

After solving the model, the Solver replace the original value of the decision variables in the spreadsheet with the optimal value, as shown in figure 7.The spreadsheet also indicates the value of the objective function, as well as the amount of each resource that is being used.

3.4 Solving a linear programming problem by Simplex method

Simplex method is an approach to solving linear programming models by hand using slack variables, tableaus and pivot variables as a means to finding the optimal solution of optimization problem. Simplex tableau is used to perform row operations on the linear programming model as well as for checking optimality.

3.4.1 Simplex method in Tabular form

The tabular form of the simplex method records only the essential information namely, (1) the coefficient of the variables (2) the constraint of the right hand sides of the equation (3) the basic variable appearing in each equation. This saves writing the symbols for the variables in each of the equation. [2]

Initialization - Introduce slack variables. Select the decision variables to be the non-basic variables (set equal to 0) and the slack variables to be the initial basic variables.

Optimality test - The current BF solution optimal if and only if coefficient row 0 is non-negative (greater than equal 0). If it is, stop; go to an iteration to obtain the next BF solution, which involves changing one non-basic variable to a basic variable (step 1) and vice versa (step 2) and then solving for the new solution (step 3).

Iteration

Step 1: Determine the entering basic variable by selecting the variables (a non-basic variable) with the coefficient having the largest absolute value (the most negative coefficient) in equation 0.Put a box around the column below this coefficient, and call this the pivot column.

Step 2: Determine the leaving basic variable by applying the minimum ratio test.

Minimum ratio test

1. Put out each coefficient in the pivot column that is strictly positive (>0).
2. Divide each of these coefficients into the right side entry for the same row.
3. Identify the row that has the smallest of these ratios.
4. The basic variable for that row is the leaving basic variable, so replace that variable by the entering basic variable in the basic variable column of the next simplex tableau.

Step 3: Solve for the new BF solution by using elementary row operations.

1. Divide the pivot row by the pivot number. Use this new pivot row in steps 2 and 3.
2. For each other row (including row 0) that has a negative coefficient in the pivot column, add to this row the product of the absolute value of this coefficient and the new pivot row.
3. For each other row that has a positive coefficient in the pivot column, subtract from this row the product of this coefficient and the new pivot row.

Iteration 0

(a)Algebraic form	(b)Tabular form								
	Coefficient of :								
	Basic variables	Eq.	Z	x_1	x_2	S_1	S_2	S_3	Right side	Minimum ratio
$Z - 5x_1 + 2x_2 = 0$	Z	0	1	-5	-2	0	0	0	0	
$3x_1 + 2x_2 + S_1 = 2400$	S_1	1	0	3	2	1	0	0	2400	800
$x_2 + S_2 = 800$	S_2	2	0	0	1	0	1	0	800	-
$2x_1 + S_3 = 1200$	S_3	3	0	2	0	0	0	1	1200	600

The tableau is not optimal (negative value in the Z row) x_1 is entering basic variable and S_3 is the leaving basic variable.(minimum ratio)

Iteration 1

Tabular form									
Coefficient of :									
Basic variables	Eq.	Z	x_1	x_2	S_1	S_2	S_3	Right side	Minimum ratio
Z	0	1	0	-2	0	0	5/2	3000	
S_1	1	0	0	2	1	0	-3/2	600	300
S_2	2	0	0	1	0	1	0	800	800
x_1	3	0	1	0	0	0	1/2	600	-

The tableau is not optimal (negative value in the Z row) x_2 is entering basic variable and S_1 is the leaving basic variable.(minimum ratio).

Iteration2

Tabular form									
Coefficient of :									
Basic variables	Eq.	Z	x_1	x_2	S_1	S_2	S_3	Right side	Minimum ratio
Z	0	1	0	0	1	0	1	3600	
x_2	1	0	0	1	1/2	0	-3/4	300	
S_2	2	0	0	1	-1/2	1	3/4	500	
x_1	3	0	1	0	0	0	1/2	600	-

0, 500, 0) with Z=3600.

3.5. Solving linear programming with the modified simplex method in Excel

Matrices are arrays of numbers, so there is no unique way to define the multiplication of matrices. As such in general the term matrix multiplication refers to a number of different ways to multiply matrices.

3.5.1 Simplex method in Matrix form

and

where, c = (c)

$$\begin{bmatrix} 2 \\ \vdots \end{bmatrix}. \quad \begin{bmatrix} \end{bmatrix} \quad \begin{bmatrix} 2 \end{bmatrix}$$

The number of decision variables are indicated by n and the number of constraints by m [1].

To obtain the augmented form of the problem, introduce the column vector of slack variables

$$.x \quad \begin{bmatrix} \end{bmatrix}$$

So that constraint become

$[A/I]\begin{bmatrix} x \end{bmatrix} = b \; and \; \begin{bmatrix} x \end{bmatrix} \geq 0$, where I is the identity matrix, and the null vector 0 now has n+m elements. In which, the n non-basic variables from the n+m element of $\begin{bmatrix} x \end{bmatrix}$ are set equal to zero. This equation can be denoted by $Bx_B = b$. x_B is the basic variables. [1]

The simplex method introduces only basic variables such that B is nonsingular, so that B^{-1} always will exist (inverse).

$$B^{-1}Bx_B = B^{-1}b.$$

Since $B^{-1}B = I$, $\quad x_B = B^{-1}b.$

Let C_B be the vector whose elements are the objective function coefficients (including zero for select variables) for the corresponding elements of x_B. The value of the objective function for this basic solution is then

$$\boxed{Z = C_B x_B = C_b B^{-1} b.}$$

3.5.2 Use Matrix Multiplication in Excel

Maximize

Subject to

and

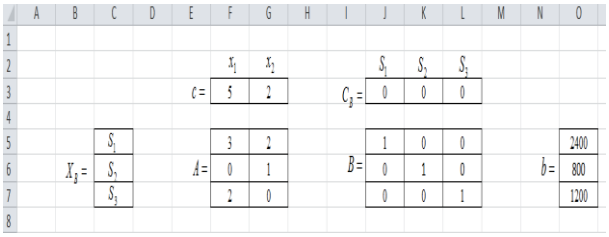

Figure 8. Entering data in the spreadsheet

To obtain the optimal test

Z	$C_BB^{-1}A$-c	C_BB^{-1}	$C_BB^{-1}b$
X_B	$B^{-1}A$	B^{-1}	$B^{-1}b$

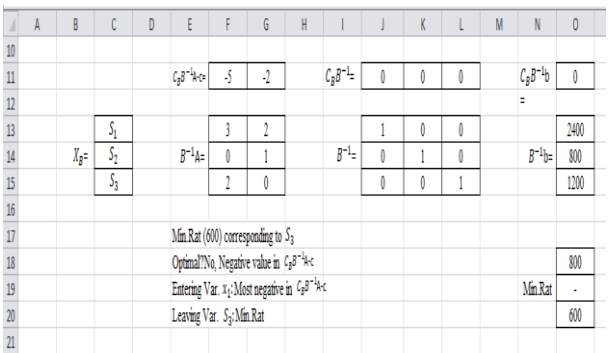

Figure 9. Evaluate and multiplication of B^{-1}

B^{-1} =First select the cell of the matrix B^{-1} and equal MINVERSE(J5:L7), then Ctrl+Shift+Enter

	=MINVERSE(J5:L7)		
$B^{-1}=$			

$B^{-1}A$= First select the cell box of the matrix $B^{-1}A$ and equal MMULT (J13:L15, F5:G7), Ctrl+Shift+Enter

	=MMULT(J13:L15,F5:G7)		
$B^{-1}A=$			

C_BB^{-1}= First select the cell box of the matrix $C_BB^{--1}$and equal MMULT (C_B: B^{-1}), then Ctrl+Shift+Enter

$C_BB^{-1}A$-c= First select the cell box of the matrix $C_BB^{-1}A$-c and equal MMULT (C_BB^{-1}: A)-c, then Ctrl+Shift+Enter

$C_BB^{-1}b$ = First select the cell box of the matrix $C_BB^{-1}b$ and equal MMULT (C_BB^{-1}:b), then Ctrl+Shift+Enter

$B^{-1}b$ = First select the cell box of the matrix $B^{-1}b$ and equal MMULT (B^{-1}:b), then Ctrl+Shift+Enter

Figure 9 is not optimal ($C_BB^{-1}A\text{-}c \leq 0$).Choose the entering basic variable in $C_BB^{-1}A$-c and the leaving basic variable by using minimum ratio test.($B^{-1}b/C_BB^{-1}A$-c, Ctrl+ Shift+ Enter).Then, x_3 column substitute in S_1 column from the original table (Figure 8) .

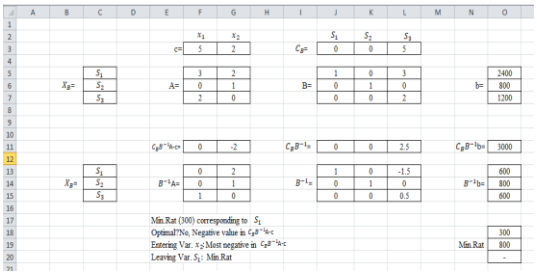

Figure 10. Substitute the variable in the spreadsheet

Figure 10 is not optimal ($C_BB^{-1}A\text{-}c \leq 0$). Choose the entering basic variable in $C_BB^{-1}A$-c and the leaving basic variable by using minimum ratio test ($B^{-1}b/ C_BB^{-1}A$-c, Ctrl+ Shift+ Enter).Then, x_2 column substitute in S_2 column from the original table (Figure 8)

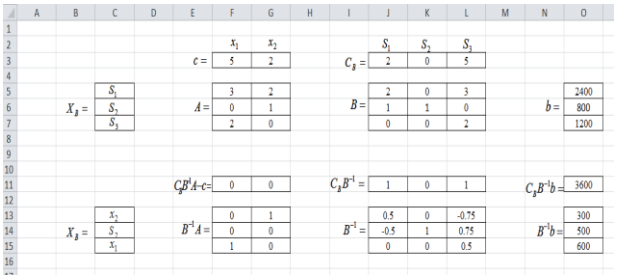

Figure 11. The spreadsheet obtained the optimal solution after solving

Figure 11 is optimal because $C_BB^{-1}A$-c is positive. The objective function $Z = C_B x_B = C_b B^{-1} b$ is 3600.

4. CONCLUSION

In this paper we can learn about the basic ideas of linear programming by using simplex method and graphical method and how to solve these methods by spread sheet.

The comparison of two methods is expressed and the advantages of these two methods are also described. The computerized system is easier to handle and more powerful than the old graphical method. Moreover, the computerized system provides the optimal kind of solution to the results.

The reader, who read this paper, can study graphical method and simplex method, also many other methods can be studied for linear programming problem.

ACKNOWLEDGEMENTS

We would like to express my sincere gratitude, Dr. Ei Ei Hlaing, Rector, University of Computer Studies (Taungoo) and Dr. Aye Theingi, Professor, Head of Department of Computational Mathematics for their encouragement to carry out this paper and a critical reading the manuscript. We have grateful to all the teachers who are work in Department of Computational Mathematics.

I am gracefully thank to Associate Professor Daw Hla Yin Moe, Department of Computational Mathematics, for her encouragement, closed guidance, critical reading the manuscript, corrected various mistakes and help to finish this paper on time.

REFERENCES

[1] C.K.Mustafi, " Operation Research, Methods and Practice", fourth edition, New Age International (P) Limited, Publishers, 2015.

[2] Frederick S. Hilliem, Gerald J. Lieberman, "Introduction to Operations Research", seventh edition, MC Graw-Hill, 2001.
[3] George B. Dantzig "Linear Programming and Extensions", Princeton University Press, Princeton, N.J, 1963.
[4] Gass,S.I, "Linear Programming: Methods and Application", 5th ed. Mc Graw-Hill, New York, 1985.

Solution and Application of Heat Equation Using Method of Separation of Variables

Kyi Pyar Moe[1], Myo Su Su Hlaing[2]
Faculty of Computing,University of Computer Studies (Dawei)
kyipyarmoe012@gmail.com, suhlaingwei@gmail.com

ABSTRACT: *In this paper introduction for heat equation is explained. Then one dimensional heat flow is expressed and the solution of it is calculated with an example. Two dimensional heat flow and the solution of it are also presented .The temperature of the plate is evaluated with an example. Finally, application of heat equation is explained.*

Keywords: Diffusivity, specific heat, homogeneous material, thermal conductivity

1. INTRODUCTION

One dimensional heat equation partial differential equation that describes how the distribution of some quantity evolves over time in a solid medium, as it spontaneously flows from places where it is higher towards places where it is lower. It is a special case of the diffusion equation. The heat equation is an important partial differential equation which describes the distribution of heat in a given region over time. Heat is a process of energy transfer as a result of temperature difference between the two points. So, the term heat is used to describe the energy transferred through the heating process. Temperature, on the other hand, is a physical property of matter that describes the hotness or coldness of an object or environment. Therefore, no heat would be exchanged between bodies of the same temperature .Suppose a function U(x, y, t) describes the temperature of a conducting material at a given location (x, y) this function can be used to determine the temperature at any position on the material at a future time. The function U changes over time as heat spreads throughout the material and the heat equation is used to determine this change in the function.

2. MEANING OF THE EQUATION

2.1 Heat flows

When heat flows into (or out of) a material, its temperature increases (respectively, decreases), in proportion to the amount of heat divided by the amount (mass) of material, with a proportionality factor called the specific heat capacity of the material.

2.1.1One dimensional heat flow

The flow of heat and the accompanying variation of temperature with position and with time in conducting solids are considered. The following empirical laws are taken as the basis of investigation.

1. Heat flows from a higher to lower temperature.
2. The amount of heat required to produce a given temperature change in a body is proportional to the mass of the body and to the temperature change. This constant of proportionality is known as the specific heat (c) of the conducting material.
3. The rate at which heat flows through an area is proportional to the area and to the temperature gradient normal to the area. This constant of proportionality is known as the thermal conductivity (k) of the material. A bar or rod of homogeneous are considered material of density ρ and having a constant cross-sectional area A Suppose that the sides of perpendicular to the area A. Take an end of the bar as origin and the direction of heat flow as the positive x-axis.

One dimensional heat equation is

$$\frac{\partial u}{\partial t} = \alpha^2 \frac{\partial^2 u}{\partial x^2},$$

Where α^2 is the diffusivity and u is the temperature at, a distance x at time t.

Solution of heat equation by the method of separation of variables.

Solve the equation,

$$\frac{\partial u}{\partial t} = \alpha^2 \frac{\partial^2 u}{\partial x^2}, \qquad (1)$$

Assume a solution of the form

$$u(x,t) = X(x).\ T(t),$$

where X is a function of x alone and T is a function of t alone.

Then (1) becomes,

$$X'T = \alpha^2 X''T$$

where $X'' = \frac{d^2x}{dx^2}$ and $T' = \frac{dT}{dt}$

i.e. $$\frac{X''}{X} = \frac{T'}{\alpha^2 T} . \qquad (2)$$

The left hand side is a function of x alone and the right hand side is a function of t alone when x and t are independent variables. (2) can be true only if each expression is equal to a constant.

So, Let $\frac{X''}{X} = \frac{T'}{\alpha^2 T}$ = k (constant) (say).

Hence, X''– kX = 0, and T'– α^2kT = 0 . (3)

The nature of solutions of (3) depends upon the values of k.

Case1. Let k =λ^2, a positive number.

Then (3) becomes,

$$X''–\lambda^2 X = 0 \text{ and } T'–\alpha^2\lambda^2 T = 0 .$$

Then, X = $A_1 e^{\lambda x} + B_1 e^{-\lambda x}$ and T =$C_1 e^{a^2\lambda^2 t}$.

Case2. Let k =$-\lambda^2$, a negative number. Then (3) becomes

$$X'' + \lambda^2 X = 0 \text{ and } T' + \alpha^2\lambda^2 T = 0 .$$

Then,X =$A_2 \cos\lambda x + B_2 \sin \lambda x$, and T =$C_2 e^{-a^2\lambda^2 t}$.

Case3. Let k = 0.

Then X'' = 0 and T' = 0.

So, X = $A_3 x + B_3$ and T =C_3 .

Hence the possible solutions of (1) are

$$u(x,t) = (A_1 e^{\lambda x} + B_1 e^{-\lambda x}) C_1 e^{a^2\lambda^2 t}$$

$$u(x,t) = (A_2 \cos \lambda x + B_2 \sin \lambda x) C_2 e^{-a^2\lambda^2 t}$$

$$u(x,t)=(A_3 x + B_3) C_3 . \qquad [2]$$

Example

A rod 10 cm long, has its ends A and B kept at 30°C and 60°Crespectively, until steady state conditions prevail. The temperature at each end is then suddenly reduced to 0°C and kept so. Find the resulting temperature function u(x,t) taking x=0 at A.

The P.D.E. of one dimensional heat flow is

$$\frac{\partial u}{\partial t} = \alpha^2 \frac{\partial^2 u}{\partial x^2} .$$

In steady state conditions, the temperature at any particular point does not vary with time. That is, u depends only on x and not on time t.

Hence the P.D.E. in steady state becomes

$$\frac{d^2 u}{dx^2} = 0 . \qquad (4)$$

By solving (4) ,

$$u = ax + b . \qquad (5)$$

The initial conditions, in steady-state , are

$$u = 30, \text{ when } x = 0 ;$$

and $$u = 60 , \text{ when } x = 10 .$$

Using these conditions , (5) becomes

$$u (x) = 3x + 30 . \qquad (6)$$

When the temperature at A and B are reduced to zero , the temperature distribution changes and the state is no more steady-state. For this transient state , the boundary conditions are

$$u (0,t) = 0 \quad \forall \quad t \geq 0 \quad (i)$$

$$u (10,t) = 0 \quad \forall \quad t \geq 0 \quad (ii)$$

The initial temperature of this state is the temperature in the previous steady-state. Hence the initial condition is

$$u (x,0) = 3x + 30 \text{ for } 0 < x < 10 . \qquad (iii)$$

Now, to find u(x,t) satisfying the conditions (i),(ii) and (iii) and (1). The suitable solution of (1) is of the form

$$u(x,t) = (A \cos \lambda x + B \sin \lambda x) e^{-a^2\lambda^2 t}. \quad (7)$$

Using (i) in (7), A = 0 .

Using (ii) in (7), B sin 10λ = 0 .

Since B ≠ 0, sin 10λ = 0

10λ = nπ

$\lambda = \frac{n\pi}{10}$, where n is any integer.

Therefore (7) reduces to

$$u(x,t) = B_n \sin \frac{n\pi}{10}x \, e^{\frac{-\alpha^2 n^2 \pi^2 t}{100}} . \qquad (8)$$

The most general solution of (1) is obtained by a linear combination of terms given by (8).

$$u(x,t) = \sum_{n=1}^{\infty} B_n \sin \frac{n\pi}{10}x \, e^{\frac{-\alpha^2 n^2 \pi^2 t}{100}} . \qquad (9)$$

Using (iii),

$u(x,0) = \sum_{n=1}^{\alpha} B_n \sin \frac{n\pi}{10}x = 3x + 30$ for $0 < x < 10$.

$\sum_{n=1}^{\alpha} B_n \sin \frac{n\pi}{10}x$ is the Fourier sine series for

$f(x) = 3x + 30$, in $0 < x < 10$.

Hence, $B_n = \frac{2}{L}\int_0^L f(x) \sin \frac{n\pi}{L}x dx$

$$= \frac{2}{10}\int_0^{10}(3x + 30) \sin \frac{n\pi}{10}x dx$$

$$= \frac{60}{n\pi}(1 - 2 (-1)^n) .$$

Substituting in (9),

$u(x,t) = \sum_{n=1}^{\alpha} \frac{60}{n\pi} (1 - 2 (-1)^n) .\sin \frac{n\pi}{10}x \; e^{\frac{-\alpha^2 n^2 \pi^2 t}{100}}$ degrees.

2.1.2 Two dimensional heat-flow

When the heat-flow is along curves instead of along straight lines, all the curves lying in parallel planes, then the flow is called two-dimensional consider now the flow of heat in a metal-plate in the xoy plane
Let the plate be of uniform thickness h, density ρ, thermal conductivity k and the specific heat c, Since the flow is two dimensional, the temperature at any point of the plate is independent of the z-coordinate. The heat-flow lies in the xoy plane and is zero along the direction normal to the xoy plane.

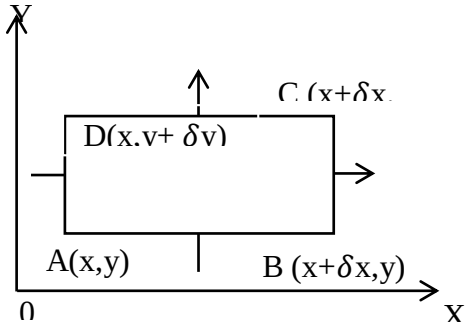

In the steady-state, u is independent of t, so that $\frac{\partial u}{\partial t} = 0$. Hence the temperature distribution of the plate in the steady-state is $\frac{\partial^2 u}{\partial x^2} + \frac{\partial^2 u}{\partial y^2} = 0$.

i.e., $\nabla^2 u = 0$, which is known as Laplace's Equation in two-dimensions.
Corollary: If the stream lines are parallel to the x-axis, then the rate of change $\frac{\partial u}{\partial y}$ of the temperature in the direction of the y-axis will be zero. Then the heat-flow equation reduces to $\frac{\partial u}{\partial t} = \alpha^2 \frac{\partial^2 u}{\partial x^2}$ which is the heat-flow equation in one-dimension.

Solution of the Equation $\frac{\partial^2 u}{\partial x^2} + \frac{\partial^2 u}{\partial y^2} = 0$.

The equation is $\frac{\partial^2 u}{\partial x^2} + \frac{\partial^2 u}{\partial y^2} = 0$. (10)

Assume the solution u(x, y) = X (x) Y (y),

Where X is a function of x alone and Y a function of y alone.

So, $\frac{\partial^2 u}{\partial x^2} = X''Y$, and $\frac{\partial^2 u}{\partial y^2} = XY''$.

The Laplace equation $\nabla^2 u = 0$ becomes

$X''Y + Y''X = 0$

i.e $\frac{X''}{X} = \frac{-Y''}{Y}$.

The left hand side of (11) is a function of x alone and the right hand side is a function of y alone. Also x and y are independent variables. Hence, this is possible only if each quantity is equal to a constant k.

Therefore, Let $\frac{X''}{X} = -\frac{Y''}{Y} = k$ (say) (12)

$X'' - kX = 0$, and $Y'' + kY = 0$. (13)

Case1. Let $k = \lambda^2$, a positive number.

Then $X'' - \lambda^2 X = 0$, and $Y'' + \lambda^2 Y = 0$.

Solving these equations, $X = A_1 e^{\lambda x} + B_1 e^{-\lambda x}$ and $Y = C_1 cos\lambda y + D_1 sin\lambda y$.

Case2. Let $k = -\lambda^2$, a negative number.

Then (13) becomes $X'' + \lambda^2 X = 0$ and $Y'' - \lambda^2 Y = 0$.

Solving these equations,

$X = A_2 cos\lambda x + B_2 sin\lambda x$ and $Y = C_2 e^{\lambda y} + D_2 e^{-\lambda y}$.

Case3. Let k = 0. Then (13) reduces to

$X'' = 0$ and $Y'' = 0$.

On solving these equations,

$X = A_3 x + B_3$ and $Y = C_3 y + D_3$.

Therefore, the possible solutions of (10) are

$u(x,y) = (A_1 e^{\lambda x} + B_1 e^{-\lambda x})(C_1 cos\lambda y + D_1 sin\lambda y)$. (I)

$u(x,y) = (A_2 cos\lambda x + B_2 sin\lambda x)(C_2 e^{\lambda y} + D_2 e^{-\lambda y})$ (II)

$u(x,y) = (A_3 x + B_3)(C_3 y + D_3)$. (III) [2]

Example

A rectangular plate with insulated surface is 10cm. wide and so long compared to its width that it may be considered infinite in length without introducing an appreciable error. If the temperature of the short edge y=0 is given by u=x for $0 \le x \le 5$ and (10-x) for $5 \le x \le 10$ and the two long edges x=0 , x=10 as well as the other short edge are kept at $0°C$.

The temperature u(x,y) at any point (x,y) of the plate can be found as follows:

$u = x$ for $0 \le x \le 5$,

$= (10-x)$ for $5 \le x \le 10$.

Select

$u(x,y) = (A \cos\lambda x + B \sin \lambda x)(Ce^{\lambda y} + De^{-\lambda y})$.

The boundary conditions are

$u(0, y) = 0, 0 < y < \infty$ (i)

$u(10, y) = 0, 0 < y < \infty$ (ii)

$u(x, \infty) = 0, 0 < x < 10$ (iii)

$u(x, 0) = x$ for $0 \le x \le 5$,

$= (10-x)$ for $5 \le x \le 10$. (iv)

Using (i) and (iii) , in II,

A = 0, C = 0.

Using (ii) ,$\lambda = \frac{n\pi}{10}$, n any integer.

Hence, $u(x,y) = Bn \sin\frac{n\pi x}{10}\, e^{\frac{-n\pi x}{10}}$, n any integer.

Therefore, the most general solution is

$u(x,y) = \sum_{n=1}^{\infty} Bn \sin\frac{n\pi x}{10}\, e^{\frac{-n\pi y}{10}}$. (14)

Using u(x,0) condition in (iv)

$u(x,0) = \sum_{n=1}^{\infty} Bn \sin\frac{n\pi x}{10}$ =given function of x.

$Bn = \frac{2}{10}\int_0^{10} f(x)dx$

$= \frac{1}{5}\left[\int_0^5 x \sin\frac{n\pi}{10} x\, dx + \int_5^{10}(10 - x)\sin\frac{n\pi}{10} x\, dx\right]$

$= \frac{1}{5}\left[\frac{-100}{n\pi}\cos\frac{n\pi}{2}\right]$

$= \frac{40}{n^2\pi^2}\sin\frac{n\pi}{2}$ for n odd.

Substituting in (14),

$u(x,y) = \sum_{n=1}^{\infty} \frac{40}{n^2\pi^2}\sin\frac{n\pi}{2}\sin\frac{n\pi x}{10}\, e^{\frac{-n\pi y}{10}}$.

3. CONCLUSION

In this paper, the derivation of one dimensional heat equation is introduced and the solutions of this equation are expressed. Application of one dimensional heat equation is also explained. Then two dimensional heat equation and its solution are presented. Finally, application of two dimensional heat equations is explained in heat transfer for rectangular plate. The heat equation is of fundamental importance in diverse scientific fields. Furthermore, this equation can be applied in solving the heat flow that is related in science and engineering.

REFERENCES

[1] Bali, N.P., "A Text Book of Engineering Mathematics,"Laxmi Publications Ltd., New Delhi, 2007.

[2] Kandasamy,P, Thilagavathy, K.,Gunavathy,K., "Engineering Mathermatics", S.CHAND & COMPANY LTD, New Delhi,2000.

[3] Kreyszig,E., "Advanced Engineering Mathematics," Tenth Edition, John Wiley & Sons, New York,2011.

[4] Thomas' Calculus, "Mathematics of Computing," Twelfth Edition, Addison- Wesley, Boston,2010.

Microcontroller Based Automatic Water Level Controller

Aung San Min[1], San San Mon[2], Hla Myat Thandar[3], Min Min Aye[4]
[1]*Department of Physics, University of Myitkyina, Myanmar*
[2]*Department of Engineering Physics, Technological University (Taunggyi), Myanmar*
[3]*Department of Physics, University of Mandalay, Myanmar*
[4] *Department of Physics, Kyaukse University, Myanmar*
[1]*aungsanmin.phys.mdy@gmail.com* , [2]*sansanmon1973@gmail.com,*[3]*drhlamyatthandar.nayla@gmail.com,*
[4]*drminminaye.1976@gmail.com*

ABSTRACT: *The aim of this research is to construct an automatic water level controller for overhead tank of water supply. In this research, the main control and processing device is PIC18F452 microcontroller. A 2-line 16-character Liquid Crystal Display is also used to monitor the conditions of water level of the tank and water pump. In our developed system, three copper rods are used as the electrodes to sense the water level. The PIC18F452 microcontroller will sense the digital signal of the water level sensor output and control the AC water pump. It also controls LCD and sends the digital data of LCD characters. The program is written with Assembly language. If the water in the overhead tank is less than the predefined level, the water pump will automatically function to pump out the water. If the water level in the overhead tank is full, the water pump will automatically close to pump out the water.*

Keywords: Automatic, PIC18F452 microcontroller, LCD, water pump

1. INTRODUCTION

Most of our building, water is provided to the housing complex by a water tank that is situated on top of the building. The water tank is supplied by a source, normally a well or another tank. Once the source has enough water it is the duty of the household to switch on the motor which then pumps water from the source to the tank that is situated on the roof or terrace [4].

For the supply of water it is very common method to use an overhead tank to which water is pumped from a ground level tank. Generally a person has to manually switch on the water pump when the overhead tank is running low of water. Also when the tank is filled a person has to switch off the water pump manually. This process is inefficient because the person has no idea about the current water level in the tank. Therefore it cannot be known when the water is going to run out and when the tank is filled up, until the actual thing occurs. This may cause unexpected cut off of water supply. Also when the water is being pumped up the person has to wait until water overflows and then switch off the water pump.

To improve this, the water level sensors can be placed in the tank to measure the water level. In our constructed system, sensors are used to measure the water level in the tank and the water pump is automatically switched on and switched off as required. This system minimizes human intervention and eliminates the inefficiencies described above.

The PIC microcontroller is used as a brain and a main controller of the overall system of this project. The motivation to create and build a water level and pump is to make an innovation and to appreciate the technology because by using this water level, it can reduce our energy without necessary to check the water level in the tank location. By using the man power, they absolutely have their limit. They cannot work in a very long hours do will and if they do, they will get tired. So, this project can work reduces the use of man power.

2. LITERATURE REVIEW

In this section, the general descriptions of the automatic water level controller are described. Firstly, the block diagram of the constructed system is discussed. Then, general features of the PIC microcontroller and electronic devices used in this project are also described.

2.1 Block Diagram of the Automatic Water Level Controller

The block diagram of the automatic water level controller is shown in Figure 1. The developed automatic water level controller consists of water level sensor, main control and processing unit, water pump driver unit, display unit and power supply unit. The main function of water level sensor is to sense whether the water level of the tank is full or not and to give the condition of the water level in the form of digital state (i.e HIGH or LOW). The digital state HIGH means that the water level is full and LOW means that the water level is less than predefined value. The function of main control and processing unit is to receive the digital state from the water level sensor, and to control display unit and water

pump driver unit by using the information of water level sensor. The main control unit also sends the digital data of LCD characters. The function of water pump driver unit is to drive the water pump for transporting the water from the underground tank to overhead tank. The main function of display unit is to show the conditions of water level and water pump. The functions of power supply unit are to provide the regulated +12 V for water pump driver unit and +5 V for other units.

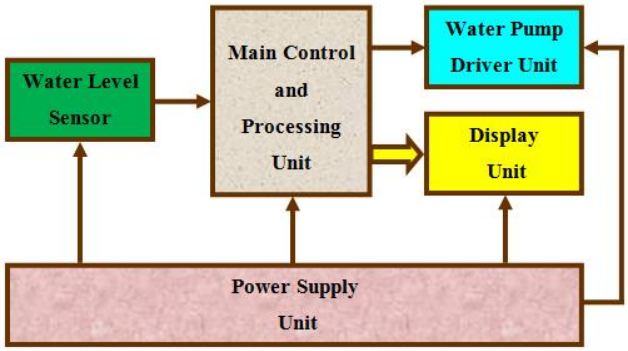

Figure 1. Block diagram of the automatic water level controller

2.2. PIC18F452 Microcontroller

PIC18F452 has five ports: PORTA, PORTB, PORTC, PORTD and PORTE. Some pins of the I/O ports are multiplexed with an alternate function from the peripheral features on the device. In general, when a peripheral is enabled, that pin may not be used as a general purpose I/O pin. Each port has three registers for its operation. These registers are: TRIS register (data direction register), PORT register (reads the levels on the pins of the device) and LAT register (output latch) [3]. Pin diagram and photograph of PIC18F452 microcontroller are shown in Figure 2 and Figure3.

The core features of PIC18F452 are:

- C compiler optimized architecture/instruction set
- High performance RISC (Reduced Instruction Set Computer) CPU
- Only 35 single word instructions to learn
- Operating speed: DC – 40 MHz clock input
- 32 Kbytes of Program Memory
- 1.5 Kbytes of Data Memory
- 256 bytes of EEPROM Data Memory

The peripheral features of PIC18F452 are:

- High current sink/source 25 mA / 25 mA
- Three external interrupt pin
- Timer0 module: 8-bit/16-bit timer/counter
- Timer1 module: 16-bit timer/counter
- Timer2 module: 8-bit timer/counter with 8-bit period register (time-base for PWM)
- Timer3 module: 16-bit timer/counter
- I^2C Master and Slave mode
- Compatible10-bit Analog-to-Digital Converter

The special features of PIC18F452 are:

- 100,000 erase/write cycle Enhanced FLASH program memory
- 1,000,000 erase/write cycle Data EEPROM memory
- FLASH/Data EEPROM Retention: > 40 years
- Programmable code protection
- Single supply 5 V In-Circuit Serial Programming via two pins
- Wide operating voltage range (2.0 V to 5.5 V)

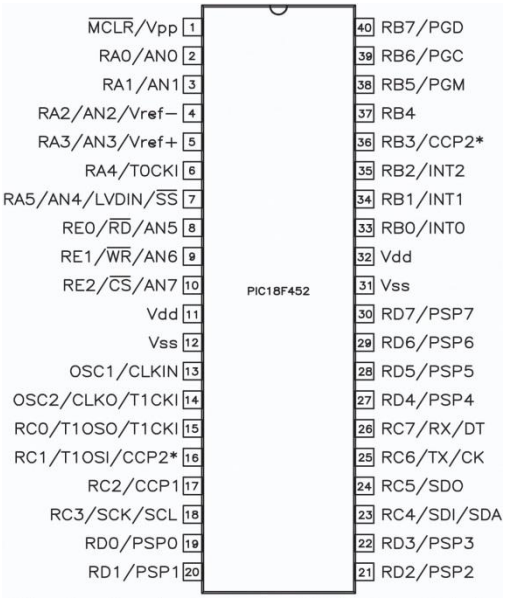

Figure 2. Pin diagram of PIC18F452 microcontroller

Figure 3. Photograph of PIC18F452 microcontroller

The PIC18F452 can be operated in eight different oscillator modes. The user can program three configuration bits (FOSC2, FOSC1 and FOSC0) to select one of these eight modes:

- LP Low-Power Crystal
- XT Crystal/Resonator
- HS High-Speed Crystal/ Resonator
- HS+PLL High-Speed Crystal/ Resonator with PLL enabled

- RC External Resistor/Capacitor
- RCIO External Resistor/Capacitor with I/O pin enabled
- EC External Clock
- ECIO External Clock with I/O pin enabled [3]

2.3. Alphanumeric LCD Display

LCDs are able to display not just numbers, but also letters, words and all manner of symbol makes them a good deal more versatile than the familiar 7-segment light emitting diode (LED) display. Even limited to character-based modules, there is still a wide variety of shapes and sizes available. Line lengths of 8, 16, 20, 24, 32 and 40 characters are all standard, in 1, 2 and 4-line versions. Most LCD modules conform to a standard interface specification. A 14-pin access is provided having eight data lines, three control lines and three power lines.

Pin 1 and pin 2 are the power supply lines, V_{SS} and V_{DD} respectively. The V_{DD} pin should be connected to the positive supply and V_{SS} to ground. Pin 3 is a control pin, which is used to alter the contrast of the display. Pin 4 is the Register Select (RS) line, the first of the three command control inputs. When this line is low, data bytes transferred to the display are treated as commands, and data bytes read from the display indicate its status. By setting the RS line high, character data can be transferred to and from the module.

Pin 5 is the Read/Write (R/W) line. This line is pulled low in order to write commands or character data to the module, or pulled high to read character data or status information from its registers. Pin 6 is the Enable (E) line. This input is used to initiate the actual transfer of commands or character data between the module and the data lines. When writing to the display, data is transferred only on the high to low transition of this signal. However, when reading from the display, data will become available shortly after the low to high transition and remain available until the signal falls low again.

Pin 7 to pin 14 are the eight data bus lines (D0 to D7). Data can be transferred to and from the display, either as a single 8-bit byte or as two 4-bit "nibbles". In the latter case, only the upper four data lines (D4 to D7) are used. This 4-bit mode is beneficial when using a microcontroller, as fewer input/output lines are required. The initial conditions of the LCD after power-on are marked with an asterisk. Most of the characters conform to the ASCII standard, although the Japanese and Greek characters are obvious exceptions [1]. The pin layout and photograph of LCD module are Figure 4 and Figure 5. Pin-out functions of an LCD module is also shown in Table 1.

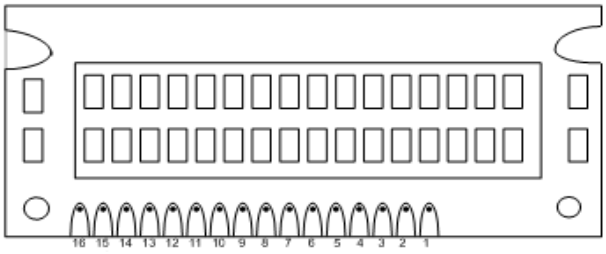

Figure 4. Pin layout of LCD module

Figure 5. Photograph of LCD module

Table 1. Pin-out functions of an LCD

Pin No.	Name	Function
1	V_{ss}	Ground
2	V_{dd}	+ve supply
3	V_{ee}	Contrast
4	RS	Register Select
5	R/W	Read / Write
6	E	Enable
7	D0	Data bit 0
8	D1	Data bit 1
9	D2	Data bit 2
10	D3	Data bit 3
11	D4	Data bit 4
12	D5	Data bit 5
13	D6	Data bit 6
14	D7	Data bit 7
15	A	LED anode
16	K	LED cathode

3. CIRCUIT CONSTRUCTION OF THE WHOLE SYSTEM

The whole system consists of water level sensor circuit, main control and processing circuit, display

circuit, water pump driver circuit and regulated power supply circuit.

3.1. Water Level Sensor Circuit

The water level sensor circuit is constructed by using three copper rods, BC547 transistors and other electronic devices. In this circuit, three copper rods are used as the electrodes to sense the water level of overhead tank. One of the three electrodes is directly applied +5 V and filtered with 10 µF capacitor to reduce other unwanted electronic noise. Each of remaining electrodes is connected to the base of BC547 transistor via 180 kΩ resistor. The emitter of the transistor is grounded and the collector is applied +5 V via 1 kΩ resistor. The collector of the upper transistor is connected to the RD0 and the collector of the lower transistor is connected to the RD1 of PIC18F452 microcontroller. When the water level of the overhead tank is less than predefined value, the output of water level sensor (RD0) is in the HIGH state. When the water level is full, the output of the sensor (RD0) is in the LOW state. Similarly, the output of the sensor (RD1) operates as described above.

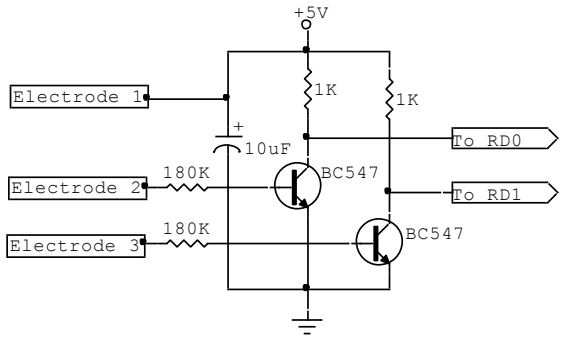

Figure 6. Schematic diagram of water level sensor circuit

Figure 7. Photograph of water level sensor circuit

3.2. Main Control and Processing Circuit

This circuit is the heart of the whole system and responsible for signal acquisition, LCD control and decision making for whether the water pump must be opened or closed. The main processing device is PIC18F452 microcontroller. RD0 and RD1 of PIC microcontroller is connected to the outputs of water level sensor. In this circuit, RD0 and RD1 are used as digital inputs and therefore bit 0 and bit1 of TRISD are required to be set. In this circuit, a 4 MHz crystal is used as the oscillator circuit of PIC18F452 microcontroller. RD2 and RD3 are used for controlling LCD display. All of PORTB are used to send the data of LCD characters. RA0 is used to control water pump driver circuit. In this circuit, RA0 is used as digital output and therefore bit0 of TRISA is required to be cleared.

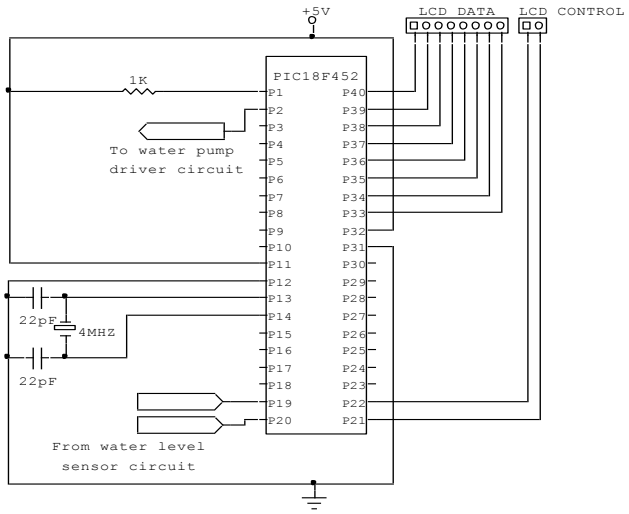

Figure 8. Schematic diagram of main control and processing circuit

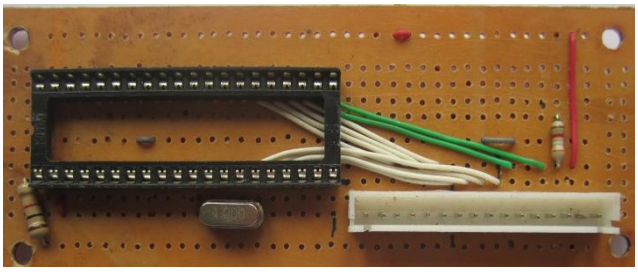

Figure 9. Photograph of main control and processing circuit

3.3. Display Circuit

In this circuit, 2- line 16- character liquid crystal display is used to show the conditions of pump and water level. The data from the microcontroller is sent to LCD by using 8-bit mode. Pin1 and Pin5 of LCD are connected to ground. Pin2 is applied by +5 V and Pin3 is connected to the ground via 3 kΩ resistor. Register Select and Enable pins of LCD are controlled by RD2 and RD3 of microcontroller respectively. All data lines (D0 to D7) of LCD are connected to PORTB of PIC18F452.

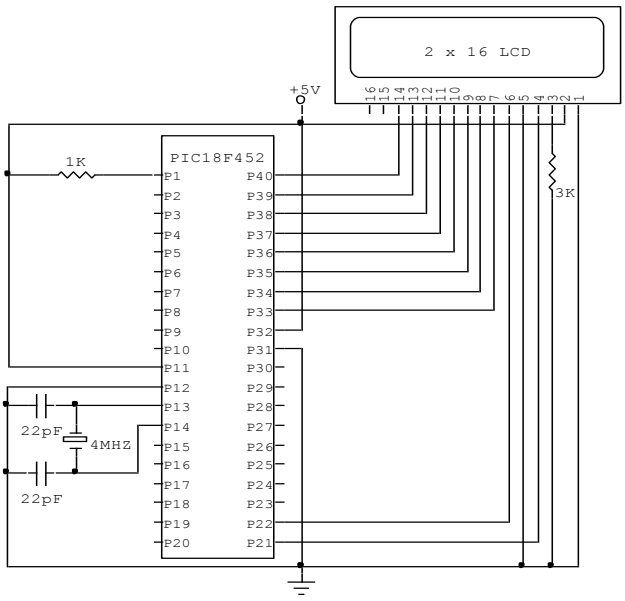

Figure 10. Schematic diagram of display circuit

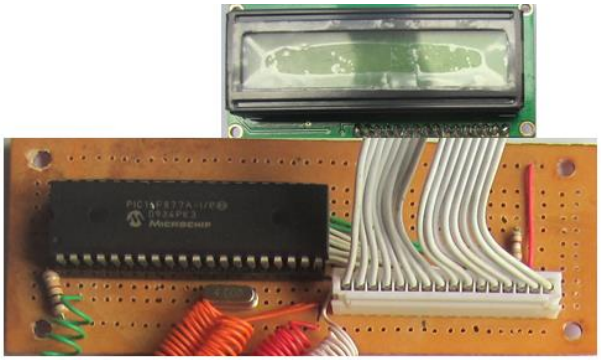

Figure 11. Photograph of display circuit

3.4. Water Pump Driver Circuit

The water pump driver circuit is constructed by using H1061 power transistor, relay, and protection diode. In this circuit, RA0 of PIC18F452 microcontroller is connected to the base of H1061 transistor by inserting 10 kΩ resistor. The emitter is directly connected to the ground. The collector is connected to one of power supply pins of relay. Another supply pin of relay is applied +12 V and a protection diode is inserted between the two supply pins of relay in the reverse direction. The output of relay is directly connected to one pin of water pump power input. Another terminal of power input of water pump is connected to the live wire of AC 220 V main line by inserting a fuse.

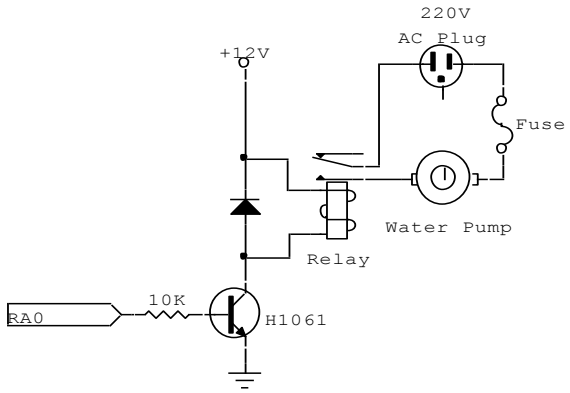

Figure 12. Schematic diagram of water pump driver circuit

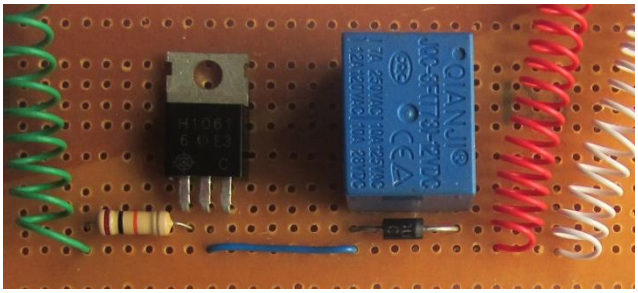

Figure 13. Photograph of water pump driver circuit

3.5. Regulated Power Supply Circuit

In this research, +5 V and +12 V regulated power supply circuits are constructed by using step-down transformer, filter capacitors, and 7805 and 7812 regulator ICs. Firstly, the AC power about 220 V from the main line is step-down to 15 V by using step-down transformer. The secondary output of transformer is rectified by full wave bridge rectifier diodes, then smoothed by filter capacitors of capacitances 1000 µF. The positive output of the bridge rectifier is connected to the inputs of the 7812 IC and 7805 IC. Pin 2 of each IC is connected to the ground. The output of 7812 IC is filtered with 0.1 µF capacitor for stabilized +12 V output voltage. The output of 7805 IC produces +5 V. The regulated +5 V line is also filtered by using 0.1 µF capacitor to filter the fluctuations. In this way, +12 V and +5 V regulated power supply are obtained. The schematic diagram of the regulated power supply circuit is shown in Figure 14. The photograph of regulated power supply circuit is also shown in Figure 15.

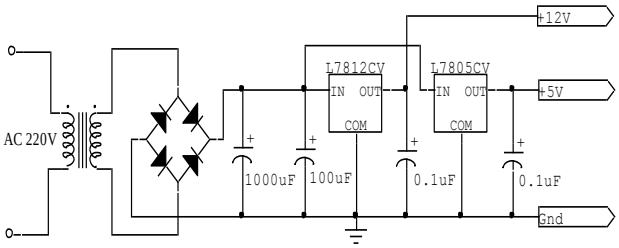

Figure 14. Schematic diagram of regulated power supply circuit

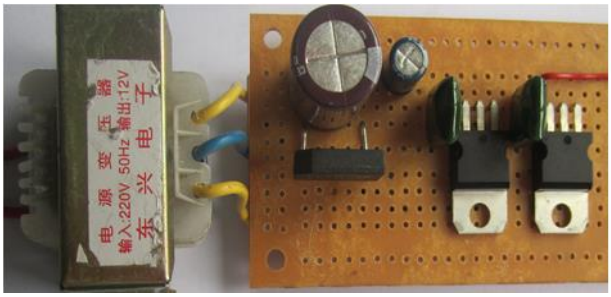

Figure 15. Photograph of regulated power supply circuit

3.6. Complete Circuit of the Whole System

The complete circuit of the whole system is obtained by combining water level sensor circuit, main control and processing circuit, LCD display circuit, water pump driver circuit and regulated power supply circuit. In this project, PORTB of the PIC18F452 microcontroller is used to send the digital data for LCD character. PORTD of the microcontroller is used for controlling the LCD. PORTA is used for controlling water pump. A 4 MHz crystal is used for oscillator circuit of the PIC microcontroller and connected at the OSC1 and OSC2 pins of the microcontroller. Therefore, the time required for executing one instruction is 1 µs.

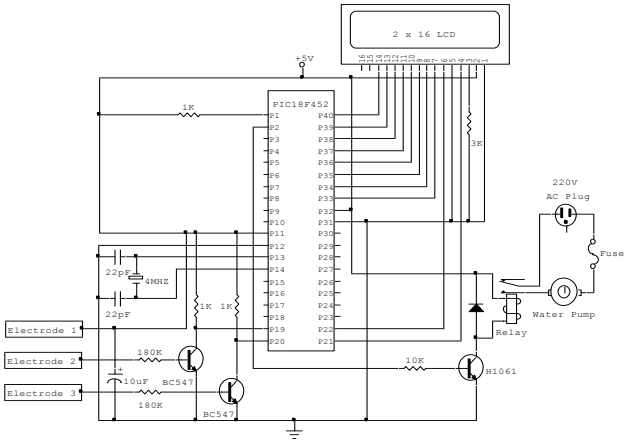

Figure 16. Schematic diagram of complete circuit

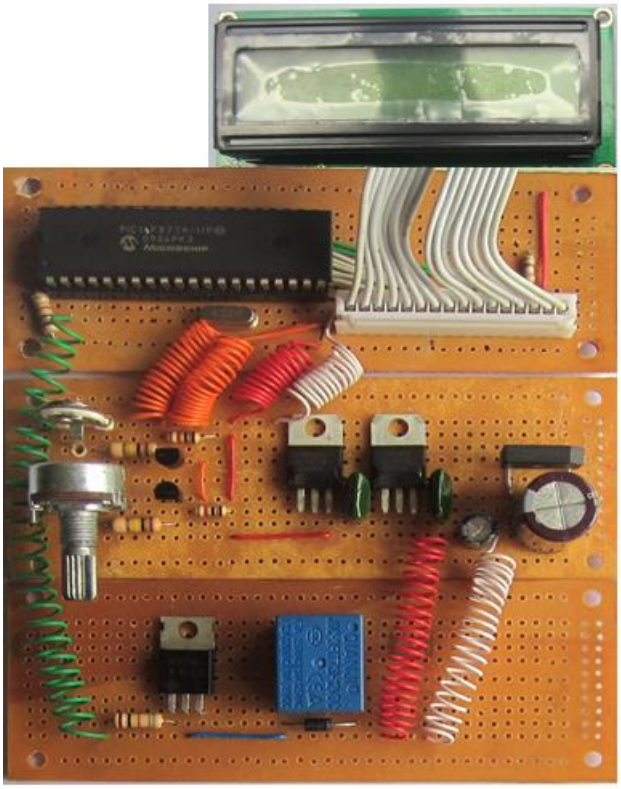

Figure 17. Photograph of complete circuit

3.7. Programming and Downloading

Firstly, Assembly program source code (Water Level Control.asm) was written in text editor. Then, it was compiled into .hex file by using MPLAB software (version 8.50). In this research, PICKIT 2 programmer board is used to write hexa code to PIC18F452 microcontroller. The resultant .hex file from the MPLAB software is imported from the USB port of the personal computer to the PICKIT 2 programmer software.

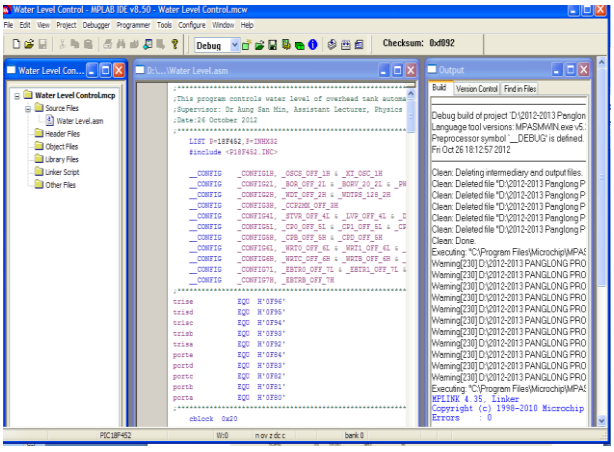

Figure 18. Photograph of MPLAB software screen (version 8.50)

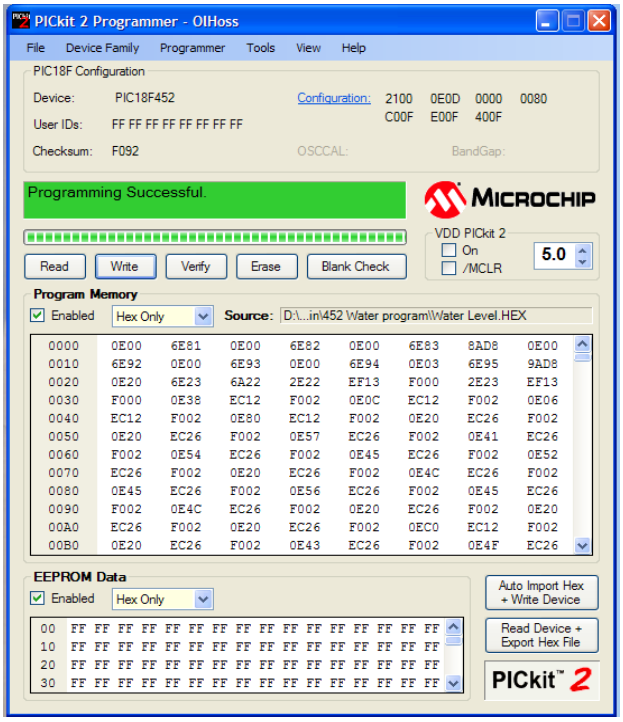

Figure 19. Photograph of writing hexa code to PIC18F452

4. DISCUSSION

To use our developed automatic water level control system, the water level sensor should be placed at the corner of overhead water tank. When the power switch is opened, PIC18F452 microcontroller monitors the output of water level sensor circuit and processes for making decision to control the water pump. The data of the water level and switching conditions of the pump can be seen on the 2-line 16-character LCD. If the water in the overhead tank is full or less than the predefined limit, the pump will automatically function to pump out the water. So the users do not have to worry about the water level in the overhead tank.

4.1. Operation of the Whole System

When the power switch is opened, ***"WATER LEVEL CONTROLLER"*** will be displayed firstly. After five seconds ***"Dr Aung San Min, Phys: Department"*** will be displayed. Then, the system waits the condition of the water level and the display will show ***"System senses water level"***. The system also performs decision making for driving water pump. When the water level is less than predefined level then the constructed system will switch on the water pump and LCD will display ***"Water pump:ON, Water level-LOW"***. The system will switch off the water pump and LCD will display ***"Water pump:CLOSE, Water level-FULL"*** when the water level of the overhead tank is full.

5. CONCLUSION

The automatic water level control system has been developed by using available electronic devices in the market. The advantages of our constructed system are:

(i) reliable sensitive
(ii) works according to the water level of the overhead tank
(iii) predefined water level can be changed
(iv) elimination of manpower
(v) can handle the load up to 1750 W
(vi) can see the conditions of water level and pump.

The constructed system can be used in every home, school and university. Therefore our constructed water level control system is very useful for automatic watering and reducing man power. By using this project framework, other researchers can develop more improved project such as automatic water level control system for both underground tank and overhead tank. We hope that the system is also useful to the university students for studying how to construct the water level sensor, how to interface between microcontroller and LCD, and how to control the water pump via relay.

ACKNOWLEDGEMENT

We would like to express our gratitude to Rector Dr Aung Win, University of Myitkyina, Pro Rector Dr Aye Aye Ko, University of Myitkyina and, Pro Rector Dr Soe Myint Aye, University of Myitkyina, for their permission to perform this research.

We are very deeply grateful to Professor Dr Mya Mya, Head of Department of Physics, University of Myitkyina for her valuable guidance, helpful advice and technical suggestions to complete this research.

REFERENCES

[1] J. Ilett, (1997), "How to Use Intelligent L.C.D.s", Wimbrone Publishing Ltd, New York.
[2] M. Bates, (2006), "Interfacing PIC Microcontrollers Embedded Design by Interactive Simulation", United State of America.
[3] Microchip Technology Inc., (2006), "PIC18FXX2 Data Sheet, 28/40-pin High Performance, Enhanced FLASH Microcontrollers with 10-Bit A/D", United State of America.
[4] V. Kumar, A. Garlapati, J. Xu, "Rural Automated Water Tank Filling System".

Numerical Solution to the Laplace Equation for a Magnetostatic Potential

San San Htwe
sansanhtwe7111967@gmail.com

ABSTRACT: *The numerical solution of equations reduces to performing arithmetic operations on the coefficients of equations and on the values of their constituent function: the process makes it possible to find solutions of equations to any predefined accuracy. Many problems of mathematics and its applications reduce to the numerical solution of equations. So a computer program in C code is generated to obtain a numerical solution for the magneto static potential which satisfies Laplace's equation. The partial differential equation is replaced with a set of finite difference equations. These can then be solved by an iteration method.*

Keywords: Laplace's equation; the partial differential equation; the finite difference equation and C programming

1. INTRODUCTION

Partial differential equations are important in all branches of physics, and often they can only be solved numerically. Owing to the diversity of boundary conditions and other factors that may apply, it is impracticable to produce special computer programs capable of solving more than one specific type of problem. For this reason it is valuable to have some practical experience of the difficulties involved in applying one of the common numerical techniques in a relatively simple situation. This work presents a method of dealing with partial differentia equation by numerical methods. It is illustrated by solving Laplace's equation for a scalar magnetostatic potential with the aid of C programming on a PC.

2. THEORY

The problem considered here is the calculation of the magnetic field in the vicinity of a uniformly magnetized rectangular permanent magnet. The magnet is assumed to be infinite in one direction. So that the problem is reduce to two dimensions. The basic magnetostatic equations are given in section 2.1.and 2.2. In there, it is show that the fields are conveniently written in terms of a scalar magnetostatic potential which satisfies Laplace's equation, and which is completely determined by the boundary conditions. Sometime it is possible to obtain an analytical solution for the potential, but usually Laplace's equation must be solved numerically. One method of doing so, and that adopted here, is to replace the partial differential equation with a set of (linear) finite difference equations. These can then be solved by standard methods, either directly by elimination or by iteration. The latter method is employed below.

2.1.The Magnetostatic potential

The magnetic induction vector B produced by a steady electric current I satisfies Ampere's law,

$$\oint_c \vec{B}.d\vec{l} = \mu_o I \qquad (2.1)$$

Where c is a contour enclosing the conductor carrying I. Employing Stokes integral theorem, $\vec{\nabla} \times \vec{B} = \mu_o \vec{J}$ (2.2)

Where $\vec{J}$ is the current density (Am^{-2}). The other basic property of $\vec{B}$ is that it forms closed loops, i.e., it satisfies

$$\vec{\nabla} \times \vec{B} = 0 \qquad (2.3)$$

A small current loop produces a field $\vec{B}$ which resembles the electric field near an electric dipole, and consequently a magnetic dipole moment can be identified with the loop. A magnetic material may be through of as containing a large number of elementary loops, giving rise to a dipole moment per unit volume, M, known as the magnetization. The magnetization contributes to $\vec{B}$ that Eq (2.2) is replaced by

$$\vec{\nabla} \times \vec{B} = \mu_o \vec{J} + \mu_o \vec{\nabla} \times \vec{M} \qquad (2.4)$$

Where $\vec{J}$ is the real current density.

A magnetic field $\vec{H}$ by

$$\vec{B} = \mu_o (\vec{H} + \vec{M}) \qquad (2.5)$$

Substituting Eq(2.5) into Eq(2.4), $\vec{H}$ satisfies

$$\vec{\nabla} \times \mu_o (\vec{H} + \vec{M}) = \mu_o \vec{J} + \mu_o \vec{\nabla} \times \vec{M}$$

$$\mu_o \vec{\nabla} \times \vec{H} + \mu_o \vec{\nabla} \times \vec{M} = \mu_o \vec{J} + \mu_o \vec{\nabla} \times \vec{M}$$

$$\vec{\nabla} \times \vec{H} = \vec{J} \qquad (2.6)$$

There are usually no true currents in a permanent magnet so that reduce to

$$\vec{\nabla} \times \vec{H} = 0 \qquad (2.7)$$

And therefore it is possible to define a scalar magnetic potential φ by

$$\vec{H} = -\nabla \varphi \qquad (2.8)$$

From Eqs(2.3) and (2.5)

$$\nabla . \vec{B} = \mu_o \nabla .(\vec{H} + \vec{M})$$

$$\nabla . \vec{B} = \mu_o (\nabla . \vec{H} + \nabla . \vec{M})$$

$$0 = \mu_o (\nabla . \vec{H} + \nabla . \vec{M}) \qquad (\because \nabla . \vec{B} = 0)$$

$$\nabla . \vec{H} = -\nabla . \vec{M} \qquad (2.9)$$

or in term of φ,

$$\nabla .(-\nabla \varphi) = -\nabla . \vec{M}$$

$$\nabla^2 \varphi = \nabla . \vec{M} \qquad (2.10)$$

This is Poission's equation for the potential and by analogy with electrostatics, the term $\nabla . \vec{M}$ plays the role of a volume magnetic charged density, and is frequently referred to as the pole density.

2.2. Boundary Conditions on Interfaces

The boundary conditions on the magnetostatic potential at the interface between two media in which true current are absent can be derived from Eqs(2.7) and (2.3).

Integration of Eq(2.7) yields

$$\oint_c \vec{H} . d\vec{l} = 0 \qquad (2.11)$$

and evaluating the line integral around a rectangular countour intersecting the boundary between two region, in which the magnetic fields are $\vec{H}_1$ and $\vec{H}_2$ as shown in fig2.1(a),

$$\vec{H}_1 . d\vec{l} - \vec{H}_2 . d\vec{l} + 0(dh) = 0 \qquad (2.12)$$

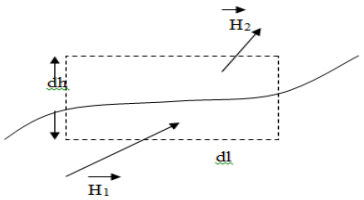

(a)

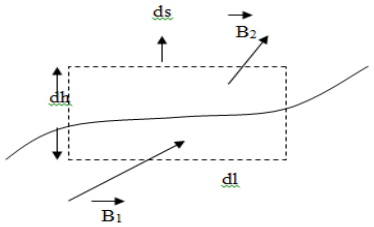

(b)

Figure 2.1 Fields near the boundary between two media illustrating the geometry and notation employed in the text to discuss the boundary conditions (a) $\vec{H}$, and (b) $\vec{B}$.

(Assuming that dh can be made arbitrarily small.) Eq (2.12) implies that the tangential components of $\vec{H}$ are expressed as

$$\hat{n} \times (\vec{H}1 - \vec{H}2) = 0 \qquad (2.13)$$

$$\hat{n} \times \vec{H}1 = \hat{n} \times \vec{H}_2$$

$$\hat{n} \times (\vec{H}_{1t} + \vec{H}_{1n}) = \hat{n} \times (\vec{H}2t + \vec{H}_{2n})$$

$$|\hat{n}||\vec{H}_{1t}|\sin 90^\circ + |\hat{n}||\vec{H}_{1n}|\sin 0^\circ$$

$$= |\hat{n}||\vec{H}_{2t}|\sin 90^\circ + |\hat{n}||\vec{H}_{2n}|\sin 0^\circ$$

Thus $|\vec{H}_{1t}| = |\vec{H}_{2t}|$

where $\hat{n}$ is a unit vector normal to the surface. In terms of the scalar potentials,

$$\hat{n} \times (\nabla \varphi_1 - \nabla \varphi_2) = 0 \qquad (2.14)$$

and, integrating along the boundary yields, in many circumstances.

$$\varphi_1 = \varphi_2 \qquad (2.15)$$

Thus the potential is continuous across the boundary.

The second boundary condition is derived from $\nabla . \vec{B} = 0$ by applying Gauss's theorem to yield

$$\int_s \vec{B} . d\vec{s} = 0 \qquad (2.16)$$

For a small cylindrical volume intersecting the boundary, indicated by the dotted lines in Fig 2.1 (b), the surface integral yields

$$\vec{B}_2 . \hat{n}\, ds - \vec{B}_1 . \hat{n}\, ds + 0(dh) = 0 \qquad (2.17)$$

$$\vec{B}_2 . \hat{n}\, ds = \vec{B}1 . \hat{n}\, ds$$

$$|\vec{B}2t||\hat{n}\, ds|\cos 90^\circ + |\vec{B}_{2n}||\hat{n}\, ds|\cos 0^\circ$$

$$= |\vec{B}1t||\hat{n}\, ds|\cos 90^\circ + |\vec{B}1n||\hat{n}\, ds|\cos 0^\circ$$

Thus $|\vec{B}_{2n}| = |\vec{B}_{1n}|$

Indicating that the normal component of $\vec{B}$ is continuous. If the two regions have magnetizations $\vec{M}_1$ and $\vec{M}_2$, substitution of

$$\vec{B} = \mu_0(-\nabla\varphi + \vec{M})$$

Yields

$$(-\nabla\varphi_1 + \vec{M}_1).\hat{n} = (-\nabla\varphi_2 + \vec{M}_2).\hat{n} \qquad (2.18)$$

This is the required boundary condition on the gradient of φ. It can be seen from Eq(2.18) that, by analogy with electrostatics, the term $\hat{M}.\hat{n}$ pays the role of a surface magnetic charge (pole) density. The normal component of the magnetic field $\vec{H}$ has a discontinuity equal to the difference of the components of the magnetization and is known as the demagnetizations field.

2.3. The Model Problem

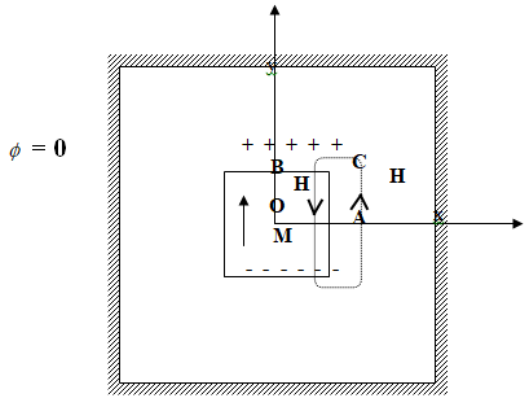

Figure.2.2. Schematic diagram showing the positions of the magnet and the outer boundary, and indicating the directions of the magnetic field. Because of symmetry it is necessary to consider only the region in the positive quadrant.

The computational problem is to determine the magnetic field in the regions inside and outside a two - dimensional rectangular magnet by solving Posson's Eq (2.10) for the scalar potential. It is assumed that the magnet is uniformly magnetized, so that M(r) is a constant vector in which case Eq(2.10) reduces to Laplace's equation,

$$\frac{\partial^2\varphi}{\partial x^2} + \frac{\partial^2\varphi}{\partial y^2} = 0 \qquad (2.19)$$

Everywhere except on the boundary of the magnet. On the latter, the potential is continuous, but the components of its gradient normal to the surface change by the normal component of the magnetization, in accordance with Eq (2.18). At large distances from the magnet the potential will resemble that of a small magnetic dipole of moment m = M V where V is the volume of the magnet,

$$\text{i.e., } \varphi(r) = -\frac{1}{4\pi}\,m.\text{grad}\left(\frac{1}{r}\right) \qquad (2.20)$$

In principal it is possible to match the numerical solutions of (2.19) to this expression of a distant rectangular boundary, but to avoid this added complication it will be assumed here that φ is essentially zero on that boundary, as shown in fig 2. The effect of this approximation on the final solutions can be investigated by increasing the size of the large rectangle.

2.4. The Finite Difference Equations

Laplace's equation (2.19) can be solved by approximating the derivatives of φ by finite difference formulae. The second derivative of a function of a single variable f(x) tabulated at equal intervals of x can be approximated, using Taylor's expansion, by

$$\frac{d^2f}{dx^2} \approx \frac{1}{h^2}\{f(x+h) + f(x-h) - 2f(x) \qquad (2.21)$$

where h is the interval. For a function of two variable, f(x,y) can be specified a points on a square mesh labeled by integers i and j, so that x = i h; y = j h (i, j = 1,2,3,…..).Eq (2.21) enables Laplace's equation to be replaced by a set of finite element equations:

$$\frac{1}{h^2}\{\varphi_{i,j+1} + \varphi_{i,j-1} + \varphi_{i+1,j} + \varphi_{i-1,j} - 4\varphi_{1,j}\} = 0 \qquad (2.22)$$

for each point (i,j). Near the boundaries of the region this equation must be modified in an appropriate way, described in detail below, to take into account the physical boundary conditions. The resulting set to equations, one equation for each mesh point, can be solved for the $\varphi_{i,j}$ either by direct matrix methods or by an iterative process. For large matrices the second method has the advantage that the zeros are preserved throughout, and consequently less computer storage is required. An iterative approach is employed here. The five values of φ in Eq(2.22) are said to form a star (fig 2.3). If four of the values are known approximately, Eq (2.22) can be employed to determine improved values for the fifth. In an iterative process initial value of φ, $\varphi^{(0)}_{i,j}$ say, must be assigned to each mesh point. Generally, it is not essential that these initial values are a close approximation to the final solution. On the boundaries the φ - values may be known exactly from the outset, but often the $\varphi^{(0)}_{i,j}$ - values inside the region can be chosen somewhat arbitrarily. Frequently they $\varphi^{(0)}_{i,j}$ are set equal to a constant value (o.5 in the program presented

here).The initial $\varphi_{i,j}^{(0)}$ can be improved by applying eq(2.22) to each mesh point in turn, giving quantities. $\varphi_{i,j}^{(1)}$ Explicitly,

$$\varphi_{i,j}^{1} = \frac{1}{4}\{\varphi_{i,j+1}^{0} + \varphi_{i,j-1}^{(0)} + \varphi_{i+1,j}^{(0)} + \varphi_{i-1}^{(0)}\} \qquad (2.23)$$

If the new $\varphi_{i,j}^{(1)}$ are substituted into Eq(2.22) the bracket on the left-hand side will not be exactly zero, but will have a residual value, R_{ij} say, which is some measure of the discrepancy between $\varphi_{i,j}^{(1)}$ and the true solution φ . Repeating the procedure, new values $\varphi_{i,j}^{2}$, can be computed from the $\varphi_{i,j}^{(1)}$ using a formula similar to Eq(2.23). This iterative is continued until the φ values do not alter, within a specified accuracy, between one scan of the mesh points and the next. Iterative formula likes Eq (2.23) employing only the old $\varphi^{(0)}$ values on the right-hand side are said to be Jacobi type. When performing the calculations with a computer it is more natural to use the newly calculated φ values in the right-hand side Eq(2.23) can be replaced by

$$\varphi_{i,j}^{(1)} = \frac{1}{4}\{\varphi_{i,j+1}^{(0)} + \varphi_{i,j-1}^{(1)} + \varphi_{i-1,j}^{(1)} + \varphi_{i+1,j}^{(0)}\} \qquad (2.24)$$

This expression gives rise to Gauss- Seidel scheme.It can be shown that this iterative process converges more rapidly than the simoler Jacobi method. More complicated iteration formulae than (2.24) have been devised which give even more rapid convergence than the Gauss-Seidel method. One such procedure, which changes the old field value by adding to it a small fraction of the old residual R_{ij} is known (amongst other names) as successive over-relaxation (SOR). For the nth iteration, assuming column by- column scanning of the mesh, the appropriate formula is

$$\varphi_{i,j}^{(n)} = \varphi_{i,j}^{(n-1)} + \frac{\alpha}{4}\{\varphi_{i+1,j}^{(n-1)} + \varphi_{i,j-1}^{(n)} + \varphi_{i,j+1}^{(n-1)} - 4\varphi_{i,j}^{(n-1)}\} \qquad (2.25)$$

Where α is a parameter which usually lies between 1 and 2 in practice. This method has been employed in the present work. Because of the symmetry of the problem it is necessary to consider only one –quarter of the total region, for example the first quadrant shown in

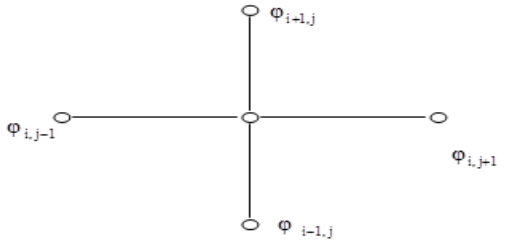

Figure 2.3 The star of function values required to approximate $\nabla^2\varphi$ mesh point (i,j) .The mesh is h assumed to be square and the mesh size is h. Fig 2.4. The iteration formulae Eq (2.23)-(2.25) cannot be employed for points on the surface of the magnet because Laplace's equation is not valid there. No can these formulae be used as they stand for points on the boundaries of the region, because some of the φ - values in the star formulae for the boundary points will be outside the region. The latter situation can be illustrated by considering the boundary OY, for which j = 1, giving for he residuals R_{i1}

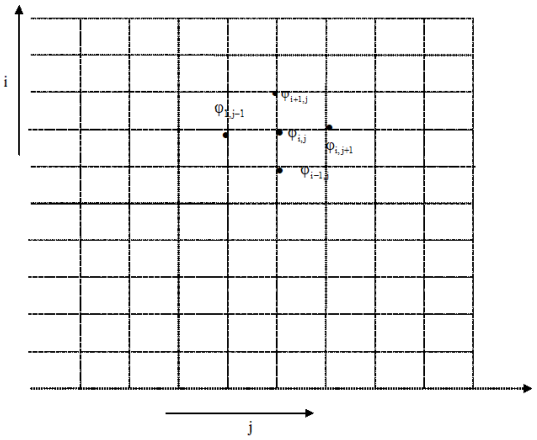

Figure 2.4 A typical mesh converging the region of interest. The area OACB represents the portion of the magnet in this quadrant.

$$R_{i1} = \varphi_{i,2} + \varphi_{i,0} + \varphi_{i+1,1} + \varphi_{i-1,1} - 4\varphi_{i,1} \qquad (2.26)$$

The values $\varphi_{i,0}$ lying outside the field region are sometimes called "fictitious" values, and are often labeled by an asterisk added as a superscript, e.g., $\varphi_{i,0}^{*}$. Because of the special conditions applying at the boundaries the fictitious values required to calculate the residuals can usually be expressed as functions of the $\varphi_{i,j}$ values inside the region.

2.4.1. The Outer Boundary

All $\varphi_{i,j} = 0$, and this boundary is excluded from the iterative process.

2.4.2. The symmetry Axis OY

The line OY lies along the Y-coordinate axis (fig 2.4). The field in the negative x region (Y > 0) is the mirror image of that in the first quadrant i.e., $\varphi(-x, y) = \varphi(x, y)$ Hence the factious field values $\varphi^*_{i,0}$ (see Fig 2.5) are given by

$$\varphi^*_{i,0} = \varphi_{i,2} \quad (2.27)$$ Employing this in the star formula for $R_{i,j}$ gives a SOR formula:

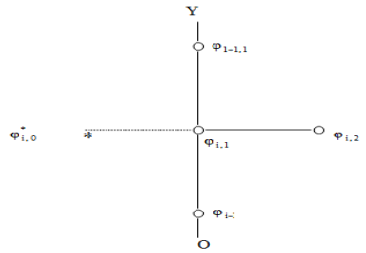

Figure2.5 Function values involved in treating typical point on the boundaries, symmetry line OY showing the position of the factious point $\varphi^*_{i,0}$

$$\varphi^{(n)}_{i,j} = \varphi^{(n-1)}_{i,j} + \frac{\alpha}{4}\{\varphi^{(n-1)}_{i,j+1} + \varphi^{(n)}_{i,j-1} + \varphi^{(n)}_{i-1,j} + \varphi^{(n-1)}_{i+1,j} - 4\varphi^{(n-1)}_{i,j}\}$$

$$\varphi^{(n)}_{i,j} = \varphi^{(n-1)}_{i,j} + \frac{\alpha}{4}\{\varphi^{(n-1)}_{i,2} + \varphi^{*(n')}_{i,0} + \varphi^{(n')}_{i-1,1} + \varphi^{(n-1)}_{i+1,j} - 4\varphi^{(n-1)}_{i,j}\}$$

$$\varphi^{(n)}_{i,j} = \varphi^{(n-1)}_{i,j} + \frac{\alpha}{4}\{2\varphi^{(n')}_{i,2} + \varphi^{(n')}_{i-1,1} + \varphi^{(n')}_{i+1,1} - 4\varphi^{(n-1)}_{i,j}\} \quad (2.28)$$

Where n' is n or (n-1) and indicates that the most the most recently calculated .φ Values are to be inserted. This formula applies for i > 1, and the origin O and point B are excluded as, they also lie on other symmetry axis.

2.4.3. The Symmetry Axis OX

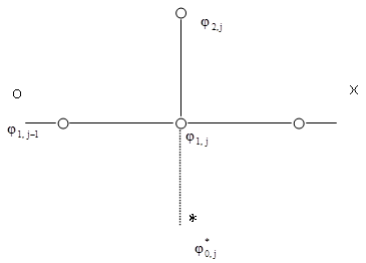

Figure 2.6 Function value involved in treating typical point on the boundaries: Symmetry line OX showing the position of the fictitious point $\varphi^*_{0,j}$;

Line OX lies along the x-axis. From the symmetry, the magnetic field $\vec{H}$ is everywhere parallel to OY, so that

$$H^y = -\frac{\partial\varphi}{\partial y} = H \quad (2.29)$$

$$H^x = -\frac{\partial\varphi}{\partial x} = H \quad (2.30)$$

The second equation means that all the φ -values on OX are equal. Furthermore, the continuity of $\vec{H}$ across OX requires that the gradient $\frac{\partial\varphi}{\partial y}$ should be continuous. Defining factious $\varphi^*_{0,j}$ as in Fig 2.6.

$$\frac{1}{h}\{\varphi_{2,j} - \varphi_{1,j}\} = \frac{1}{h}\{\varphi_{1,j} - \varphi^*_{0,j}\}$$

$$\varphi^*_{0,j} = 2\varphi_{1,j} - \varphi_{2,j} \quad (2.31)$$

Substitution into the star formula for the residual, SOR iteration formula becomes

$$\varphi^{(n)}_{1,j} = \varphi^{(n-1)}_{1,j} + \frac{\alpha}{4}\{\varphi^{(n')}_{1,j+1} + \varphi^{(n')}_{1,j-1} - 2\varphi^{(n-1)}_{1,j} \quad (2.3\ 2)$$

Where n' is n or (n- 1) depending on how the boundary mesh points are scanned. In fact this equation is redundant because they φ are all equal by Eq (2.30). Hence, since φ is zero on the outer boundary, it is necessary to set φ = 0 at all point on the line, including the origin O.

2.4.4. The Magnet Boundary AC

The condition on tangential $\vec{H}$ requires that φ is continuous on the boundary. Since the magnetization has component perpendicular to A C, the continuity of normal component of $\vec{B}$ implies that $\frac{\partial\varphi}{\partial x}$ is continuous.

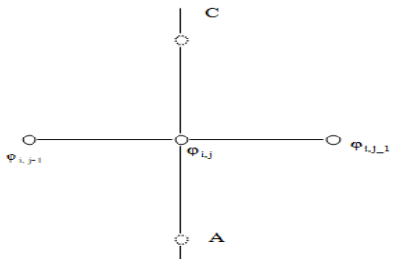

Figure. 2.7 Function values involved in treating typical points on the boundaries: Magnet boundary AC;

$$\frac{1}{h}\{\varphi_{i,j-1} - \varphi_{i,j}\} = \frac{1}{h}\{\varphi_{i,j} - \varphi_{i,j+1}\}$$

$$\varphi_{i,j} = \frac{1}{2}\{\varphi_{i,j+1} + \varphi_{i,j-1}\} \quad (2.33)$$

$$\varphi_{i,j}^{(n)} = \varphi_{i,j}^{(n-1)} + \frac{\alpha}{4}\{\varphi_{i,j+1}^{(n')} + \varphi_{i,j-1}^{(n')} - 2\varphi_{i,j}^{(n-1)}\} \quad (2.34)$$

2.4.5. The Magnet Boundary BC

Again φ is continuous but now from equation (2.18) the gradient in Y has a discontinuity equal to $\vec{|M|}$, i.e.,

$$\frac{\partial\varphi}{\partial y}|_{in} + \vec{M} = \frac{\partial\varphi}{\partial y}|_{out} \quad (2.35)$$

In terms of finite differences, this becomes (see fig 2.8)

$$-\frac{1}{h} = \{\varphi_{i+1,j} - \varphi_{i,j}\} = -\frac{1}{h}\{\varphi_{i,j} - \varphi_{i-1,j}\} + M$$

$$\varphi_{i,j} = \frac{1}{2}\{\varphi_{i+1,j} + \varphi_{i-1,j} + Mh\} \quad (2.36)$$

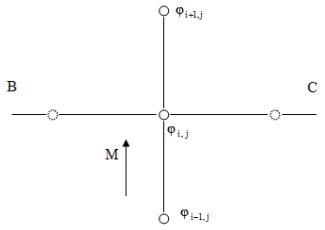

Figure.2.8 Function values involved in treating typical points on the boundaries: Magnet boundaries B C;

Therefore, excluding point C, but including point B,

$$\varphi_{i,j}^{(n)} = \varphi_{i,j}^{(n-1)} + \frac{\alpha}{2}\{\varphi_{i+1,j}^{(n')} + \varphi_{i-1,j}^{(n')} + Mh - 2\varphi_{i,j}^{(n-1)}\} \quad (2.37)$$

2.4.6. The Point C

This point is difficult to treat satisfactorily. Only a very approximate expression for φ will be used here, it being assumed that a simple average of the expressions for AC and BC, gave by (2.33) an (2.36), is appropriated. Hence, adding,

$$2\varphi_{i,j} = \frac{1}{2}\{\varphi_{i,j+1} + \varphi_{i,j-1}\} + \frac{1}{2}\{\varphi_{i+1,j} + \varphi_{i-1,j} + Mh\} \quad (2.38)$$

$$\varphi_{i,j} = \frac{1}{4}\{\varphi_{i,j+1} + \varphi_{i,j-1} + \varphi_{i+1,j} + \varphi_{i-1,j} + Mh\}$$

$$\varphi_{i,j}^{(n)} = \varphi_{i,j}^{(n-1)} + \frac{1}{4}\{\varphi_{i,j+1}^{(n')} + \varphi_{i,j-1}^{(n')} + \varphi_{i+1,j}^{(n')} + \varphi_{i-1,j}^{(n')} + Mh - 4\varphi_{i,j}^{(n-1)}\} \quad (2.39)$$

3. COMPUTATION

The iteration scheme is readily programmed for a computer, and a suitable C coding is given in this chapter. The flow diagram indicates a few practical dealings. The iteration loop for the $\varphi_{i,j}$ is included in the main routine.

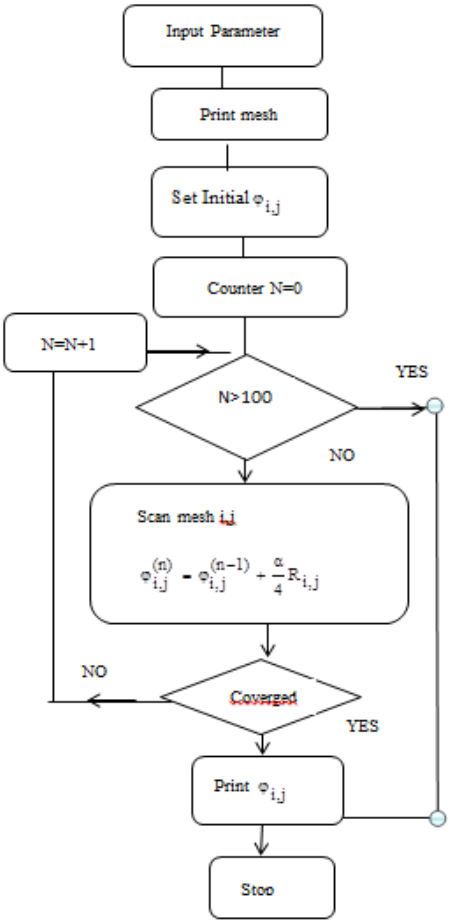

Figure 3.1. Flow diagrams for the computer program

It is necessary to keep a running count of the number of iterations performed, so that the process can be terminated if it shows no sign of converging to the required accuracy. There are several criteria for satisfactory convergence that can be employed, and in the appended program two different criteria are used in series. In the first, the residual with the largest magnitude is determined the n^{th} iteration and if this is less than some prescribed value, R_m say, the process is terminated. In some cases this criterion might be too strong, for it is conceivable that all but a few residuals are must smaller

that R_m, and the solution for the $\varphi_{i,j}$ might be acceptable at that stage. Therefore the second criterion used is that the root- mean- square average residual over the total number of scanned mesh points N is less than some value R_{ms}. i.e.,

$$\left[\frac{1}{N}\sum_{i,j} R_{i,j}^2\right]^{1/2} < R_{ms}$$

The iteration is terminated when one of these two criteria is first satisfied.

5. RESULTS AND DISCUSSION

The small list of input parameters is as follows:

I N, J N — Number of mesh point in the x and y directions, respectively.

IM, JM — Number of mesh points in the x and y directions occupied by the magnet.

H — mesh size (metres) (written as h in the text).

ALPHA — Convergence parameter ($1 < \alpha < 2$).

AMAG — The magnetization (A m^{-1}).

The physical quantities are measured in S I units. In this system the magnetic induction vector $\vec{B}$ has unit of testla (T), and both the magnetization $\vec{M}$ and the magnetic field $\vec{H}$ have units of ampere per meter (Am^{-1}). The values of $|\vec{M}|$ for typical permanent magnets are in the range 10^5 -10^6 A m^{-1}. Special dimensions are measured in metres. Since M and h enter the potential equations only through the product Mh, that the magnitude of the magnetic field $\vec{H}$ depends on the value of h in each case, through the gradient, and further, the magnitude of $\vec{H}$ scales linearly with M. A typical set of input parameters is as follows:

10 9 5 4 0.1 1.5 5.0

(IN) (JN) (IM) (JM) (H) (ALPHA) (AMAG)

The value of the input data is printed out immediately followed by a mesh pattern showing the position of the magnet. The next three numbers printed give information on the convergence of the iteration process. The parameters determining the conditions for termination of the iteration have been presented in the program. The largest residual REMAX, and the root mean square of the residuals, RESUM, is determined after each scan of the mesh. There are compared with two parameters, EPMAX and EPSUM respectively, which have both been given values of 10^{-4}. If REMAX is less than EPMAX or if RESUM is less than EPSUM it is assumed that the solution is sufficiently accurate for the present purpose. From the typical results given here it is seen that iteration has terminated when RESUM (= 0.95 x 10^{-4}) become smaller than 10^{-4}. The largest residual at that time was reasonably close to 10^{-4} (REMAX = 2.4 x 10^{-4}), giving confidence in the solution obtained. The number of iterations needed is also printed out, being 28 in example given. A control in the program stops the calculations if the integer NCOUN, counting the number of iterations exceeds 100. It is a simple matter to change the preset parameters by making minor modifications to the program coding. Finally, the arrays containing $\varphi_{i,j}$ are printed out. There are several functions that can be performed with the computer program given here, simply by changing the input parameters. For instance it is instructive to investigate how the convergence of the iterative process depends on the successive over relation parameter α (ALPHA). The following table shows the final iteration numbers for α ranging from 1.0 to 1.9 insteps of 0.1.

Table 1 The final iteration numbers for α ranging from 1.0 to 1.9 insteps of 0.1

relaxation Parameter α	1.0	1.1	1.2	1.3	1.4	1.5	1.6	1.7	1.8	1.9
Final iteration number	75	64	53	44	36	28	23	29	43	89

The relaxation parameter α indeed controls the rate of convergence and its optimal value is 1.6.

6. THE COMPUTER PROGRAM OUTPUT

```
Enter itmax:100

NO OF ITERATION=28   REMAX=0.000222   RESUM=0.000088

                MAGNETOSTATIC POTENTIAL

0.00 0.00 0.00 0.00 0.00 0.00 0.00 0.00 0.00
0.14 0.14 0.13 0.11 0.09 0.06 0.04 0.02 0.00
0.30 0.29 0.26 0.22 0.17 0.12 0.08 0.04 0.00
0.47 0.45 0.41 0.34 0.26 0.18 0.11 0.05 0.00
0.66 0.65 0.59 0.48 0.33 0.22 0.13 0.06 0.00
0.90 0.88 0.82 0.65 0.38 0.23 0.14 0.06 0.00
0.63 0.61 0.55 0.43 0.30 0.20 0.12 0.06 0.00
0.40 0.38 0.34 0.27 0.21 0.14 0.09 0.04 0.00
0.19 0.19 0.17 0.13 0.10 0.07 0.05 0.02 0.00
0.00 0.00 0.00 0.00 0.00 0.00 0.00 0.00 0.00
```


ACKNOWLEDGMENTS

I would like to express my sincere gratitude and special thanks to Rector, Dr. Ei Ei Hlaing University of Computer Studies (Taungoo) for her kind permission to carry out my research paper.

REFERENCES

[1] A D Boardman 1980 “Physics Programs”
(New York : Wiley)
[2] B Sprit 1988 “Reference Guide for Turbo C”
(New York: Borland)
[3] Electromagnetics “Second Edition”
(Kraus and Carver)
[4] F Scheid 1988 “Numerical Analysis”
(New York: Interscience)
[5]SCHAUM’S OUTLINE SERIES “THEORY and PROBLEM of NUMERICAL ANALYSIS”
(by FRANCIS SCHEID)

Influence of Reducing Agents on the Formation of Reduced Graphene Oxide

Lwin Ko Oo[1], Nan Thidar Chit Swe[2], Than Zaw Oo[3], Ye Chan[4]
1. *Assistance Lecturer, Universities' Research Centre, University of Yangon*
2. *Associate Professor, Department of Physics, Sagaing University of Education*
3. *Professor, Universities' Research Centre, University of Yangon*
4. *Professor and Head of Department, Universities' Research Centre, University of Yangon*
oolwinko9@gmail.com, nchitswe@gmail.com, thanzawoo06@gmail.com, yechann@gmail.com

ABSTRACT: *Graphene oxides (GO) were synthesized directly from graphite according to Hummers method. Reduced graphene oxides (rGOs) were prepared by chemical reduction of GO with different reductants such as ascorbic acid (AA) and sodium borohydride ($NaBH_4$) and comparatively characterized by UV-Visible spectroscopy (UV-Vis), Fourier Transform Infrared spectroscopy (FTIR), Scanning Electron Microscope (SEM), X-ray powder diffractometer (XRD) and Raman spectroscopy method. GO and rGO have different morphologies, UV-Vis absorption peaks, functionalized groups and structural properties. SEM images show the ultrathin, wrinkled, paper-like morphology of graphene sheets. UV-Vis and FTIR spectrum show disorder in the graphene sheets. In the XRD spectra, the characteristic peaks at 10.85°, 26.606° and 26.625° for GO, rGO (AA) and rGO ($NaBH_4$), respectively. The intensity ratio (I_D/I_G) of GO and rGO were 0.99, 0.85 (AA) and 1.25 ($NaBH_4$) in Raman result. RGO sheets with a high degree of reduction and low sheet stacking were obtained using ascorbic acid as the reducing agent.*

Keywords: graphene oxide, reduced graphene oxide, chemical reduction, ascorbic acid, sodium borohydride

1. INTRODUCTION

Graphene has the two dimensional structure, excellent electronic, mechanical, optical and thermal properties. For these purposes, the mass production of graphene materials at low costs is one of the essential requirements. Actually, graphene sheets have already existed in the nature and we need to exfoliate them. The exfoliation of graphite to graphene can be realized either physically or chemically. Among the various methods, chemical reduction of graphene oxide (GO) to reduce graphene oxide (rGO) is attractive because of its capability of producing single layer graphene. Especially, it has many applications in the electronics world since it is the thinnest, transparent, strongest, and conductive material [1].

Synthesis of graphene oxide (GO) is achieved by placing graphite in concentrated acid in the presence of an oxidizing agent. The oxidation method is the most widely used to produce graphene [2, 3]. In the most successful processes, the chemical reduction of GO was conducted using hydrazine or hydrazine hydrate. However, these are highly poisonous and explosive [4] that precautions must be taken when large quantities are used. Consequently, new approaches for effectively converting GO to reduced graphene oxide (rGO) under mild conditions needed to be explored [5]. Ascorbic acid (AA) and sodium borohydride ($NaBH_4$), having a mild reductive ability and nontoxic property, are naturally employed as a reducing agent in living things [6] and have also been used as a primary reductant when graphene oxide was converted to reduced graphene oxide [7, 8]. More significantly, in comparison with the conventional reductants used in GO reduction, such as hydrazine and hydrazine hydrate, AA itself and the oxidized products are environmentally friendly [9].

In this study, reduced graphene oxide has been produced with different parameters. The graphene oxide (GO) was converted to reduced graphene oxide (rGO) by chemical reduction using ascorbic acid and sodium borohydride as the reducing agent. Reduced graphene oxide derivatives were characterized by UV-visible spectroscopy, FTIR, Scanning Electron Microscopy (SEM), X-ray powder Diffraction (XRD) and Raman spectroscopy. In addition, the rGO presents the best characteristics to be used in the future development of hybridization electronic applications.

2. EXPERIMENTAL

2.1 Materials

Graphite powder is widely used to get graphene. It has been widely explored for the applications in electronics. Analytical grade Graphite powder (99%), Sodium nitrate ($NaNO_3$), Potassium permanganate ($KMnO_4$), Sulfuric acid (concentrated) (H_2SO_4, 98%), Hydrochloric acid (concentrated) (HCl), Hydrogen peroxide (H_2O_2, 30%), Ascorbic acid, and Ammonia (NH_3) are purchased from Chemical Reagent Co, Ltd. Distilled water (DW) was used throughout the whole experiments. All chemicals were used without any purification.

2.2 Synthesis of Graphene Oxide

Graphene oxides were synthesized directly from graphite according to Hummers method (a

chemical process that can be used to generate graphite oxide through the addition of potassium permanganate to a solution of graphite, sodium nitrate and sulfuric acid). In a typical procedure, 1.5 g of graphite powder was added to 35 ml of concentrated sulfuric acid and sodium nitrate while stirring in an ice bath. Potassium permanganate (4.5 g) was added slowly to keep the temperature of the suspension lower than 20 °C. And then, this reaction system was transferred to a 40 °C oil bath and stirred for about 45 min. Distilled water (DW) (75 ml) was added and stirred for 20 min at 95 °C. Furthermore, 250 ml of DW was added in this solution. Hydrogen peroxide (30 %) (7.5 ml) was added slowly in the solution, it was changed from dark brown to yellow color. The mixture was filtered and washed with 1:10 HCl aqueous solution to remove metal ions. This solution is Graphite Oxide aqueous dispersion. The solution was washed several times for neutralization to pH 6-7. And then, the solvent was put overnight. Its precipitate was made by filtration method and dispersed in water. The graphite oxide dispersion was centrifuged at 3000 rpm for 20 min (7 times) to remove the unexfoliated graphite. The graphite oxide aqueous dispersion was further sonicated for 1hr to exfoliate. The yellow color graphite oxide solution changed into yellowish brown color. The solution was absolutely graphene oxide (GO).

2.3 Preparation of Reduced Graphene Oxide

Ascorbic acid (1.2 g) and the obtained GO suspension (250 ml, 1 g/ml) were mixed, and then ammonia solution (100 µl) was added to adjust the pH 8-10. Then the suspension was heated to 95 °C under vigorous stirring and kept for 2 hr. The black reaction mixture was allowed to cool down to the room temperature and was filtered by whatman paper. The resulting was reduced graphene oxide (rGO). The filtrate was dried in vacuum at room temperature for 2-4 days.

For the second way of reduction, sodium borohydride ($NaBH_4$) was used as the reducing agent. Synthesized GO (200 mg) was added to 200 ml water and ultra-sonicated for 1 hr while maintain the pH 8-9. Sodium borohydride (1.6 g) was added to well disperse graphene oxide solution and stirred at 70-80 °C for 2 hr. Finally, the reduced graphene oxide (rGO) was obtained.

2.4 Characterization

Centrifuge machine (Kokusan H-200 series) and Sonicator (AS ONE) were used to separate the layers by layers from the solution. GO dispersions were freeze-dried and used for morphological and structural characterizations. Scanning Electron Microscopic (SEM) images of GO and rGO were measured using Scanning Electron Microscope (JEOL-JSM 5610LV) with the accelerating voltage of 15kV. UV-visible was recorded on a Perkin Elmer Lambda 35 spectrophotometer. Fourier transform infrared (FTIR) spectra were taken out by the use of a FTIR-8400 SHIMADZU. The structural characterizations of GO and rGO were confirmed by X-ray powder diffractometer (Rigaku-RINT 2000). The solution of GO and rGO in DW were used for FTIR analysis by filtration method on what man filter paper. Raman spectra of the sample were recorded with Raman spectrometer by using 532 nm excitation wavelengths.

3. RESULT AND DISCUSSION

3.1 UV-Vis Analysis

The synthesis of graphene oxide and reduced graphene oxide were confirmed by UV-visible spectroscopy. The UV-visible spectra of GO and rGO are shown in Figure 1. There are two characteristic absorption bands in the UV-visible spectra of GO. The absorption band centered at 229.5 nm (green line) is attributed to $\pi \rightarrow \pi^*$ transitions (electronic transitions) of aromatic C-C bonds. The shoulder centered at 302 nm is corresponding to $n \rightarrow \pi^*$ transition of C=O bonds (carbonyl groups). After reduced by ascorbic acid (AA), the peak of rGO is observed at 248.34 nm (yellow line). And then, another reductant with sodium borohydride ($NaBH_4$) of the rGO is found at 259.71 nm (red line). The absorption of reduced graphene oxide red shifts from 229 nm to 248 nm and 259 nm and the other absorption band at 302 nm is completely removed. The UV-visible spectra results demonstrate that the oxygen containing functional groups on the surface of GO are mostly removed and electronic conjugation within graphene sheets is restored via reduction reaction. The peak suppression in red line indicates that there are thick and crumple graphene sheets obtained in this sample. The similar results were obtained by Ciplak et al [10].

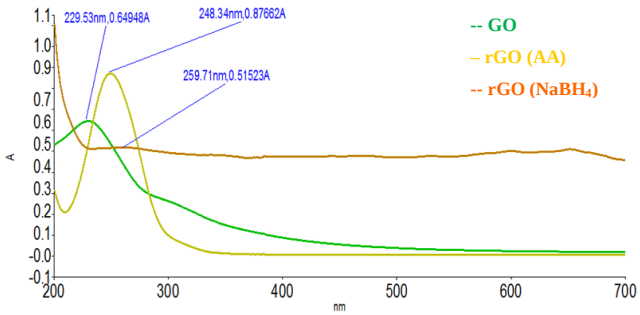

Figure 1. UV-Visible spectra of GO and rGO

3.2 FTIR Analysis

FTIR spectra of GO (Figure 2a) shows the characteristic functional groups of GO: C-O-C (round about 1000 cm^{-1}), C-O (1207 cm^{-1}), carboxyl C=O stretching band at 1730 cm^{-1}, O-H deformation band at 1423 cm^{-1}, and C=C (round about 1600 cm^{-1}) bonds. The O-H stretching vibrations in the region of 3600-3000 cm^{-1} are attributed to the hydroxyl and carboxyl groups of GO and residual water between GO sheets. As expected,

due to the reduction reaction by AA (Figure 2b) and $NaBH_4$ (Figure 2c), these characteristic bands of GO are relatively weaker (lower transmittance after the reduction) or completely removed in the FTIR spectra of rGO. The majority of carbonyl and epoxy groups can be changed into hydroxyl groups in the GO by chemical reduction (AA, $NaBH_4$). This result indicates that rGO was successfully obtained after reduction reaction.

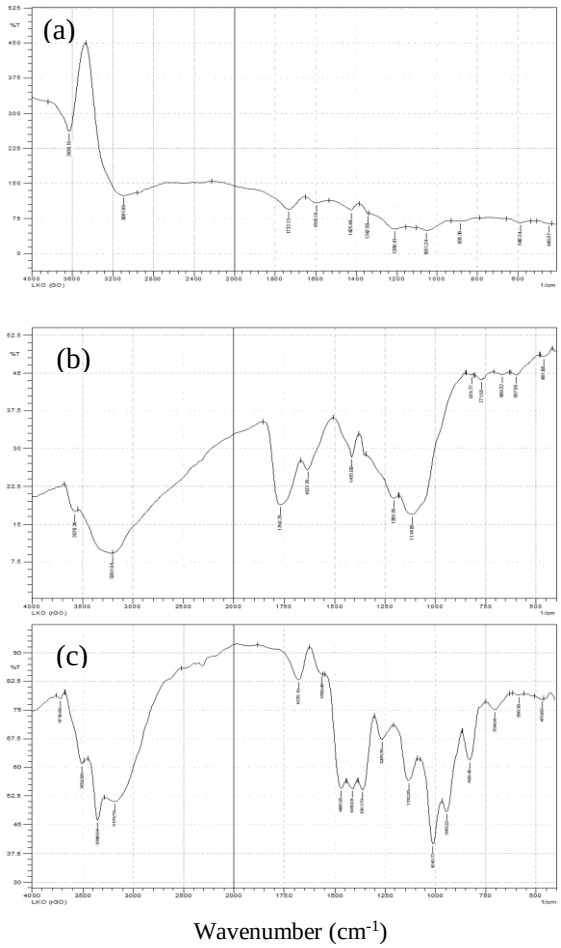

Figure 2. FTIR spectra of (a) graphene oxide (GO) (b) reduced graphene oxide (rGO) with ascorbic acid & NH_3 and (c) reduced graphene oxide with $NaBH_4$

3.3 SEM Analysis

To confirm the results of microscopic image, the detailed surface morphology of graphene oxide and reduced graphene oxide (AA, $NaBH_4$) were carried out by using Scanning Electron microscope (SEM). Figure 3(a) reveals the existence of crumple structure for graphene oxide. This is due to the exfoliation of graphite to become oxide and results in deformation upon the exfoliation and restacking. Figure 3(b) and (c) show the images of reduced graphene oxide (rGO) by using different reducing agent such as ascorbic acid and $NaBH_4$. In Figure 3(b) the thin sheets of folded and wrinkled structure has been observed while as in Figure 3(c) the large crumple structure has been observed in SEM image which agrees with UV measurements.

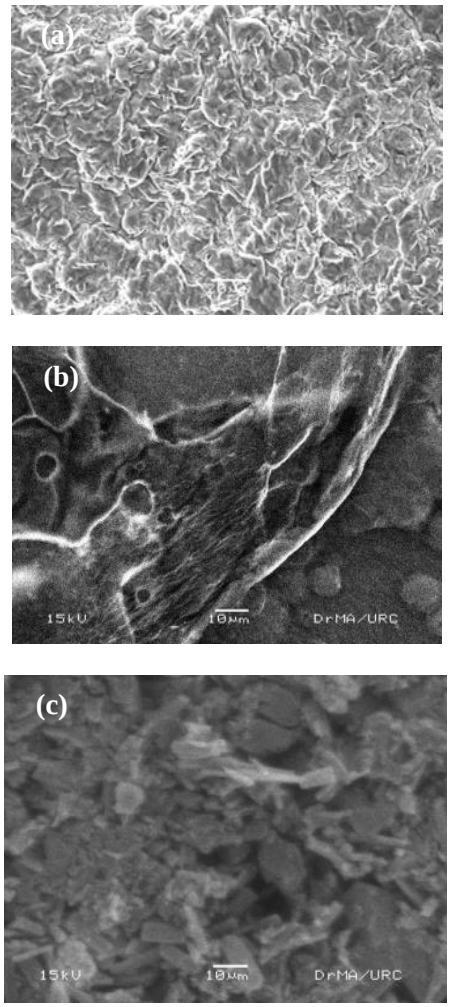

Figure 3. SEM images of (a) GO sheet (b) rGO sheets by using ascorbic acid as a reducing agent (c) rGO sheets by using sodium borohydride as a reducing agent

3.4 XRD Analysis

In addition, X-ray diffraction can also be used to characterize the crystal structure of GO and rGO using different reducing agents. The XRD spectrum of resulting powder and sheets of GO and rGO samples were shown in Figure 4 (a-c). A sharp peak at $2\theta \sim 10.85°$, corresponds to the reflection from the (111) plane, was observed in XRD spectra of GO. This pattern reveals that the phase precipitated out in the sample is hexagonal structure. The inter planner spacing d (002) between individual graphene layers (3.35 Å) can be used as an indicator of the degree of graphitization. Reduced graphene oxide has a peak around $2\theta \sim 26.606°$ for AA (Figure 4b) and $2\theta \sim 26.625°$ for $NaBH_4$ (Figure 4c). The change in peak positions and FWHM of the peaks could be due to the exfoliation of GO sheets after removal of the intercalated carboxylic groups. The

comparison of XRD results indicate that the graphene oxide was fully reduced into rGO by using reducing agents.

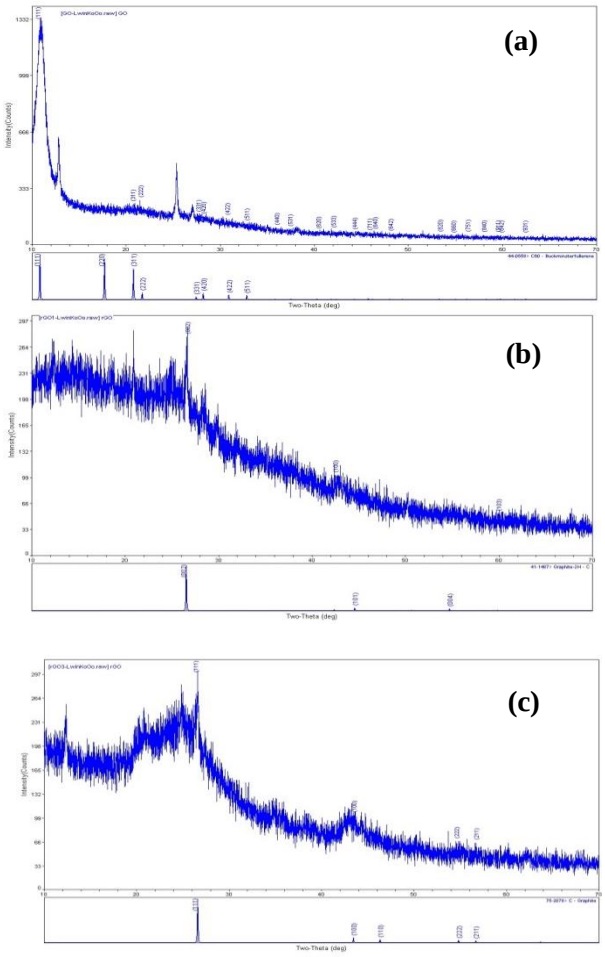

Figure 4. XRD spectra of (a) graphene oxide (b) reduced graphene oxide with ascorbic acid & NH_3 and (c) rGO with $NaBH_4$

3.5 Raman Analysis

Raman spectra are a powerful tool to characterize carbonaceous materials. Raman spectra of synthesized GO and rGO are presented in Fig 5. In the Raman spectra of GO, the band at 1585 cm^{-1} is called G band, this band arise from the first order scattering of the E2g mode. The band at 1347 cm^{-1} is the D band that corresponded to decrease of the size of in plane sp^2 domains. GO and rGO have both D and G bands. In the Raman spectrum of graphene and other sp^2 carbon samples containing defects, several additional symmetry-breaking features are found. After reduction reaction, D/G intensity ratio (I_D/I_G) of rGO increases from 0.85 to 1.25. This increase is due to formation of domains that are numerous in number and smaller in size with respect to ones present in GO.

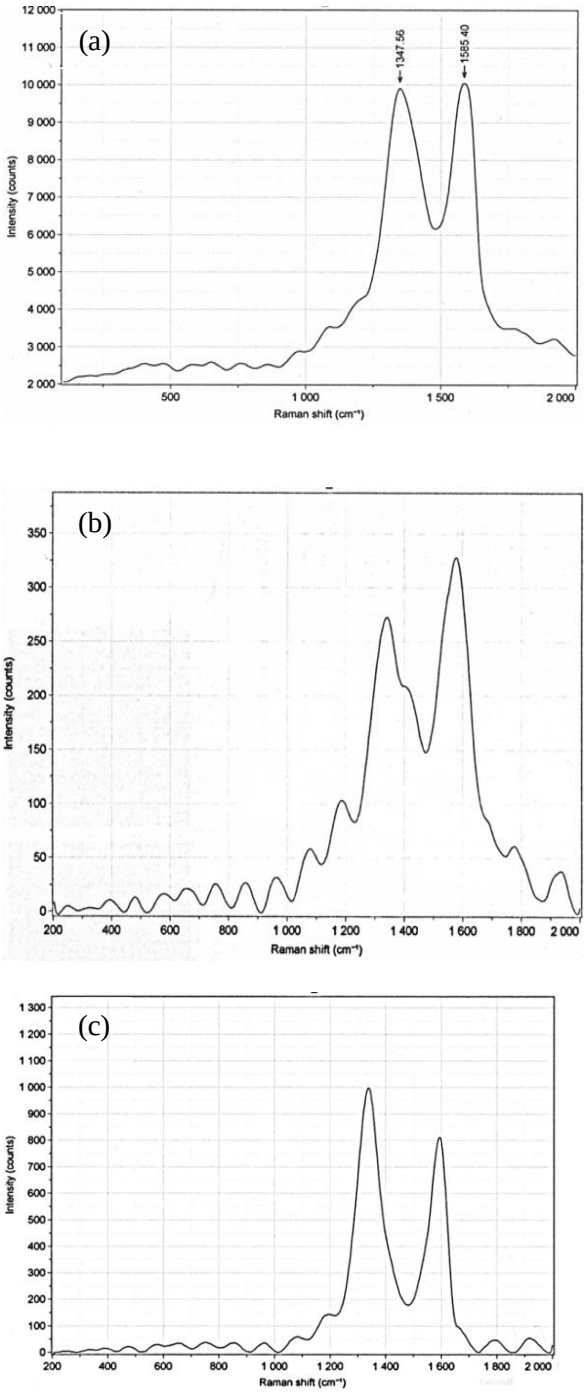

Figure 5. Raman spectra of (a) graphene oxide (b) reduced graphene oxide with ascorbic acid & NH_3 and (c) reduced graphene oxide with $NaBH_4$

Compare the results of graphene oxide and reduced graphene oxide through different characterization techniques are summarized in table 1.

Table 1. Determination of GO and rGO with ascorbic acid and $NaBH_4$

Analysis	GO	rGO by using Reducing Agents	
		(AA)	($NaBH_4$)
UV	229.5nm {attributed to $\pi \rightarrow \pi^*$ transitions} corresponding to $n \rightarrow \pi^*$ transition of C=O bonds (carbonyl groups)	peak shift to 248.34nm (optical absorption is changing with the number of layer)	peak shift to 259.71nm (less than 10 layers)
FTIR	hydroxyl group (carbonyl and epoxy)	conjugated carbonyl group (stretching)	conjugated carbonyl group (stretching)
SEM	crumple structure (exfoliation)	folded and wrinkled structure	large crumple structure
XRD	$2\theta \sim 10.85°$ corresponds to the reflection from (111)plane	$2\theta \sim 26.606°$ corresponds to the reflection from (002)plane	$2\theta \sim 26.625°$ corresponds to the reflection from (111)plane
Raman	$I_D/I_G = 0.99$	$I_D/I_G = 0.85$	$I_D/I_G = 1.25$

4. CONCLUSIONS

In this study, graphene oxide and reduced graphene oxide were synthesized by Hummers method and chemical reduction method. During this study, the effect of different reducing agents such as ascorbic acid and $NaBH_4$ on morphology and structure of GO and rGO were investigated. The detailed study to investigate the effect of reducing agents on the structure and morphology of rGO by using SEM, XRD, UV-visible and Raman spectrometer, FTIR spectroscopic techniques. In XRD, inner planner spacing showed the formation of GO and rGO. SEM images displayed the random wrinkled and crumpled wave's morphologies of graphene oxide and reduced graphene oxide. RGO sheets with a high degree of reduction and low sheet stacking were obtained using ascorbic acid as the reducing agent. Therefore, the ascorbic acid is a good candidate to successfully reduced graphene oxide.

ACKNOWLEDGEMENTS

The authors would like to thank University of Yangon and Department of Higher Education for the financial support in this research work.

REFERENCES

[1] S. V. Morozov, K. S. Novoselov, M. I. Katsnelson et al., "Giant intrinsic carrier mobilities in graphene and its bilayer," Physical Review Letters, vol. 100, no. 1, Article ID 016602, 2008. View at Publisher · View at Google Scholar · View at Scopus

[2] M. Hirata, T. Gotou, S. Horiuchi, M. Fujiwara, and M. Ohba, "Thin-film particles of graphite oxide 1: high-yield synthesis and flexibility of the particles," Carbon, vol. 42, no. 14, pp. 2929–2937, 2004. View at Publisher · View at Google Scholar

[3] T. Nakajima, A. Mabuchi, and R. Hagiwara, "A new structure model of graphite oxide," Carbon, vol. 26, no. 3, pp. 357–361, 1988. View at Publisher · View at Google Scholar · View at Scopus

[4] A. Furst, R. C. Berlo, and S. Hooton, "Hydrazine as a reducing agent for organic compounds (catalytic hydrazine reductions)," Chemical Reviews, vol. 65, no. 1, pp. 51–68, 1965. View at Publisher · View at Google Scholar · View at Scopus

[5] L. Shahriary and A. A. Athawale, "Graphene oxide synthesized by using modified Hummers approach," International Journal of Renewable Energy and Environmental Engineering, vol. 2, no. 1, 2014. View at Google Scholar

[6] G. Wang, J. Yang, J. Park et al., "Facile synthesis and characterization of graphene nanosheets," The Journal of Physical Chemistry C, vol. 112, no. 22, pp. 8192–8195, 2008. View at Publisher · View at Google Scholar · View at Scopus

[7] M. B. Davies, J. Austin, and D. A. Partridge, Vitamin C: Its Chemistry and Biochemistry, Royal Society of Chemistry, London, UK, 1991.

[8] M. Ambrosi, E. Fratini, V. Alfredsson et al., "Nanotubes from a vitamin C-based bolaamphiphile," Journal of the American Chemical Society, vol. 128, no. 22, pp. 7209–7214, 2006. View at Publisher · View at Google Scholar · View at Scopus

[9] Y. Wang, P. H. C. Camargo, S. E. Skrabalak, H. Gu, and Y. Xia, "A facile, water-based synthesis of highly branched nanostructures of silver," Langmuir, vol. 24, no. 20, pp. 12042–12046, 2008. View at Publisher · View at Google Scholar · View at Scopus

[10] Z. Ciplak, N. Yildiz and A. calimli, "Investigation of Graphene/Ag nanocomposites synthesis parameters for two different synthesis methods," Fullerenes, Nanotubes and Carbon Nanostructures, vol. 23, 2014, pp-361-370.

Influence of Dopant Calcium Concentration on Electrical Behavior of Pbtio$_3$ Ceramic Capacitor

Lae Lae Khine[1], Nwe Ni Soe[2]
Department of Engineering Physics, Thanlyin Technological University, The Union of Myanmar.
Department of Engineering Physics, Thanlyin Technological University, The Union of Myanmar.
laelaekhine.tu@gmail.com, nwenisoenns1971@gmail.com

ABSTRACT: Ca modified $Pb_{1-x}Ca_xTiO_3$ ferroelectric ceramic capacitor was fabricated. The fabrication process comprises five stages: the specification, purchase and storage of raw materials, the preparation of a composition in powder form, forming the powder into a shape, sintering, finishing. The stating regents for $Pb_{1-x}Ca_xTiO_3$ synthesis have been lead oxide (PbO), titanium dioxide (TiO_3) and calcium oxide (CaO), x=0.05,0.10,0.15,0.20 , and then they were mixed by standard solution method and calcined at 600°C in O_2 ambient for sintering time 1 hour and dried again in air atmosphere. The samples were covered with Cu electrode to be electrical contact. The maximum capacitance frequencies were at 1 kHz and between 20kHz to 100kHz, where the latter is the largest quality factor. The maximum quality factor was at 100 kHz, and PCT ceramic capacitor was suitable for low frequency application. The objective of fabrication is to produce a material with specific properties, and a body of required shape and size within specified dimensional tolerances are needed to fulfill the economic cost. According to data, fabricated PCT was promising device for memory device application.

Keywords: ceramic capacitor, metal/ceramic/metal semiconductor device, PCT, frequency, quality factor

1. INTRODUCTION

Semiconductor gives difficulty in maintaining stoichiometry, and obtaining the correct chemical ratio for the compound's difficult constituent elements, while at the same time controlling the thermal parameters and determining the crystalline perfection are required. The oxide ceramics has the general chemical formula ABO_3 perovskite like structure. The simple cubic perovskite structure is still probably the most important ferroelectric prototype. Lead titanate $PbTiO_3$ has been promising compound for piezoelectric sensor material. This research work is dealt with preparation and characterization of ferroelectric $Pb(Ca)TiO_3$ ceramic capacitor.

2. MATERIALS USED

2.1. PbO Powder

Lead reacts easily with silica to from melting lead silicates of high glass deep character. Lead is very easy to use. It is the heaviest oxide and produces incredible colors and surface characteristics.

Lead also has "blemish healing" and flow characteristics that are unmatched lead glazes tend to have high resistance to chipping. In addition, Lead is a "forgiving materials" that tends to hide imperfections on the finished fired surface. Furthermore, lead has very good quality such as promoting low expansion, a low firing range, and it decreases viscosity and tendency to devitrify.

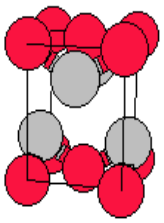

Figure 1. Crystal structure of PbO

2.2. TiO_2 Powder

Titanium is a complex material because it opacities, variegates and crystallizes glazes. It also modifies existing color from metal like Cr, Mn, Fe, Co, Ni, and Cu. Titanium can acts as a modifier and within a narrow range it will combine with fluxes to make a glass. It can also act in a flux-like way in very high silica melts $TiO_2$is considered an impurity in ball clays and kaolin used to make porcelain because it can react with any iron present to from rutile crystals which detrimentally affect body color and translucency.

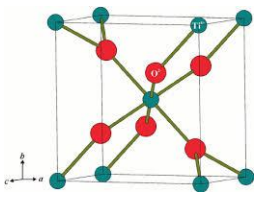

Figure 2. Crystal structure of TiO_2

2.3. CaO Powder

Calcium oxide is the principle flux in medium and high temperature glazed beginning its action around 1100°C. It must be used with care in high fire bodies

because its active fluxing action can produce a body that is too volatile. Calcium usually hardens a glaze and makes it more scratch and acid resistant. This is especially so in alkaline and lead glazes. Calcium and silica alone resist melting even at high lottery temperatures, but soda and potash are added, calcia becomes very active in both oxidation and reduction. CaO contributed by wall astatine is more readily fusible than that contributed by whittling (calcium carbonate). This energy between CaO and other fluxes and differences in the mechanism of its fluxing action generates some disagreement among experts regarding the nature of CaO since it does not appear to the stand-alone flux compare to other.

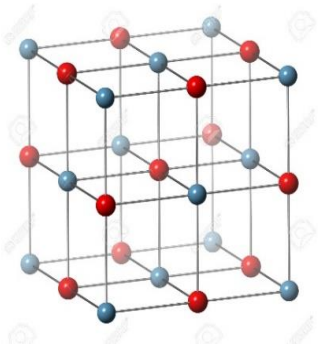

Figure 3. Crystal structure of CaO

2.4. Lead Titanate ($PbTiO_3$, PT)

Lead titanate is a ferroelectric material having s structure similar to $BaTiO_3$ with a high Curie point (490°C). On decreasing the temperature through the Curies point a phase transition from the para electric cubic phase to the ferroelectric tetragonal phase takes place. Lead tatanate ceramic are difficult to fabricate in the bulk form as they undergo a large volume charge on coating below the Curies point. It is the result of a cubic (c/a=1.00) to tetragonal (c/l=1.064) phase transformation leading to a strain of .6%. Hence, pare $PbTiO_3$ ceramic crack and fracture during fabrication.

The spontaneous strain developed during cooling can be reduced by modifying the lead titanate with various dopant such as Ca, Sr, Ba, Sn and W to obtain a crack free ceramic. One representative modified lead titanate composition that has been extensively investigated recently is $(Pb_{0.76}Ca_{0.24})(CO_{0.50}W_{0.50}I_{0.04}Ti_{0.96})O_3$ with 2 mol % MnO added to it. This composition has a decreased c/a ratio and Curie point 255°C.

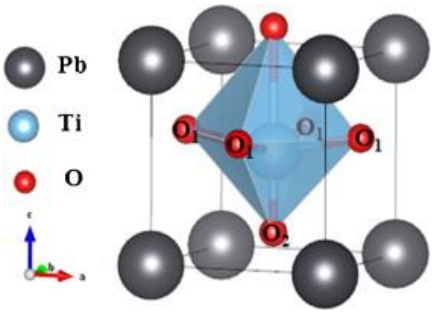

Figure 4. Crystal structure of $PbTiO_3$

3. STARTING MATERIALS

The objective of fabrication are to produce a material with specific properties, a body of a required shape and size within specific tolerances and the required component of an economic cost.The material properties are basically controlled by the composition but with also be affected by the gain size and porosity of the sintered ceramic, and the latter features are affected by the method of fabrication. The stages in the fabrication of ceramic are calcinations and sintering, which are sometimes combined. During these processes the constituent atoms redistribute themselves in such a way as to minimize the free energy of the system. This involves a consideration moment of ions, the minimization of the internal surface area and increase in grain size.

4. FABRICATION PROCESS AND PROCEDURE

The fabrication process comprises five stages: processing of raw materials, the preparation of a composition in powder form, shaping, sintering and finishing.

The first stage is to weigh out the raw material with due allowance for impurity and moisture content. The next step is mixing, elimating aggregations and/or reducing the partied size. If compound formation is to occur during calcining or firing, the matter of neighboring particle must inter diffuse end of the time taken to complete the process. Apart from breaking up agglomerates and forming an intimate mixture of constituents, a milling process introduces defects into the crystals which may enhance diffusion and accelerate sintering.

Moreover, calcination can be considered to be part of the mixing process. The calcinations condition are important factor for controlling shrinkage during sintering. The main requirements is that calcinations should yield a very consistent product.

Shaping is one of the most important factor for fabrication process. The treatment of the milled powders depends on the method of fabricating shape from it. Unless the material concerned contains as substantial quantity of dry (usually 10% or more), it is necessary to incorporate an organic binder. The main function of the binder is to give the dry shape sufficient strength to survive the handling necessary between shaping and sintering, but it may also essential to the method of shaping.

The last stage of the fabrication process is dry-pressing. It is carried out in a die with movable top and bottom punches. A cavity is formed with the bottom punch in a low position and this is fill with free-flowing granulated powder which is then struck off level with the top of the die. The most important factor for this procedure is the time taken, which varies form 0.2 seconds for pieces of diameter around 1mm to 5 seconds for large complex shape of pressing on an automatic machine.

5. EXPERIMENTAL PROCEDURE

The first step is to weigh the starting material according to desirable composition. In general, PbO and TiO2 powder were mixed in cleaned crucible with stoichiometry composition in uniform ratio, to obtain homogeneous and uniform grain size of solution. It was dried at room temperature and then grounded by an agate motor. The mixture powder was mixed with 2 drops of ethanol that can be bonded with the powder, stirred in the crucible and put in the container and ball mailing. This mixed solution was given heat treatment at primary temperature 600°C for 1 hour in atmosphere and subsequently put off the solution from oven.

Then it was cool down at room temperature to be crystalline, the mixed solution was shaped by dry-pressing and pressed with 6 tons to obtain 1.8 cm diameter pallets. Calcium doped $PbTiO_3$ was heated at secondary temperature 800°C and dry at room temperature. Size at 0.8 cm diameter of Cu (Copper) foils was attached with silver paste and sandwiched with the pallets. Finally, Cu/Pb(Ca)TiO3/Cu (Metal/Insulator/Metal) semiconductor device was obtained.

6. MEASUREMENT

The oldest way of finding the resistivity ρ (ohm-centimeter) is using a rectangular sample of known dimensions. And the relation $R = \rho \frac{l}{A}$ is suitable expression to measure the resistance "R" where "l" is the sample length and "A" is cross-sectional area. The advantage of having the value of resistivity is that it can be mentioned as the contact-resistance term for semiconductors. Moreover the result can be minimized by plotting measured resistivity versus applied voltage. This resistivity will ordinarily decrease as the voltage increases and finally becomes relatively constant. If injection from the contacts has not become excessive at the point, the resistivity is probably no more than a few percent high. Injection difficulties can arise only with long-lifetime materials such as silicon and germanium but should seldom be a problem. In this research work, the direct method can be used to find the electrical conductivity and resistivity. Fig 5 shown the fabrication process of Ca modified $Pb_{1-x}Ca_xTiO_3$ ferroelectric ceramic capacitor

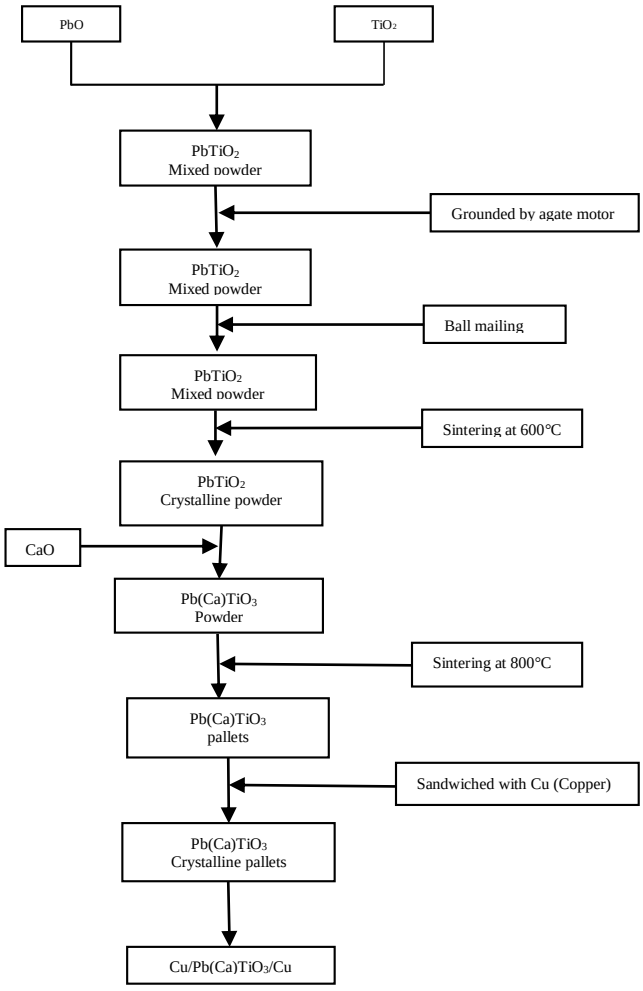

Figure 5. Block diagram of preparation of Cu/Pb(Ca) TiO_3/Cu ceramic capacitor

7. RESUTS AND DISCUSSION

When MIM ceramic diode was measured, the crystal was sandwiched by two copper (Cu) electrodes and it was served as dielectric. When the potential voltage was applied, the current passed through the two electrodes simultaneously. Therefore, the crystal was

paralleled with the power supply and the emitted currents were recorded by the fluke meter. The recorded data were shown by straight line. Thus the electrical conductivity was found with the formula,

$$f = y_0 + ax$$

And the values of electrical conductivity were shown in Table (1).

To know the true characteristic nature of straight line from I-V curve, the non-linearity factor was also analyzed. The value of non-linearity factor were 0.5,0.3, 0.62 and 0.7. The value of electrical conductivity were -1.77097, 1.998, 0.571495 and 0.83264.

Table 1. Electrical conductivity values all Pb(Ca)TiO_3 ceramic capacitor

	Electrical conductivity (νm^{-1})
PCT5	-1.77097
PCT10	1.998
PCT15	0.571495
PCT20	0.83264

7.1. Resistivity and Conductivity

Resistivity was measured with direct method intense of 2-probe method or 4-probe method. The value of resistivity for Pb(Ca)TiO_3 ceramic capacitor (x=0.05~0.20) are shown in Table (2) and Fig 6. Hence, it can be concluded that the resistivity increases from 0.06 to 2.5 Ωm as the PCT values increase.

Table 2. Resisitivity for all Pb(Ca)TiO3 ceramic capacitor

	Resistivity (Ωm)
PCT5	0.0641
PCT10	0.282
PCT15	1.841
PCT20	2.564

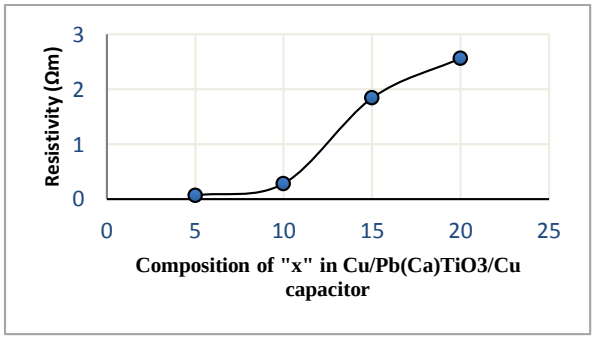

Figure 6. Resistivity value of Ca doped $PbTiO_3$ ceramic

7.2. C-F Measurement

To classify the memory nature to the fabricated sample, the capacitance values are measured at various applied frequencies with sample RC circuit as an integrator in which sample is served as circuit element. To know the charge storage capacity of fabricated sample, the charge storing values were measured at the difference applied frequencies from 0 kHz to 100 kHz. Two distant regions were found in the plot. The value of the capacitance decreased abruptly with increasing the value of frequency. The maximum capacitance value in accumulation region for all Pb(Ca)TiO_3 ceramic capacitor were 7 pF, 8 pF, 9 pF and 7 pF. Fig 7 shows the capacitive values of our fabricated ceramic capacitor.

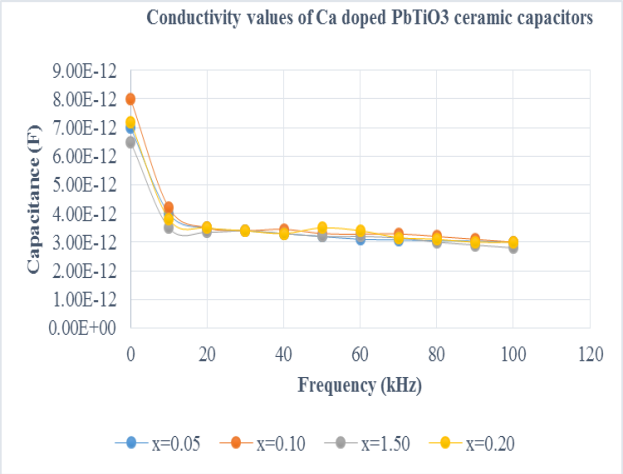

Figure 7. Conductivity values of Ca doped PbTiO3 ceramic capacitors (x=0.5~0.20)

7.3. Quality Factor Measurement

To know the device performance of our fabricated sample, quality factor was measured for LCR meter at zero bias potential. At the low frequency region, the quality factor was nearly unity and the quality factor was larger than unity at the high frequency region. The maximum quality factor for all Pb(Ca)TiO_3 were 9.8, 8, 8.2 and 9.5. The values of quality factor for all ceramic capacitors and characteristic are shown in Table (3) and Fig 8.

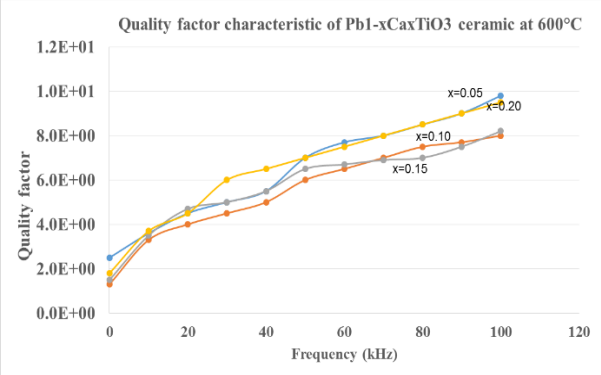

Figure 8. Quality factor value of Ca doped $PbTiO_3$ ceramic capacitors (x=0.5~0.20)

Table 3. Quality factors and transition frequencies for all ceramic capacitors

	Quality factor
PCT5	9.8
PCT10	8
PCT15	8.2
PCT20	9.5

7.4. Dissipation Factor Measurement

To know the device performance of $Pb(Ca)TiO_3$ ceramic capacitor, zero bias quality factor and dielectric lass measured for LCR meter were analyzed immediately. The more capacitance value for our fabricated ceramic capacitor, the better to switch current flowing. The dissipation factor decreased slowly from 0 kHz to 20 kHz. The first transition frequency was found at 12 kHz and the minimum and maximum dissipation factors were 0.58 and 0.1. The transition frequency changing from the first region to the second region was found at 14 kHz, where the maximum the transition frequency occurred. The maximum and minimum dissipation factor were 0.61 and 0.11. The transition frequencies changing from one region to another region for all $Pb(Ca)TiO_3$ ceramic capacitor with desire molar rations (x=0.05~0.20) are 12 kHz, 14 kHz, 20 kHz and 11 kHz and collected in Table(4). The characteristics of dissipation factor are shown in Fig 9.

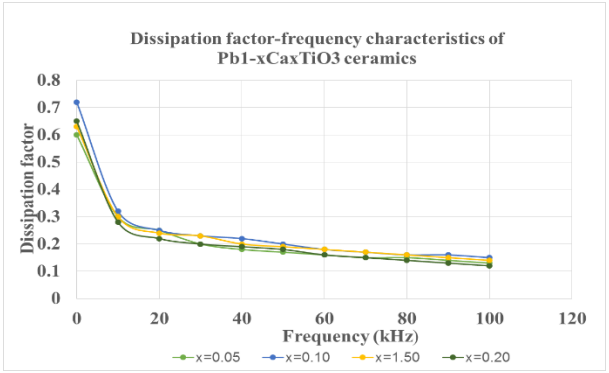

Figure 9.Dissipation factor value of Ca doped $PbTiO_3$ ceramic capacitors (x=0.5~0.20)

Table 4.Dissipation factors and transition frequencies for all ceramic capacitors

	Maximum dissipation factor	Minimum dissipation factor	Transition Frequency (kHz)
PCT5	0.58	0.1	12
PCT10	0.72	0.14	14
PCT15	0.63	0.12	20
PCT20	0.61	0.11	11

8. CONCLUSIONS

With ferroelectric Cu doped lead-titanate ceramic capacitor, the fabrication and characterization of PCT configuration have been investigated. The results calculated from ferroelectric, dielectric and electrical characterization, the choice of material system, fabrication technique and multilayers design in this study are promising for device technology.

I-V characterization also shows the rectification effect. The forward bias to the Cu/ calcium doped lead titanate ceramic capacitor and this forward rectification parts of the curve could be explained, and the calcium doped lead titanate ceramic capacitor is p-type conductivity. In the case of PCT, the zero bias barrier height would increase as dopant concentration increases, and it might be the energy band gap variation with dopant concentration. Generally, the electrical conductivity values can be seen as increasing trend when the PCT values increase. For quality factor, it is ascending as the PCT values increase except for PCT5. When the frequency increases, the dissipation factor decreases but the values are stable between 50 and 100 kHz. C-F significant capacitance dispersion over frequency was observed for all cases above 1 kHz. According to the results and data conducted, it can be observed that the maximum dissipation factors are

increasing but the minimum values are nearly constant about 0.1, and the transition frequencies are in the range between 11 and 20.

Therefore, various modifications into calcium doped lead titanate have been studied with the aim of obtaining improved properties to make them potential useful in practical application. The present result in this research which is indicated our fabricated memory devices with new sol-based method are very promising for memory device application.

ACKNOWLEDGMENT

The author is deeply grateful to Professor Dr. Khin Hla Hla Win, Head of Department of Engineering Physics, Technological University (Thanlyin), for giving me such opportunity to complete my research paper.

I am also deeply indebted to Professor Dr. Than Than Win, Professor of Department of Physics, Pinlon University, for her suggestion for the choice of the technique, valuable advice of this study.

At last but not the least, the author thanks to my parents for always supporting my choices. I want to mention my thanks to all my colleagues of Department of Engineering Physics, Technological University (Thanlyin) for giving me valuable suggestions.

REFERENCES

[1] A.P.Chen et al, Strong oxygen pressure dependence of ferroelectric in BaTiO3/SrRuO3/SrTiO3 epitaxial heterostructurs, Journal of applied physics 114, 124101, Japan: 2013.

[2] Akira Ariizumi, Kiyoshi Kawamura, Ichiro Kikuchi and Iwao Kato, Electrical Properties of $PbTiO_3$ Thin Films by Thermal Decomposition of Organometallic Compounds, The Japan Society of Applied Physics, Japan, 1985.

[3] Dissipation factor/ESR-Illinois Capacitor. Available: [Online] http://www.illioniscapacitor.com > impedence - dissipation-factor-ESR.

[4] Hairai T et al, J Appl Phys 36 pp5908, 1997.

[5] Handbook of Ceramic Composition(2006).Available: [Online]. http://www. www.Quantum modeling of ferroelectric PbTiO2 ceramic

[6] .Robert S Rath, Classification of perovskite and other ABO3 type, Journal of Research of National Bureau of Standard, Vol. 58, pp, 75-88, Feb, 1956

.

Design and Construction of Mosfet Inverter

Myint Myint Swe[1], San San Htwe[2], Sandar Win[3]
[1]*Lecturer, Faculty of Natural Sciences, University of Computer Studies (Taungoo)*
[2]*Associate Professor, Faculty of Natural Sciences, University of Computer Studies (Taungoo)*
[3]*Assistant Lecturer, Faculty of Natural Sciences, University of Computer Studies (Taungoo)*
myintmyintswe.ms@gmail.com

ABSTRACT: *This project focuses on the design and construction of an inverter using MOSFETs (Metal-Oxide-Semiconductor-Field-Effect-Transistors). An inverter is a circuit that transform from DC to AC current. Inverters are very useful electronics products for compensating emergency power failure, as it performs DC to AC conversion. AC can't be stored for future use but DC can be stored for future use in a battery. The stored DC can be converted back to AC by using power inverters. MOSFETs inverters are more efficient, low power consumption than those of using BJTs (Bipolar Transistors). For the region in our country where the electricity cannot available can be obtained electrical energy by solar cells, small hydroelectric station, wind mills and fuel used generators. For this reason, inverter is widely used in both cities and country sides. It also intends to continue contributing to progress toward a low-carbon society by developing technologies that will help make inverters more widely used.*

Keywords: Design and construction; Inverter; MOSFETs; Electrical energy; DC to AC convertor

1. INTRODUCTION

An inverter is a device that delivers AC power when energized from a source of DC power. Although varieties of inverters design have been reported, a simple inverter circuit is constructed by CMOS 4047 IC and 555 IC. Actually DC voltage from a battery gets into circuit. It produces AC voltage, 50Hz frequency. But this is too low current. Use the power switching such as the power transistors or MOSFETs. But AC voltage still is 12V. Next, Transformer inductance voltage to rises into 220V AC 50Hz to apply load. A circuit in which the emphasis is on such parameters as efficiency, regulation, over load capability, and in which may operate at audio of low supersonics frequencies, may qualify as in inverter even though its operating principle is similar to that of an oscillator. All the inverters covered thus far have been self-oscillatory. Most of them can be driven from an external oscillator if their feedback circuits are disabled or omitted. In essence, the inverters becomes amplifiers. Most often, they are designated as class D amplifiers because they reproduces square waves and operate in switching mode. That is, they are earlier driven to collector-current saturation, or they are completely turn-off. Thus, the opportunity for high operational efficiency is retained. In addition, there are other advantages. A driving type inverter generally uses a linear output transformer; this greatly diminishes the spike problem. In as much as core losses are less in linear transformers than in saturating transformer, operating efficiency tends to be high. Finally, such as an arrangement neatly circumvents problems associated with starting.

2. WAVEFORM GENERATORS

Waveform generators are used to produce a large variety of electronic waveforms such as sine waves, square waves and triangular waves or other non-sinusoidal waves. An oscillator is a circuit, which produces a periodc waveforms. The output can be sine waves, square waves, triangular waves,sawtooth waves, pulses or any of several other shapes. The impontant things are that the waveform is periodic.

2.1. Step–Up Design

In our design, The MOSFET is a driven type. It is designed with the oscillator, power amplifier, battery charger circuit and step up transformer. The oscillator is designed using a 4047 CMOS IC, four IRF 540 N-channel E-MOSFETs are used as a power amplifier. The block diagram of the whole system is shown in figure (2.1).

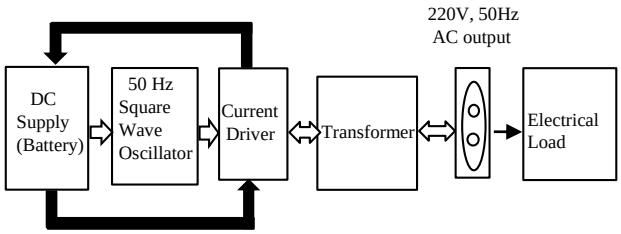

Figure 2.1. Block diagram of the MOSFET-Inverter

2.2. Gated Oscillator

The simplest way to make the square wave generator is to wire two inverters stage in series and used the RC feedback network shown in the basic two stage astable multivibrator circuit of figure (2.2).The circuit is suitable for used in many clock generator applications. For practical circuits, the calculated oscillation period deviates sometimes strongly from the real oscillation period. For long oscillation periods, the input of the first NOT gate needs to be protected by a resistor. This makes it even more difficult to determine the oscillation period. Occasionally the oscillation fails to start.

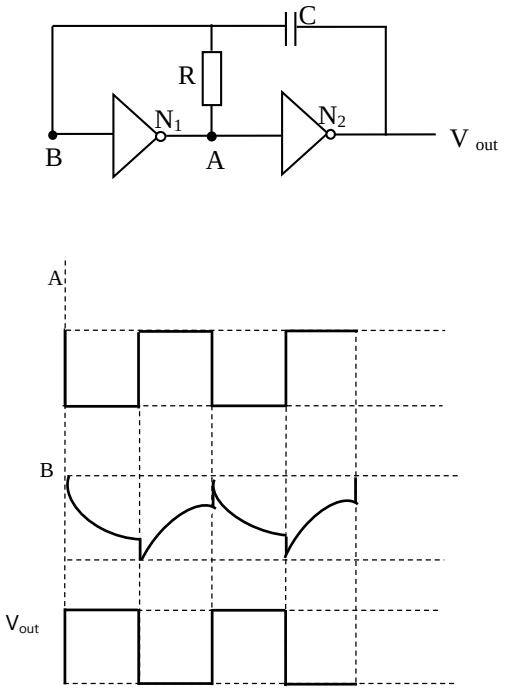

Figure 2.2. NOT gate oscillator and output waveforms for each node of circuit

2.3. 555 Timer IC

Basically, the 555 timer IC is a highly stable integrated circuit capable of functioning as an accurate time-delay generator and as a free running multivirator (or astable multivibrator). When use as an oscillator the frequency and duty cycle are accurately controlled by only two external resistors and a capacitor.

If the circuit is connected as shown in figure (2.3), it will triggered itself and free ran as a multivibrator. The external capacitor charges through R_A and R_B and discharge through R_B only. Thus the duty cycle may be set precisely by the ratio of these two resistors.

In this mode of this operation, the capacitor charges and discharges between 1/3 V_{cc} and 2/3 V_{cc}. As in the triggered mode, the charge and discharge times and hence the frequency is independent of the supply voltage. The charge time output is given by:

$$t_1 = 0.693(R_A + R_B)C_T \quad (2.1)$$

The discharge time (output low) is given by:

$$t_2 = 0.693(R_B)C_T \quad (2.2)$$

Thus, the total period is given by

$$T = t_1 + t_2 = 0.693(R_A + 2R_B)C_T \quad (2.3)$$

and the frequency of the oscillation is then:

$$f = \frac{1}{T} = \frac{1.44}{(R_A + 2R_B)C_T} \quad (2.4)$$

The duty cycle is given by

$$D = \frac{R_A + R_B}{(R_A + 2R_B)} \quad (2.5)$$

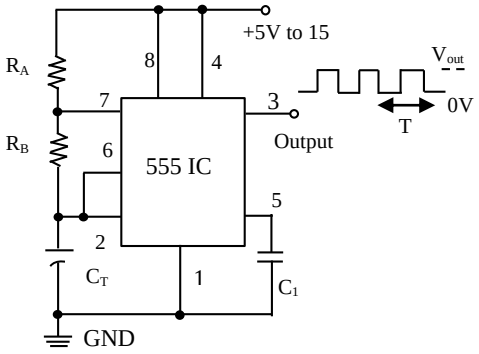

Figure 2.3. Circuit diagram of NE 555 astable multivibrator

2.4. CMOS 4047 IC Timer

CD4047 is a CMOS Low Power mono stable/ astable multivibrator mainly used. CD4047 is a 14 pin IC that operates on a logic techniques with an ability to allow negative or positive edge-triggered monostable multivibrator action layered with retriggering and external counting options. Accurate and complemented buffered output with low power consumption make this IC an ideal choice for Frequency Division and Time Delay applications. No matter what type of operation this IC undergoes, an external resistor is permanently connected between RC-Common and R timing terminals and an external capacitor is connected between RC-Common and C timing terminals. The 4047 can be used as a free running astable multivibrator (square wave generator) by connecting it as shown in figure (2.4).

Alternately, the output may be taken via the internal divided-by-2 element as shown in figure (2.5), in which case the output is perfectly symmetrical (50% duty cycle) and has a period of 4.4 CR.

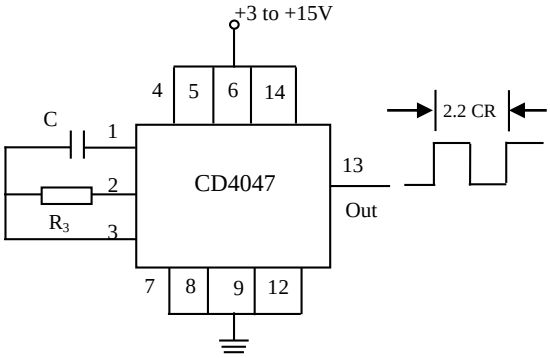

Figure 2.4. Wiring diagram of 4047B astable multivibrator

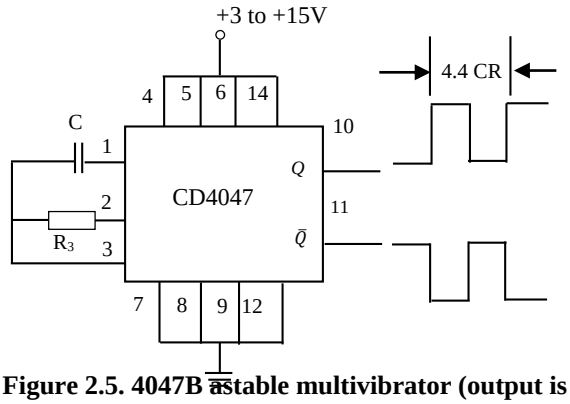

Figure 2.5. 4047B astable multivibrator (output is 50% duty cycle)

2.5. The Components List

Table 2.1. The Component List

Symbols used	Number of pieces
IC1 : CD 4047 IC	1 pcs
BR1 :bridge rectifier with1N4001diodes	4 pcs
C_1, C_2 : 0.047uF 100V Mylar capacitors	2 pcs
C_3 : 22 u F 100V Mylar capacitors	1 pcs
C_4 : 0.022 u F	1pcs
C_5: 0.1 u F	2 pcs
Diode:1N-4001	2 pcs
Diode:1N-4148	1 pcs
R_1,R_2 :100 ohm resistors	2 pcs
R_3,R_4 :10 K ohm resistors	2 pcs
Variable Resister 500 K	1 pcs
2Kohm resistors	2 pcs
330 ohm resistor	1 pcs
S_1:switch Low/High	1 pcs
F_1:1A fuse	1 pcs
F_2:15A fuse	1 pcs
Q_1, Q_2, Q_3, Q_4 : IRF540-NPN transistors	4 pcs
T1 : 220V-12 V transformer	1 pcs
7.5V Zener diode	1 pcs
12V 5A relay	1pcs
12 V Battery	1pcs

3. MOSFET POWER AMPLIFIER

3.1. Metal Oxide Semiconductor Field Effect Transistors

The metal–oxide–semiconductor field-effect transistor also known as the metal–oxide–silicon transistor (MOS transistor, or MOS), is a type of field effect transistor. It has an insulated gate, whose voltage determines the conductivity of the device. This ability to change conductivity with the amount of applied voltage can be used for amplifying or switching electronic signals. The MOSFET is the basic building block of modern electronics. These transistors are identified by various manufactures as HEXFET, VMOS or DMOS, depending on the geometry of the gate structure, respectively hexagonal, V-shaped, or D-shaped. A key advantage of a MOSFET is that it requires almost no input current to control the load current, when compared with bipolar transistors (bipolar junction transistors, or BJTs). In an *enhancement mode* MOSFET, voltage applied to the gate terminal increases the conductivity of the device. MOSFETs also consume much less power, and allow higher density, than bipolar transistors. The MOSFET is also cheaper and has relatively simple processing steps, resulting in a high manufacturing yield. Since MOSFETs can be made with either p-type or n type semiconductors (PMOS or NMOS logic, respectively), complementary pairs of MOS transistors can be used to make switching circuits with very low power consumption, in the form of CMOS (complementary MOS) logic.

3.2. Measuring Power MOSFET Characteristics

The circuit shown in figure (3.1) is used to measure the I-V characteristics of MOSFET. The gate to source is biased by the 7.5 V zener diode and the require voltage V_{GS} is adjusted by 50 kΩ resistor. The drain to source voltage can varied for each value of V_{GS} by variable power supply. The results are shown in table (3.1) and the MOSFET characteristics is illustrated in figure (3.2).

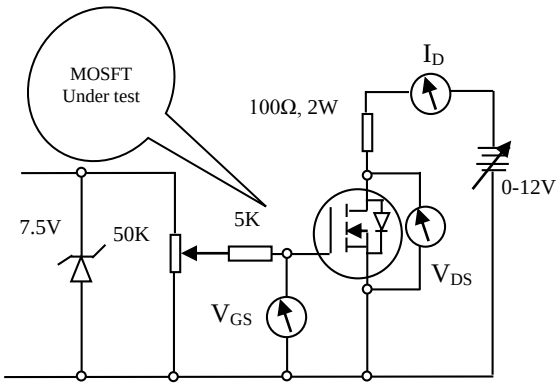

Figure 3.1. Wiring diagram for measurement of MOSFET characteristic

Table 3.1. MOSFET V-I characteristics data for V_{GS}=2V and 4V

V_{GS} (V)	V_{DS} (V)	I_{DS} (mA)	V_{GS} (V)	V_{DS} (V)	I_{DS} (mA)
2	0	0	4	0	0
	0.5	10		0.5	15
	1	20		1	32
	1.5	23		1.5	34.5
	2	24		2	36
	2.5	25		2.5	37.5
	3	25.3		3	37.95
	3.5	25.4		3.5	38.1
	4	25.5		4	38.2
	4.5	25.7		4.5	38.55

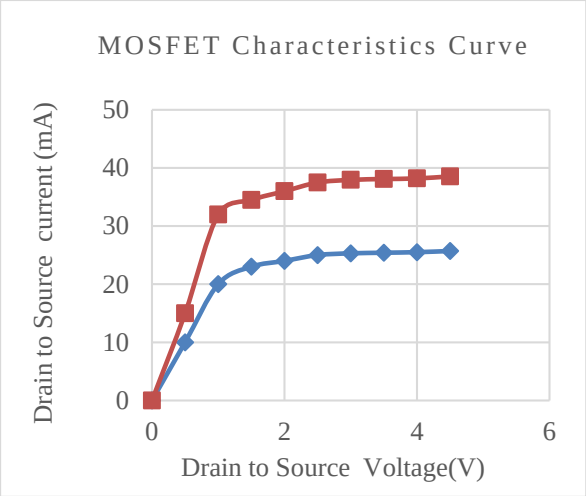

Figure 3.2. MOSFET characteristics drawn by measured results

4. CONSTRUCTION OF MOSFET INVERTER

4.1. Oscillator

The oscillator used in our circuit is constructed by 4047B and this IC is used as a free-running astable multivibrator (square wave generator) by connecting it as shown in figure (4.1). The output may be taken from pin -10 and -11) via the internal divided-by-2 element, in which case the output is perfectly symmetrical (50% duty cycle) and has a period of 4.4 CR. The output frequency can be calculated as:

$$f = \frac{0.23}{RC} \qquad (4.1)$$

For the C = 0.022 µF, R=220 KΩ

$$f = \frac{0.23}{RC}$$

$$= \frac{0.23}{220\times10^{3}\times0.022\times10^{-6}}$$

$$= 47.5Hz \cong 50Hz$$

In the practical circuit, 50 Hz frequency can be achieved accurately by adjusting the preset VR_1.

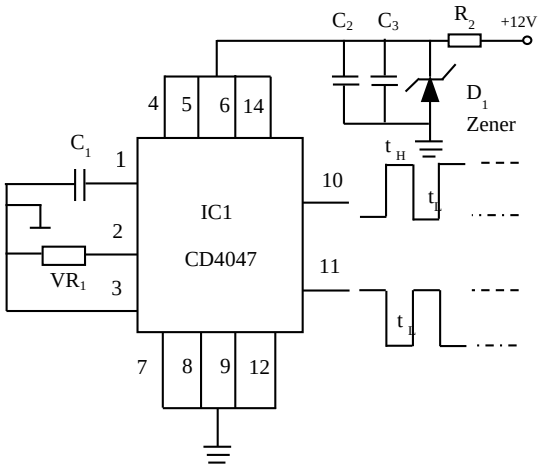

Figure 4.1. CD 4047 free-running astable multiviibrator

4.2. Transformer Design

The transformer is a basic necessary in operation of several electronics devices. The transformer used in the inverter circuit is step-up transformer, which transforms 12 volts to 220 volts. It is used to transform a low voltage current to a high voltage current. A step-up transformer can be designed by several ways, considering its core type, winding arrangement and coil size. Beside classification of the transformer should be thought out when it is designed. The output power of transformer is the basic requirement of the transformer design.

Theoretically, for an ideal transformer the input power is equal to the output power. But in practice the output power is less than the input power by 10% or 20%. To recover the power loss the input power is increased by % of the output power and expressed by the following equation:

$$input\ power = 1.10 * output\ power \qquad (4.2)$$

To design a transformer the following steps are needed to calculate.

$$primary\ current\ I_p = input\ power / primary\ voltage \qquad (4.3)$$

Cross-sectional area of the iron core $A = \frac{\sqrt{P_{in}}}{5.58}$

In practice, to recover the flux leakage the size of the iron core should be greater than 10% of the calculated valve.

The turns per volts for the winding can be calculated by the following equation:

$$N = \frac{10^8}{4.44 \times f \times B \times A}$$

Where, N= number of turns per volt
V= voltage in a wire coin
F= frequency
B= magnetic flux density
A= cross-sectional area of iron core

For our inverter transformer design, the required factors are calculated as follow:

The output power P_{out}=150W
So input power P_{IN}=1.1×150=165W
Primary current I_p=165/12=13.75A

Since the output signal of the inverter is a square wave, the output voltage is not a sin wave (rms). The relation between the square wave and a sin wave voltage (rms) is:
Square wave voltage = 1.1× sin wave voltage (rms)
To achieve the 240 V (rms), the output of the inverter transformer must be 240×1.1=266.4 V.
Secondary current I_s=150/266.4=0.563 A,

Cross- sectional area of iron core A=$\frac{\sqrt{165}}{5.58}$=2.302 square inches, and the actual size of core area= 2.302×1.1= 2.532 square inches.
To calculate turns per volt B was taken 6000 weber and f was 50Hz. So, the turn per volts

$$N = \frac{10^8 \times 1}{4.44 \times 50 \times 6000 \times 2.532} = 2.965 \text{ turns/volt}$$

Iron core area=1.5″×1.7″
Primary No. of turns=12V × 2.965 turns/volt 36 turns
For a center tap transformer, total primary windings = (36+36) turns.
Secondary no. of turns = 266.4 V ×2.965 turns/V
= 789.876
= 790 turns

The loss of energy in the transformer occurs in the transmission through a well-insulated wire depends also on two factors, the current and the resistance of the wire. The resistance of coil changes some energy of source to the heat energy and it is wasted. The coil sizes determine the allowable current carrying capacities of conductors in amperes. That is why a suitable coil size must be chosen to minimize the heat effect.

4.3. Power Amplifier

The current driver circuit for inverter is as shown in figure. The parallel combination of two MOSFETs is used for each tap of transformer to share the load current, MOSFETs connect in parallel share the current equally due to the positive temperature of $R_{DS\ (ON)}$, so there is no need for series current sharing resistors.

If two MOSFETs are in parallel, the device with the lower resistance $R_{DS\ (ON)}$ will try to draw more current than the other. Since P = I_D^2 $R_{DS\ (ON)}$), the device conducting the higher current will dissipate more power, rising the junction temperature, and in turn increasing the ON state resistance ($R_{DS\ (ON)}$),which will limit the current. This self-limiting characteristics forces an even distribution of current in two MOSFETs. Hence, in our power amplifier circuit, more current will drive than that of a single stage MOSFET and this circuit can be used safely at high current operation.

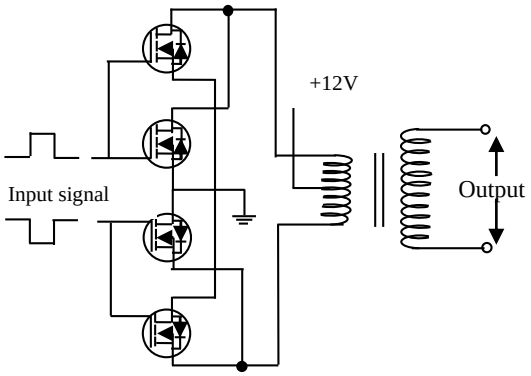

Figure 4.2. Power Amplifier for MOSFET Inverter

4.4. Charging Battery through MOSFET

The power MOSFET consists the internal body diode within its structure and it provides a direct internal path for the current to flow in the reverse direction (from source to drain) across the junction, which becomes forward biased. This diode is very useful for most switching application, since it provides a freewheeling current path. In this work, these diodes are used as rectifier diodes to charge the battery. When Main line power supply is in normal condition, the inverter mode is halt and serves as battery charger. The transformer serves as step down transformer. The diodes in the MOSFET ac like a full wave rectifier and the output produced is full-rectified sine wave. The circuit diagram for charging operation is illustrated in figure (4.3). During the first half cycle of an AC input, the diode in the lower MOSFET conducts and the diode in the upper MOSFET is conducted in the second half cycle of AC input.

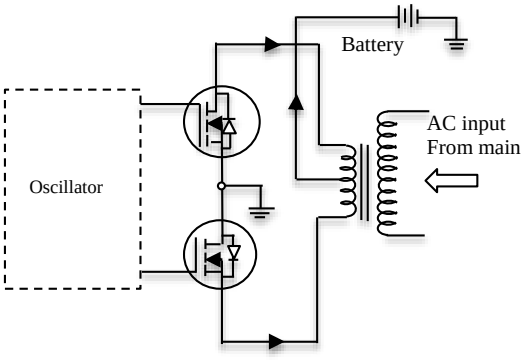

Figure 4.3. Operation of charging mode

4.5. Operation of Inverter

To operate the inverter system normally, required DC power can be obtained from the DC power source or a battery. As the inverter is switch on, DC power is delivered to the oscillator IC (4047).

The IC (4047) low power astable /monostable multivivrator constitutes an excellent heart for a simple inverter which can provide a 220 V AC output from a 12V DC input. For this application, of course, the IC is in the astable mode, the symmetrical square wave signals available at pin-10 and pin-11 outputs. Therefore, the output signals of 4047 are applied to the power amplifier that formed MOSFETs. Since these signals are square wave, MOSFETs operates as electronic switch. If the signal is applied and on the first half cycle, upper MOSFETs will start switching on, current will flow in one half of transformer's primary and will be transformed into the load. On the next half cycle upper MOSFETs will be off and lower MOSFETs driven on, current will flow in the other half of transformer's primary and the load.

The amplified output signal from the power amplifier is then fed to the primary winding of an inverter transformer. The 220 V AC output is then available at the secondary winding of the transformer. The complete circuit diagram of current will MOSFET inverter is shown in figure (4.4).

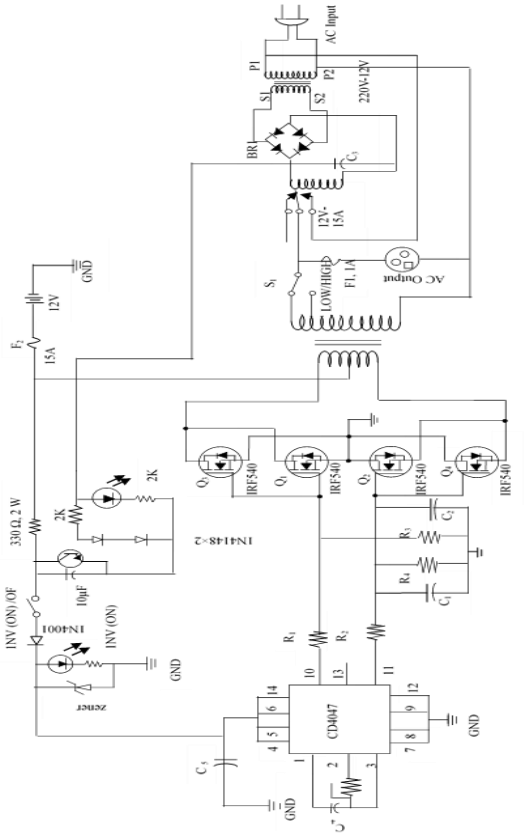

Figure 4.4. Complete circuit diagram of 150 W MOSFET Inverter.

5. CONCLUSIONS

The heart of an inverter is the oscillator circuit and it converts DC voltage to an AC voltage. So, the frequency of the output AC signal mainly depends on the frequency of the oscillator and the stability of the oscillator is an important role in the inverter circuit. The output frequency the oscillator mainly depends on the three factors: components tolerances, temperature and supply DC voltage.

In this project, a MOSFET inverter was constructed by using locally available integrated circuits and desire electronics components. Although the oscillator can be constructed by using the other ICs CD4047 is a low coast device and less external components are require to produce symmetrical square wave output since it has internally fabricated divided two circuit. The frequency adjustment was carried out using oscilloscope. The output potential depends on two conditions: the load used from external circuit and the type of the power supply (battery).

Overloading will causes to decrease the output voltage. The lead-acid battery should have enough capacity to supply the current for a requirement of inverter. The higher capacity battery can provide more over output then the lower capacity battery. The results from performance test of inverter are illustrated in table (5.1) and figure (5.1). Since the output of the inverter is square wave it is not suitable to used inductive load devices such as motors, fans, computers and TV in long term used. But there is no significantly effect on the resistive devices such as lamp for lighting.

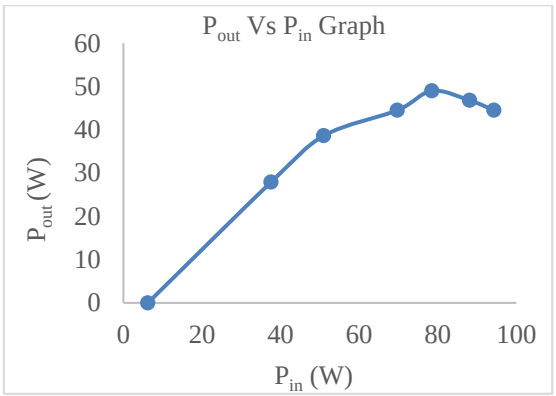

(a)

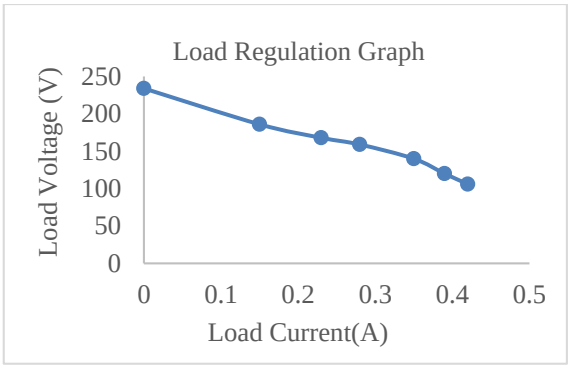

(b)

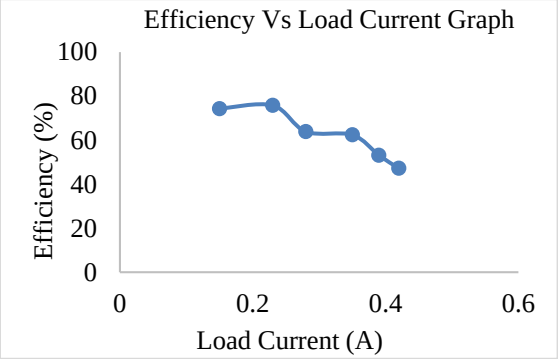

(c)

Figure 5.1. (a) P_{out} versus P_{in} Graph, (b) Load Regulation Graph, (c) Efficiency versus Load Current Graph

Table 5.1. Measurement Results obtained from inverter performance test

Load (W)	V_{dc} (V)	I_{dc} (A)	P_{in} (W)	V_{rms} (V)	I_{rms} (A)	P_{out} (W)	Eff (%)
No	12.94	0.48	6.21	234	0	0	-
40	12.78	2.94	37.57	186	0.15	27.9	74.26
60	12.75	4.0	51	168	0.23	38.64	75.76
80	12.68	5.5	69.74	159	0.28	44.52	63.84
100	12.67	6.2	78.55	140	0.35	49	62.38
120	12.59	7.0	88.13	120	0.39	46.8	53.1
140	12.58	7.5	94.35	106	0.42	44.52	47.19

ACKNOWLEDGEMENT

I would like to express my particular thanks Rector Dr. Ei Ei Hlaing, University of Computer Studies (Taungoo), for her permission to carry out this research work. Thanks should also go to all the teachers, University of Computer Studies (Taungoo), for their kind help during this work.

REFERENCES

[1] Ahmed, A 1999 "Power Electronics for Technology", (New Jersey: Prentice-Hall)

[2] Floyd, TL 1996 "Electronics Devices"(New Jersey: Prentice-Hall)

[3] Gottlieb, IM1985"Power Supplies: Switching Regulators, Inverter & Converter (New Delhi: Manish Jain)

[4] Malvino, AP 1993 “Digital Computer Electronics” (New York: McGraw-Hill).

[5] Marston RM 1996 "Modern CMOS Circuits Manual (Oxford: Butterworth-Heinemann)

[6] Zbar, PB Sloop, 1977 "Electricity-Electronics for Technology", (New York: McGraw-Hill).

[7] http://www.tpub.com

[8] http://www.teachcd.net/Qstore

[9] http://sales.digikey.com

[10] https://en.wikipedia.org/wiki/MOSFET

Design and Construction of Dual Axis Solar Tracker in Pyay

Zarchi San[1], Pan Wint Hmone Htwe[2], K Khaing Wint[3]
[1,2]*Lecturer*, [3]*Assistant Lecturer*
[1]*zarchisan2012@gmail.com*, [3]*kkhaingwint19@gmail.com*

ABSTRACT: *The main importance for this paper is that sixth year students can be used laptop and projector in presentation for their mini thesis though the light is off. As four 90W solar panel is connected in parallel, total power is 360W that is reliable for our loads. In this paper, the comparison between single axis and dual axis tracker radiation for Pyay District is expressed. Myanmar is more suitable solar power to store energy in battery during sunny days as renewable. Rotating motor forward and reversing is done by using PIC microcontroller. Proteus Software is used for simulation result. Due to the energy crisis and environmental problem such as pollution and global warming, solar energy is a very attractive solution for places with solar density. Dual-axis tracker has both horizontal and vertical axis can track the sun's apparent motion almost anywhere in the world. So solar panel can produce maximum power output.*

Keywords: single axis and dual axis tracker, radiation, PIC, solar panel, Proteus Software

1. INTRODUCTION

Solar tracker is a device used to orient a solar panel towards the sun. Since the sun position in the sky changes with the time of day, solar tracker is used to track the maximum amount of light produced by the sun. It is discovered that the instantaneous solar radiation collected by photovoltaic modules, assembled in a tracking system, is higher than the critical irradiance level for longer hours than in fixed system. The following solar energy technologies can be successfully propagated: solar cookers; solar water heating systems for industrial application; solar distillation units for battery charging; solar photovoltaic systems for water pumping, battery charging, and power supply to children's hospitals for operating vital equipment. Solar air driers can be used for agricultural and industrial products. Since Myanmar is a land of plentiful sunshine, especially in central and southern regions of the country, the first form of energy- solar energy could hopefully become the final solution to its energy supply problem. The direct conversion of solar energy into electricity using photovoltaic system has been receiving intensive installation not only in developed countries but also in developing countries.

It is mainly intended to present solar energy potential and application in Myanmar. It is also wanted to get the benefits of using solar energy for people in remote areas which are not yet connected to the national grids because of the high price of fossil fuel. MEPE (Myanma Electric Power Enterprise) experimental measurements indicate that irradiation intensity of more than 5kWh/m^2/day was observed during the dry season. If solar panel is installed in fixed position, solar power can absorb when the sun faces with solar panel. Even single axis moves, the efficiency of solar power can prove by comparing with dual axis as sun orbit is changing all the year. Nowadays, there are many types of solar trackers invented but the two basic categories of trackers that are widely-used are single-axis and dual-axis tracker. Single-axis tracker can either has a horizontal or a vertical axis, while dual-axis tracker has both horizontal and vertical axis, thus making them able to track the sun's apparent motion almost anywhere in the world.

The overall block diagram for solar tracker in P.T.U E.P Department is shown in Figure 1. After light dependence resistors had sensed where the sun is, the motors can move the solar panel due to PIC microcontroller. The battery either can store energy from solar during sunny days or can give supply when the rainy or cloudy days. The maximum 360 W loads such as laptop and projector can draw from solar tracker through inverter.

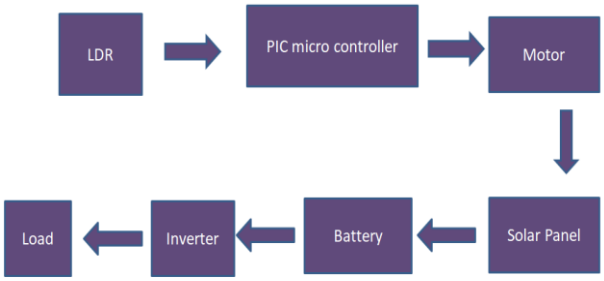

Figure 1. Overall block diagram of solar tracker

2. METHODOLOGY

As stated before, the aim of this research is the performance of dual axis solar tracking system. It consists of three main structures which are the inputs, the controller and the output. In this research, the main controller is PIC and then the controller sends the signal to the DC motor in order to determine the movement of the solar panel. This research can also be divided into two parts which are hardware and simulation software.

2.1 Light Dependent Resistor (LDR)

Photo resistors, also known as light dependent resistors (LDR) are light sensitive devices most often used to indicate the presence or absence of light or to measure the light intensity. This used as a sensor in the detention of light level in a variety of applications.

The use of this type of sensor is a relatively simple task which relies on the linear reduction of the resistance of a LDR with the increase in the intensity of the light. If the light intensity is lower than the setting, the resistor of the LDR is high. The result is a logic low signal on the output of the comparator.

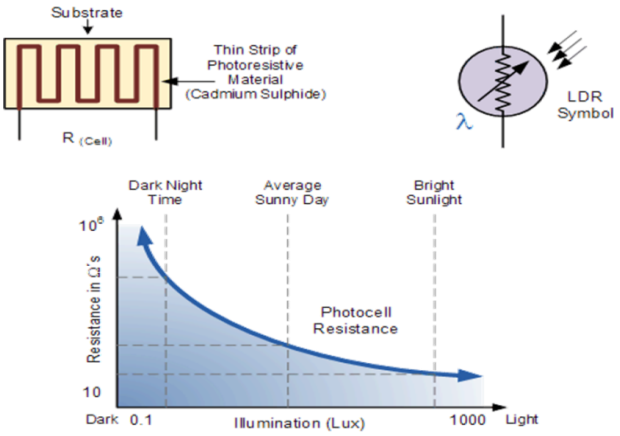

Figure 2. The Light Dependent Resistor Cell

When the light intensity exceeds the required level, the output of the comparator changes to a logic high state. In this research, the intensity of light sensed by the LDR becomes an input to the comparator. Figure 2 is shown the light dependent resistor cell. LDR is a component that has a resistance that changes with the light intensity that falls upon it. LDRs are made from semiconductor materials to enable them to have their light sensitive properties.

2.2 PIC Microcontroller

Microcontrollers are widely used in today's control system. It is a computer on chip used to control electronic device. PIC microcontroller is to provide the system reading the signal from the sensor during the operation sending the data. Moreover, it can be also used to control the motor driver that holds the motor to turn left, turn right and stop. PIC16F887A is one of the most commonly used microcontrollers especially in automotive, industrial, appliances and consumer applications. It can be reprogrammed and erased up to 10,000 times. Therefore it is very good for new product development phase. This PIC supports build-in PWM function for motor speed control. PWM is the most commonly technique for motor speed control. PIC16F887A microcontroller is used to control motor driver to drive DC motors. Pin Configuration of PIC16F887A Microcontroller is shown in Figure 3.

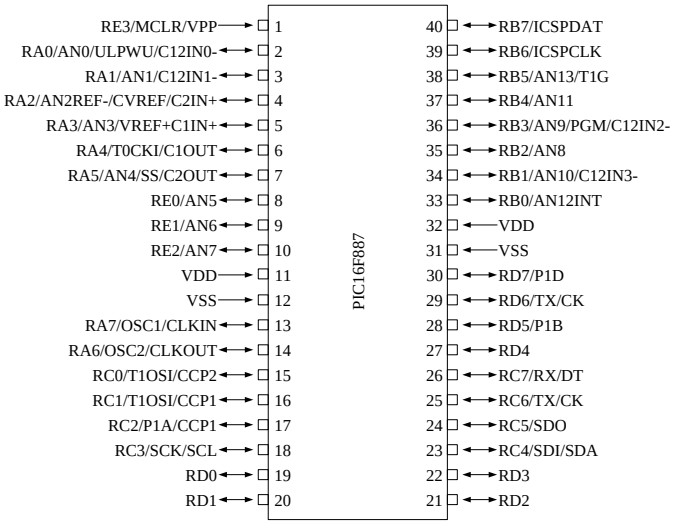

Figure 3. Pin Configuration of PIC16F887A Microcontroller

A microcontroller is a compact standalone computer, optimized for control applications. Entire processor, memory and the I/O interfaces are located on a single piece of silicon, so it takes less time to read and write to external devices. Features of PIC16F887A Microcontroller can be seen in Table 1.

Table 1. Features of PIC16F887A Microcontroller

CPU	8 – bit PIC
Number of pin	40
Operating Voltage (V)	2 to 5.5V
Number of I/O pins	33
ADC Module	8ch, 10bit
Timer Module	8 – bit (2), 16 – bit (1)
Comparators	2
External Oscillator	Up to 20MHz
Program Memory Type	Flash
Program Memory (KB)	14KB
RAM Bytes	368
Data EEPROM	256 bytes

2.3 Solar Panel

In this system, a poly-crystalline solar panel is used to convert energy from light energy to electrical energy. Solar PV panel produces power output proportional to their size. A small PV panel will produce

small power and a large PV panel will produce large power. Table 2 is Specification of Poly-crystalline Solar Panel.

Table 2. Specification of Poly-crystalline Solar Panel

Module Type		SYM 90P
Cell Material		Poly Crystalline
Maximum Power	P_{max}	90 W
Maximum Power Voltage	V_{pmax}	18.37 V
Maximum Power Current	I_{pmax}	4.9 A
Open Circuit Voltage	V_{oc}	22.05 V
Short Circuit Current	I_{sc}	5.15 A
Weight	W	20 lb

2.4. Electric Motor

An electric motor is an electrical machine that converts electrical energy into mechanical energy. There are many different electrical motor types, all with their good and bad sides. Motion control is the art and science of precisely controlling the position, velocity and torque of a mechanical drive. Motion-control systems comprise a numerical controller that performs path generation, such as DSP, an amplifier and a motor. DC motors are widely used in practice, particularly in applications where accurate control of speed or position of the load required. The DC motor can provide high starting torque for applications requiring quick stoppage or reversals. Speed control over a wide range is relatively easy to achieve in comparison with all other electro-mechanical energy-conversion devices; in fact, this has traditionally been the DC motor's strength.

2.5 Automatic Solar Tracking Control System

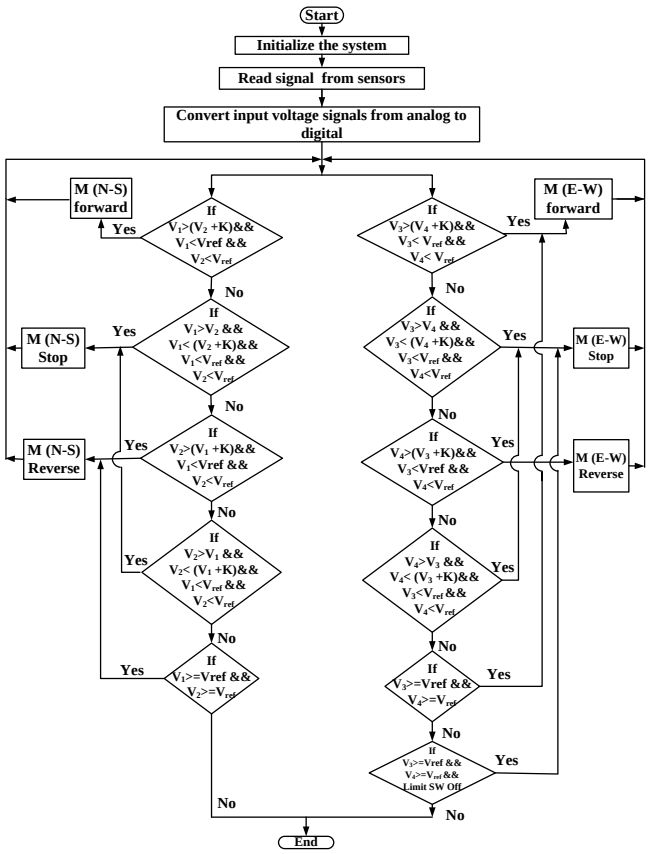

Figure 4. Flow Chart of the Solar Tracking Control System

3. SIMULATION RESULT

Total numbers of sensor are four which are known the Sun is shiny or not. After these sensors sense light, the outputs of LDR are inputs of PIC. As PIC is programming, the motor is running forward direction when light falls on the LDR. If there is no light that is dark, the motor moves reverse direction that is solar panel reaches east that is ready for next day. Simulation of dual axis solar tracker is done with Proteus Software and is shown in Figure 4.

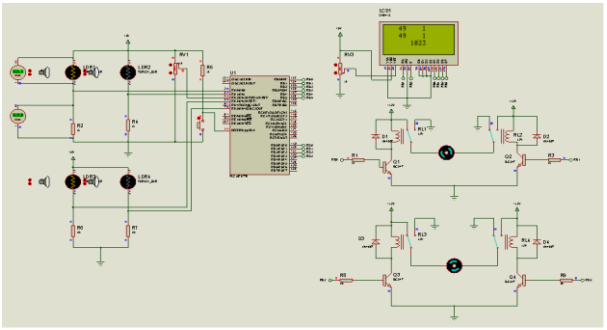

Figure 5. Simulation of Dual Axis Solar Tracker

When the light of the Sun reaches LDR 1 and 3, the value of LDR 1 and 3 will be greater than LDR 2 and 4. As k=40 that is value between LDR 1, 2, 3 and 4, the direction of the motor moves reverse when the value of LDR 2 and 4 are greater than LDR 1 and 3. Table 3 is shown Simulation Result of Motor Forward and Reverse.

Table 3. Simulation Result of Motor Forward and Reverse

LDR1, LDR3	LDR2, LDR4	Motor
49	1	Forward
49	93	Reverse
49	49	Stop

4. TEST RESULT

Figure 5 is shown Display of LDR values, Motors moving Forward and Reverse. Due to dual axis Solar tracker, there are two numbers of motor which move as the direction of the Sun. If one motor moves East to West, other one can move North and South. We need many components such as LDR, solar panel, PIC microcontroller, L298 Motor Driver, motors, Display and so on. Prototype and Display of Motor Forward and Reverse can be seen in Figure 5.

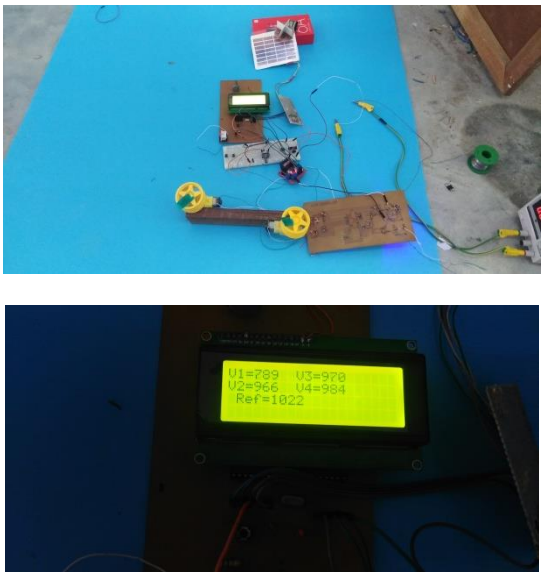

Figure 6. Prototype and Display of Motor Forward and Reverse

Table 4 is Test Result of Motor Forward and Reverse. When LDR 1 and LDR 3 are 789 and 970, motor 1 is running reverse direction. As LDR 2 and LRD 4 are 966 and 984, motor 2 is stop condition. If the value of LDR is greater than other one, the motor moves forward. When the value of LDR is greater than the reference value, LDRs are reset.

Table 4. Test Result of Motor Forward and Reverse

LDR 1	LDR 2	LDR 3	LDR 4	Ref	M 1	M 2
789	966	970	984	1022	Reverse	Stop
973	964	752	982	1015	Forward	Stop

5. CONCLUSION

In this research, the automatic solar tracking system was developed which is based on PIC microcontroller and it can track the sun's position with the simple and effective sensor module. After experimental testing, it can be said that the proposed solar tracking system is a feasible method of maximizing the energy received from solar radiation. This research is proposed to have solar trackers as standard PV systems in residential areas. . Solar trackers are beneficial and dependent on various factors including weather, location, obstruction and cost. The large solar panel arrays would cost in thousands of dollars, so the addition of a solar tracker is very cost effective. Moreover, another benefit is the space saved rather than adding extra panels. As four 90W solar panel are connected in parallel, laptop and projector can cover from this 360W solar panel. Pyay can get the efficient solar radiation so solar power is very suitable in this place.

6. RECOMMENDATION

As this solar tracker is only functional, we have many plans to continue this project. We can substitute DC motor with stepper motor to be very definite. The stepper motor can move step by step very detail. We can add charge controller circuit and the circuit to overcome for battery overcharging. Moreover, we can collect more data with measuring instruments with time schedule such as daily, monthly and yearly. We should consider how much cost effective and energy efficiency by comparing 360W fixed solar panel and equal power dual axis. Another recommendation is that PIC16F887A can be substituted other.

ACKNOWLEDGEMENT

Our Energy and Machine Research group also acknowledges Dr. Nyunt Soe, Rector, Pyay Technological University. Our group also likes to express special thanks to Dr. Soe Winn, Professor, Head of Electrical Power Engineering, Pyay Technological University. Our Head looks like our brother who can give the best way for every case. Our research group would like to say thanks to everyone who help us to do many researches directly or indirectly. Finally and specially, our heartfelt thanks to our parents, family, our pupils, friends and colleagues. Without getting the help from our students from Pyay Technological University, we cannot do any research.

REFERENCES

[1] Ahmed F.Zobaa and Ramesh C.Bansal: *Handbook of Renewable Energy Technology*, 2011

[2] Gilbert M. Master, ISBN 0-471-28060-7): Renewable and Efficient Electric Power System

[3] H.P.Garg and J.Prakash, Solar Energy Fundamentals and Application, New Delhi: Tata MC Graw – Hill, 2005, pp7

[4] Moh Moh Lwin : Master Thesis :Design and Implementation of Photovoltaic Solar Powered Water Pumping System in Hngetpyittaung Village

[5] Swe Swe Mar : Master Thesis: Performance Analysis of Dual-Axis Solar Tracking System using DC Motor

[6] Solar Energy Potential and Applications in Myanmar, Thet Thet Han Yee, Su Su Win, and Nyein Nyein Soe

[7] Thi Thi Aung and Nang Saw Yuzana Kyaing, "Performance Analysis of Dual-Axis Solar Tracking System and a Fixed System by Test Experiment", MTU Journal of Science, Engineering and Technology, 2015.

Evaluation of Quality Control Parameters of Four Different Brands of Paracetamol Tablets

Soe Kyaw Kyaw[1], Yu Yu Hlaing[2]
#1 Dr, Lecturer, Department of Chemistry, University of Yangon
#2 Dr, Assistant Lecturer, Department of Chemistry, East Yangon University
[1]drsoekyawkyawdawei@gmail.com, [2]yuyuhlaing.yyh90@gamil.com

ABSTRACT: *Paracetamol is a non-steroidal anti-inflammatory drug frequently prescribed for relief of pain and fever. The purpose of this project was to evaluate the quality control parameters of four different brands of paracetamol tablets marketed in Yangon Region. Four different brands of paracetamol were taken from market. The tablets used are BPI, PARACAP, Para-Denk and BAL 500. The project study to perform various the quality control paracetamol including weight variation, hardness, disintegration time, identification test and drug assay. The tablets were evaluated to examine if they comply with the specification of BPI. All the tablets of the brands met with the specification of BPI expect the BAL 500 tablets did not satisfy the requirement for the drug assay test.*

Keywords : paracetamol, weight variation, hardness, disintegration, drug assay

1. INTRODUCTION

Paracetamol also known as acetaminophen is active metabolites of phenacitin. Paracetamol or acetaminophen is active metabolites of phenacitin (Figure 1). It is a widely used over-the-counter analgesic and antipyretic. Chemically, it is 4-hydroxy acetanilide [1]. It is a non-steroidal anti-inflammatory drug frequently prescribed for relief of pain and fever [2]. It is also used to treat the headache. The chemical name of acetaminophen is N-acetyl-Para aminophenol [4]. Acetaminophen structure paracetamol or acetaminophen is commonly used as nonprescription drug for analgesic and antipyretic purpose and also called over the counter (OTC) product [10]. Acetaminophen exerts its inflammatory and antipyretic effect in several ways but yet not confirmed. Analgesic effect of acetaminophen is due to prostaglandins (PGs) has been proposed [6], [8].

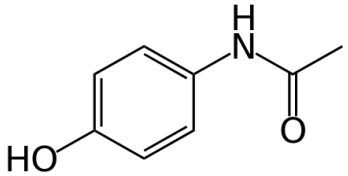

Figure 1. Structure of paracetamol or acetaminophen

Paracetamol, known as acetaminophen is an over-the-counter non-steroidal anti-inflammatory drug (NSAID). It is commonly used as an analgesics and antipyretic agent to treat pain and fever. Unlike the other NSAIDs, the ability of paracetamol to inhibit the function of cyclooxygenase (COX) enzyme is not significant, that is, it's a weak anti-inflammatory drug. The most commonly consumed daily used, 1000 mg results in roughly 50 % inhibition of both COX-1 and COX-2 in whole body assays ex vivo in healthy volunteers [9]. It is used to release mild to moderate pain from headaches, muscle aches, menstrual periods, colds and sore throats, toothaches, backaches, osteoarthritis and reactions to vaccinations (shots) and to reduce fever [1].

Unlike opiates it is almost ineffective in intense pain and has no depressant effect on respiration. It is available in a tablet, capsule, suspension or solution (liquid), drop, extended-released (long-acting) tablet, orally disintegration tablets, suppository, intravenous, and intramuscular form [1]. Generally, the consumption of paracetamol at a recommended dose and under the doctor's instruction is safe. Paracetamol has a low side effect on the gastrointestinal tract and at over dosages, it can cause the hepatic damage severely. Therefore, following the instructions and doctors' advices and knowledge on dosages is primary requirement. However the safety and efficacy of a pharmaceutical dosage form can be guaranteed when its quality is reliable. The efficacy of pharmaceutical dosage forms generally depends on their formulation properties, and manufacturing methods, hence it is likely that the quality of dosage form may vary [3].

2. MATERIALS AND METHODS

All the experimental procedures involved in this research. The chemical supplier, viz., "British Drug House Chemicals Ltd., Poole, England" Kanto Chemical Co., Unc., Tokyo, Japan" are simply abbreviated as BHS and Kanto, respectively.

2.1 Sample Collection

Four different brands (BPI paracetamol, PARACAP, paradenk, and BAL) of 500 mg paracetamol tablets were collected from marked distribution in Yangon Region in December, 2017 as shown in figure 2.

Figure 2. Four different brands of paracetamol tablets

2.2 Weight Variation of Paracetamol Tablets

The 20 tablets were taken from each brand and each tablet was weight individually using the analytical balance. The average weight of the tablets was also calculated.

2.3 Hardness Test of Paracetamol Tablets

Six tablets were taken from different brands of paracetamol and each tablet was placed between two anvils, force was applied to the anvils, and the crushing strength that caused the tablet to break was recorded (Figure 3). The reading was recorded in kg [7], [9].

Figure 3. Hardness Tester

2.4 Disintegration Test of Paracetamol Tablets

First of all, the disintegration tester was assembled. Then 900 mL beaker was filled with distilled water and the temperature was maintained at 37±2°C. After that, one tablet was placed in each of the 6 tubes and the apparatus was operated in Figure 4 for the prescribed time.

Figure 4. Disintegration tester

2.5 Identification of Active Ingredient of Paracetamol Tablets

Paracetamol (0.5 g) was powered and extracted with acetone, filtered and evaporated. The residue was dried in drying oven at 105°C. For the preliminary test, sample (0.1 g) of dried residue was dissolved in 10 mL of distilled water and 0.5 mL of ferric chloride was added. For the confirmatory test, sample (0.1 g) of dried residue was dissolved in 2 mL of 0.2 M HCl and boiled for 3 minutes. And then distilled water was added and cooled. After that 2 or 3 drops of potassium dichromate was added and confirmed the color changed [9].

2.6 Melting Point of Paracetamol tablets

Paracetamol (0.5 g) was powered and extracted with acetone, filtered and evaporated. The residue was dried in drying oven at 105°C. A small amount of dried residue was transferred to the capillary tube and inserted into the melting point apparatus and the melting point was recorded [7], [9].

2.7 Drug Assay (Percentage Content of Paracetamol) of Paracetamol Tablets

Drung assay (percentage content of paracetamol) was determined by UV spectrophotometer (SHIMADZU UV mini-1240). A 20 tablets were weighed and powered. The powder (0.2 g) was dissolved in 50 mL of NaOH and diluted with 100 mL of distilled water. Then the solution was shaken well for about 15 min with the help of shaker. And then sufficient distilled water was added to make the 200 mL solution with 200 mL volumetric flask and filtered. 10 mL of filtrate was taken and diluted to 100 mL with distilled water using 100 mL volumetric flask. From this solution, 10 mL was again taken and 10 mL of NaOH was added and then diluted to 100 mL with distilled water.

The spectrophotometer was warmed-up. One cuvette was rinsed with distilled water. And the cuvette was filled with distilled water and put in the sample compartment. Then the wavelength was set at the maximum wavelength of 257 nm and the absorbance was set to zero.

A second cuvette was rinsed with distilled water and once with sample solution. After that the cuvette was filled with sample solution and put in the sample compartment. Then the absorbance was measured at 257 nm and the absorbance was recorded. The content of the paracetamol was calculated by taking 715 as the value of A (1%, 1cm) at the maximum wavelength of 257 nm [7], [9].

3. RESULTS AND DISCUSSION

3.1 Preliminary Information and Physical Appearance of Four Different Brands of Paracetamol Tablets

Four different brands of paracetamol tablets have collected in market. Preliminary information (manufacturing date, expiry date, batch number and REG No.) were recorded. And then physical appearance such as colour, shape, scoring and logo were also recorded. This information of four different brands of paracetamol tablets were shown in Tables 1 and 2.

Table 1. Preliminary information on the drug samples used

Sample	Manuf. Date	Exp. Date	Batch number	REG No.
BPI Paracetamol	Nov, 2017	Oct, 2020	7031B1	R2108L0 174
PARACAP	Jan, 2018	Jan, 2022	0053	R1909A 3679
Para-Denk	Oct, 2016	Sep, 2021	3218	R1608A 8950
BAL 500 paracetamol	Dec, 2017	Nov, 2021	UBPM17 110	R2011A 1720

Table 2. Physical appearance of different brands of paracetamol tablets

Brand	Color	Shape	Scoring	Logo
BPI paracetamol	White	Round	Yes	Yes
PARACAP	White	Cylindrical	Yes	Yes
Para-Denk	White	Round	Yes	Yes
BAL 500 paracetamol	White	Round	Yes	Yes

3.2 Weight Variation of Paracetamol Tablets

The percentage weight variation was calculated to determine whether the individual weight is within the range or not. According to British Pharmacopoeia (BP), the weight for tablets weighing greater than 325 mg, there should not be more than two tablets deviating from the average by no more than 5 % [5].

The average weight of BPI paracetamol, PARACAP, Para-Denk and BAL 500 were shown in Table 3 and Figure 5. According to the results the tablets of all paracetamol brands (BPI, PARACAP, Para-Denk, and BAL 500) meet the specification indicating the uniform distribution of the active ingredient. All of four brands were showed percentage weight variation of 0.1 to 2.6 %, which is outside the acceptable range of 5 %. The test was performed as per the official producer, 20 tablets were randomly selected and weighed individually and also average weight was calculated. The difference between average and individual was calculated; further % weight variation was calculated and compared with the BP limits. All of the four brands showed percentage weight variation within the range of ± 5 and therefore the four different brands have passed the quality control parameter and satisfied the specification of BP.

3.3 Hardness

Hardness test indicates dissolution profile of tablets. If tablets are harder it is difficult to dissolve in prescribed time. The average hardness of BPI Paracetamol, PARACAP, Para-Denk and BAL 500 were mentioned in Table 4 and Figure 6. The tablets need to meet the requirement to have a certain amount of strength or hardness to withstand the mechanical shock of handling and transportation. It is one of the primary requirements that the hardness of the tablets are within the range since it is related to the disintegration. Tablets with increased hardness value tend to have increasing disintegration time and a minimum hardness of 4 kg is essential. According to the results, the tablets of all paracetamol brands satisfied the specification.

Table 3. Mean weight and standard deviation of paracetamol tablets

Brand	Mean Weight (g) n=20	Standard Deviation
BPI Paracetamol	0.5467	0.005182
PARACAP	0.5759	0.005274
Para-Denk	0.6131	0.003268
BAL 500	0.5931	0.009602

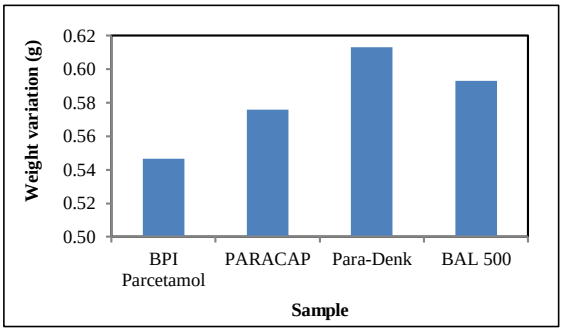

Figure 5. Weight variation (mean values) of the four different brands of paracetamol tablets

Table 4. Mean hardness and standard deviation of paracetamol tablets

Brand	Mean Hardness	Standard Deviation
BPI Paracetamol	11.366	0.5957
PARACAP	11.65	2.0078
Para-Denk	9.438	0.6509

BAL 500	12.76	1.4288

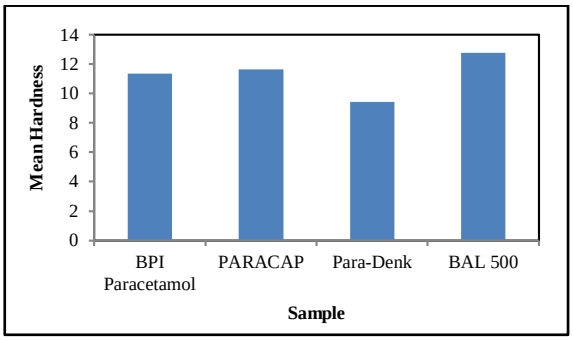

Figure 6. Hardness (mean values) of four different brands of paracetamol tablets

3.4 Disintegration Time of Paracetamol Tablets

The disintegration time of the tablets of all paracetamol brands (BPI, PARACAP, Para-Denk and BAL 500) were in the range that they all met the specification of BP where the maximum disintegration time of 15 minutes as shown in Table 5 and Figure 7.

Table 5. Mean disintegration time and standard deviation of paracetamol tablets

No.	Brand	Mean time (sec) n = 6	Standard Deviation
1	BPI Paracetamol	2.317	0.2137
2	PARACAP	1.550	0.5128
3	Para-Denk	1.133	0.9158
4	BAL 500	1.450	0.1049

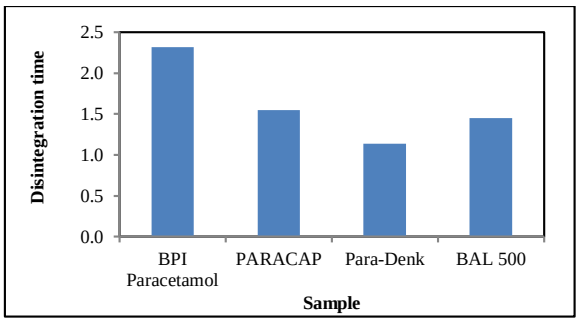

Figure 7. Disintegration time (mean value) of four different brands of paracetamol tablets

3.5 Identification of Tests

3.5.1 Identification of Active Ingredient of Paracetamol Tablets

The identification of active ingredient for BPI paracetamol, PARACAP, Para-Denk and BAL 500 were identified. It was found that the preliminary test for all brands observed a blue color. And then the confirmatory test observed a violet color solution. Therefore, all brands of paracetamol tablets were found to be present 4-hydroxyacetanilide as shown in Table 6. **A**ll the tablets under the study showed the positive results in the preliminary test and confirmatory test. All brands of tablets were contained the active ingredient 4-hydroxyacetanilide.

3.5.2 Melting Point of Paracetamol Tablets

The melting point of BPI paracetamol, PARACAP, Para-Denk and BAL 500 were characterized by melting point in Table 7 and Figure 8. The melting points of all brands of tablets were found to be showing in the range all of the tablets were melted between 169 and 170ºC and BP puts the melting point to be 169ºC. According to the results, the tablets of all paracetamol brands satisfied the specification of BP.

3.5.3 Drug Assay of Paracetamol Tablets

This third identification test plays a very important role in pharmaceutical analysis. The absorbance of BPI paracetamol, PARACAP, Para-Denk and BAL 500 were measured by UV-visible spectrometer. It was found that the percent content of paracetamol of BPI paracetamol, PARACAP, Para-Denk and BAL 500 tablets shown in Table 8 and Figure 9. According to the results, tablets of the three different brands (BPI, PARACAP, Para-Denk) met the specification of BP where the percentage content of paracetamol tablets needs to be in the range of 95 to 105 %, except the tablets of BAL-500 which failed to meet the requirement containing only 94 % of paracetamol.

Table 6. Results of the qualitative analysis of paracetamol tablets for four different brands

Test	Observation	Inference
Preliminary test	A blue color was observed.	4-hydroxyacetanilide may be presented.
Confirmatory test	A violet color was observed.	4-hydroxyacetanilide is present.

Table 7. Melting point of paracetamol tablets

Brands	Melting Point (°C)
BPI Paracetamol	168.6

PARACAP	169.8
Para-Denk	170.3
BAL 500	169.7

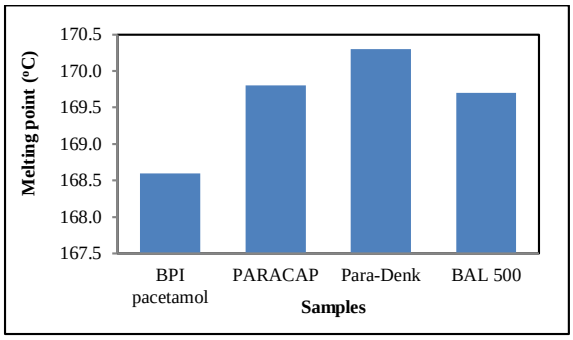

Figure 8. Melting point of four different brands paracetamol tablets

Table 8. Percentage content of paracetamol tablets

Brand	Average weight of tablet (g)	Sample weight (g)	*A	Content (%)
BPI paracetamol	0.5467	0.201	0.637	97
PARACAP	0.5759	0.201	0.650	104
Para-Denk	0.6131	0.203	0.600	101
BAL 500	0.5931	0.203	0.577	94

*A (1 %, 1 cm) at the maximum wavelength 257 nm = 715

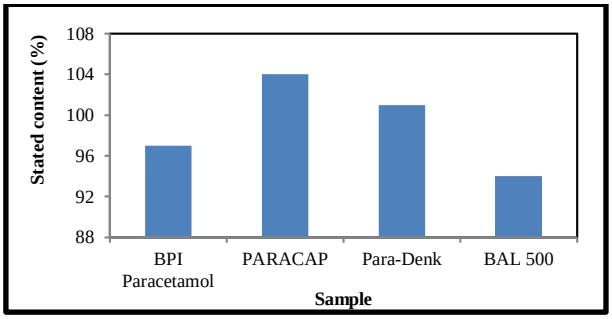

Figure 9. Stated content (%) of four different brands of paracetamol tablets

4. CONCLUSIONS

Paracetamol is a nonprescription drug. It is well established drug used for antipyretic and analgesic purpose. From the study of comparative quality control of paracetamol tablets marketed in Yangon Region, the following inferences can be deduced. Preliminary information (manufacturing date, expiry date, batch number and REG No.) were recorded. The identification of tests for BPI paracetamol, PARACAP, Para-Denk and BAL 500 were identified. All the tablets under the study showed the preliminary test for all brands observed a blue color and then the confirmatory test observed a violet color solution. Therefore, all brands of tablets were contained the active ingredient 4-hydroxyacetanilide. It was observed that all the tablets of the four different brands complied with the specification of BP, expect for the BAL 500 tablets which did not meet the drug assay test. In this study, all the tablets of the four different brands needs to meet the all the parameter to have the full therapeutic efficacy. From these results of the study, it can be concluded that the four different brands (BPI, PARACAP, Para-Denk and BAL 500) meet the very basic requirements of the quality control test that they have the full potential of therapeutic efficacy.

ACKNOWLEDGEMENTS

The authors would like to express my deep appreciation to professor and head, Dr Ni Ni Than, Department of Chemistry, University of Yangon, for her kind provision of the research paper and comments offered to me during the course of this research work.

REFERENCES

[1] (2012) MedlinePlus website. [Acetaminophen]. Available: http://www.nlm.nih.gov/medlineplus/druginfo/meds/a681004.html#other-uses

[2] A. Burke, E. Smyth, and G. A. FitzGerald, *Goodman & Ilman's the Pharmacological Basis of Therapeutics*, 11th ed., Analgesic-Antipyretic Agents; Pharmacotherapy of Gout. In L.B. Brunton, J.S Lazo, & K.L. Parker Ed., New York: McGraw-Hill, 2005.

[3] A. K Nayak, "Comparative in vitro dissolution assessment of some commercially available paracetamol tablets," *International Journal of Pharmaceutical Sciences Review and Research*, vol. 2, pp. 29-30, May. 2010.

[4] A. Kar, M. N. Amin, M. S. Hossain, M. H. E. Mukul, M. S. U. ashed, and M. Ibrahim, "Quality analysis of different marketed brands of paracetamol available in Bangladesh," *International Current Pharmaceutical Journal*, vol. 4, pp. 432-435, Aug. 2015.

[5] British Pharmacopoeia, *British Pharmacopiea Volume I and II, Monograph: Medicinal and Pharmacuetical Substances, Paracetamol*, British Pharmacopeia Commission, UK, 2013

[6] F. Asim, K. H. Daulat, D. I. Umair, K.Izzatullah, W. Rai, T. Saad, F. Anum and S. Muhammad, "Comparative study of commercially available brands of acetaminophen in lahore, Pakistan," *World journal of pharmacy and pharmaceutical sciences*, Vol. 5, pp. 155-162, Oct. 2016.

[7] L. Lachman, H. A. Lieberman, and I. L. Kanig, *The Theory and Practice of Industrial Pharmacy*, 3rd ed., Lea & Febiger. Lippincott Williams & Wilkins, Philadelphia, USA., 1986.

[8] L. Teklu, E. Adugna, and A. Ashenef, "Quality evaluation of paracetamol tablets obtained from the common shops (kiosks) in addis ababa, ethiopia,"

International Journal of Pharmaceutical Sciences and Research, Vol. 5, pp. 3502-3510, Jan. 2014.

[9] M. Zinia, "Determination of the quality control parameters of paracetamol tablets in bangladesh pharma market," Degree Bachelor of Pharmacy thesis, Department of Pharmacy, East West University, Aftabnagar, Dhaka, July 2012.

[10] P. Karmakar, and M. G. Kibria, M. G. "In-vitro comparative evaluation of quality control parameters between paracetamol and paracetamol/caffeine tablets available in Banglades," *International Current Pharmaceutical Journal*, vol. 1, pp. 103-109, 2012.

Removal of Organic Dye (Methylene Blue) by Activated Bentonite Clay

[1]Pyae Sone Aung, [2]Zaw Naing
[1]*Demonstrator, Department of Chemistry, University of Medicine (2), Yangon*
[2]*Associate Professor, Department of Chemistry, Dagon University*
pyaesoneaung248@gmail.com, zawzawnaing999@gmail.com

ABSTRACT: *This research work is designed to investigate the removal of organic dye (methylene blue) from aqueous solution by bentonite and activated bentonite. Bentonite was collected at the foot site of Mount Poppa from Kyauk Padaung Township, Mandalay Region. The bentonite was heated at the optimum temperature of 400 ºC to form activated bentonite and then characterized by EDXRF and SEM techniques. The physicochemical properties such as pH, bulk density, moisture content and surface area were also determined. The adsorption capacity as a function of contact time, initial concentration and dosage on bentonite and activated bentonite have been studied. From these investigations, the dye adsorption increased with the increasing adsorbent dosage and decreased with increasing initial dye concentration. It was found that the adsorption was rapid process with 73-84 % of the dye removed within the first 10-20 min. Therefore, bentonite can be used as environmental and eco-friendly sorbent material for the removal of organic dyes from waste water.*

Keywords: Methylene Blue, Bentonite, Sorption Studies, EDXRF spectrometer, SEM analysis

1. INTRODUCTION

1.1 Bentonite Clay

Bentonite clay is a fine-grained clay that contains primarily montmorillonite minerals. Bentonite is formed by the weathering of volcanic ash, usually in a marine environment [1]. Bentonite clay, chemical formula, $Al_2O_3 4SiO_2 H_2O$, comes in a broad range of colors, including light olive green, brick red, gray, brown and yellow. Bentonite clay feels greasy, slippery or like plastic when wet, but its absorbent properties make it great to use as a paste [2].

There are two basic kinds of bentonite, and their names depend on the primary elements found in the clays. Sodium bentonite swells when it gets wet, allowing it to absorb a very high volume of liquid [3]. Calcium bentonite, commercially called pascalite, fats and oils found in a solution. This type of bentonite clay is the primary active ingredient of Fuller's Earth, which was one of the first industrial cleaners. [4]

Bentonite has many applications to a broad range of industrial and other activities. Major domestic uses, which include binding foundary sand, absorbing grease, oil and and improving the properties of many drilling muds. Bentonite clay is used in many commercial personal care products, including baby powder, eczema lotion, face creams, mud packs and sunburn lotions. Speciality uses of bentonite include serving as an ingredients for ceramics; water proffing and sealing in civil engineering projects (e.g. blocking seepage loss from landfill sites, nuclear waste repositories, irrigation ditches, treatment ponds) [5].

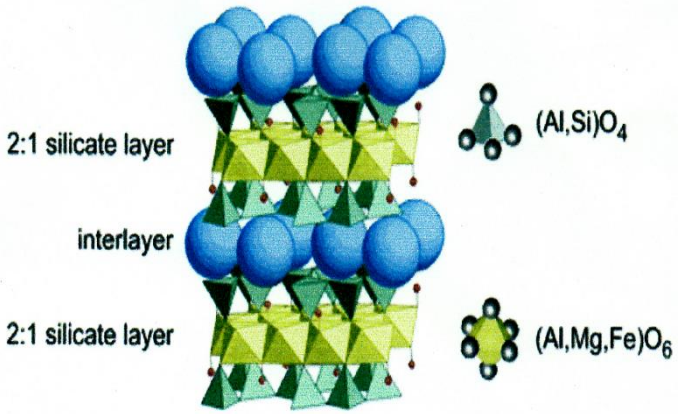

Figure 1. Layer structure of bentonite clay

1.2 Methylene Blue

Methylene blue is a heterocyclic aromatic chemical compound with the chemical formula $C_6H_{18}N_3SCI$. It has many uses in biology and chemistry, for example it can be used as a stain for pharmaceutical drug. At room temperature it appears as a solid, odorless, dark green powder, it yield a blue solution when dissolved in water. New methylene blue nor with the methylene violet often used as a pH indicator [6].

Methylene blue injection is used to treat a condition called methemoglobinemia. This condition occur when the blood cannot deliver oxygen to where it is needed in the body. Methylene injection is also used as a dye to stain certain parts of the body before or during surgery. Methylene blue (MB) is a cationic dye having various applications in chemistry, biology, medical science and dyeing industries. Long term exposure of methylene blue can cause vomiting, nausea, and hypertension [7].

2. MATERIALS AND METHODS

2.1 Collection and Preparation of Samples

The bentonite clay sample was collected from Kyauk Pataung Township, Mandalay Region. After collection, the bentonite sample was washed with tap water to remove impurities and then air-dried under the shade to prevent some reaction of sunlight. Then the bentonite was ground to fine particles and sieved into 90 μm aperture size and stored in air tight plastic bag so that the sample was free from getting molds and can prevent moisture, as well as other contaminations and was ready to be used for the experimental works. Then, this bentonite sample was heated at 400 ºC in furnace to get activated bentonite. Deionized water was used through the experiment. Stock solution (1000 mg/L) of methylene blue solution was prepared in deionized water. The stock solution was diluted as required to obtain the standard solutions.

Figure 2. Sample collection site

Figure 3. Bentonite clay sample

2.2 Adsorption Methods

Sorption measurements were made by a batch technique at room temperature. Bentonite clay was used as adsorbent and characterized by EDXRF and SEM analyses. Different concentrations of methylene blue solutions were used as adsorbate. The batch mode was selected because of its simplicity and reliability. In all experiments, the required volume (25 mL) of the adsorptive compound solution was added to bentonite clay absorbent at room temperature. The solutions were then shaken vigorously for a given time period to reach equilibrium. After completion of a selected shaking time, the suspensions were then filtered. The amount adsorbed was determined by using UV-visible spectrophotometer.

3. RESULTS AND DICUSSIONS

3.1 Physicochemical Properties of Bentonite

Physicochemical properties of prepared raw bentonite and activated bentonite were determined. The physicochemical properties, such as moisture content, bulk density, pH and surface area of raw bentonite and activated bentonite are presented in Table 1. It was found that raw bentonite was higher moisture content than those of activated bentonite. The moisture content has no effect on its adsorption proporties. pH values of raw bentonite and activated were nearly the same. Moreover, it was also found that activated bentonite has higher bulk density and surface area than those of raw bentonite. The greater the surface area, the larger the adsorptive properties of adsorbent samples. Surface area and porosity is the main factor for increasing the adsorptive power of an adsorbent sample.

Table 1. Physiochemical Properties of Bentonite

No.	Physical Properties	Raw bentonite	Activated bentonite
1.	Moisture (%)	1.01	0.99
2.	Bulk density (g cm^{-3})	1.48	1.57
3.	pH	6.82	6.90
4.	Surface Area (m^2g^{-1})	44	47

3.2. Energy Dispersive X-Ray Fluorescence (EDXRF) Analysis

The chemical constituents of prepared raw bentonite and activated bentonite were detected by using EDXRF analysis. Figures 4(a) and 4(b) show the EDXRF spectra of raw bentonite and activated bentonite. According to the EDXRF spectra of raw bentonite and activated bentonite, iron which was the main component, silicon which was the second major component and others were trace constituents. These data were shown in Table 2.

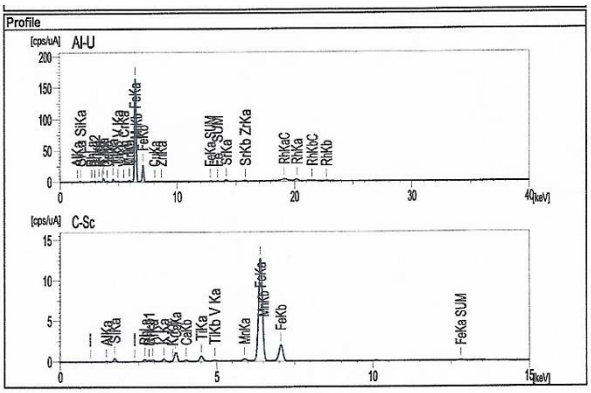

Figure 4(a). EDXRF spectrum of raw bentonite

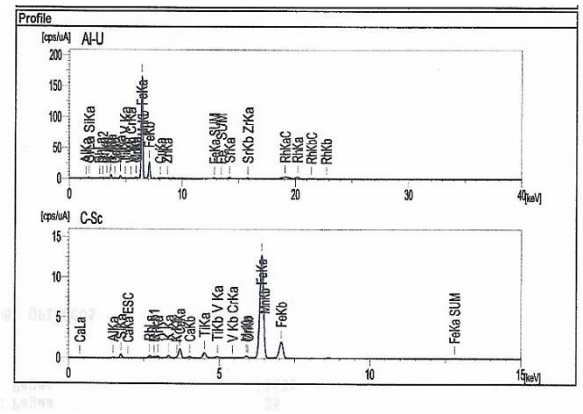

Figure 4(b). EDXRF spectrum of activated bentonite

Table 2. Relative Abundance of Elements Present in Raw Bentonite and Activated Bentonite by EDXRF Spectrometry

Element	Relative Abundance (%)	
	RB	AB
Fe	36.642	37.376
Si	33.148	32.812
Al	16.937	16.741
Ca	6.818	6.579
K	2.504	2.571
Ti	2.489	2.497

***RB = raw bentonite, AB= activated bentonite**

3.3 Scanning Electron Microscopy (SEM) Analysis

Raw bentonite and activated bentonite samples were examined by scanning electron microscope (SEM) for a visual inspection of external porosity and micro-texture. Activated bentonite powder can remove the mineral elements and improve the hydrophilic nature of surface. The SEM micrographs of activated bentonite is formed by sheets and every sheet clinged closely to each other. Consequently, raw bentonite and activated bentonite have a large surface area and leads to adsorption of waste and impurities from water. The SEM micrographs of raw bentonite and activated bentonite are shown in Figure 5(a) and 5(b).

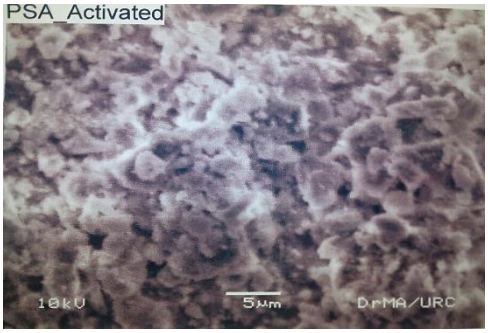

Figure 5(a). SEM micrograph of raw bentonite

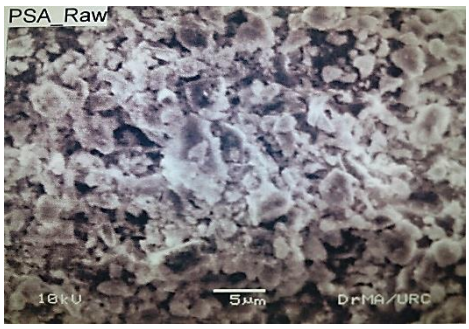

Figure 5(b). SEM micrograph of activated bentonite

3.4 Removal of Methylene by Raw Bentonite and Activated Bentonite

3.4.1 The Effect of Contact Time on Dye Removal

The effect of contact time on the removal of methylene blue was studied. The amount of raw bentonite and activated bentonite (500 mg / 25 mL) for each dye solutions was used and the solutions were equilibrated. Table 3 and corresponding Figure 6, showed effect of contact time on the removal of methylene blue.

In activated bentonite and dye system, it was observed that adsorption were enhanced between the adsorbed dye molecule and activated bentonite. The removal percent increases with increasing time. From the results of the Figure 6, there was an effect of contact time on the adsorption of organic dye by raw bentonite and activated bentonite. The removal percent of dye on raw bentonite sample was lower than that of the activated bentonite sample.

Table 3. The Removal Percent of Methylene Blue at Different Contact Times by Raw Bentonit and Activated Bentonite

Volume = 25 mL, Initial concentration = 50 ppm, Dosage = 0.4 g

Contact Time (min)	Removal percent of dye (%)	
	RB	AB
10	65.71	73.58
20	73.29	84.91
30	76.41	87.78
40	80.07	92.34
50	85.33	97.69
60	90.1	97.4

Table 4. The Removal Percent of Methylene Blue at Different Concentrations by Raw Bentonite and Activated Bentonite

Volume = 25 mL, Dosage = 0.4 g, Time = 1 h,

Initial Concentration (ppm)	Removal Percent of Dye (%)	
	RB	AB
10	95.5	99.8
20	93	99
30	92.8	98.8
40	91.7	98.6
50	90.1	97.4
60	78.8	82.61
70	75.9	79.84
80	72.7	76.45
90	66.23	72.1
100	57.4	65.15

e

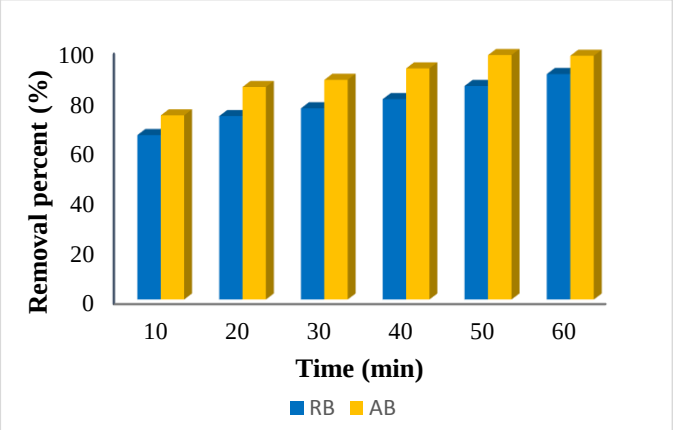

Figure 6. Effect of contact time on removal percent of methylene blue by raw bentonite and activated bentonite

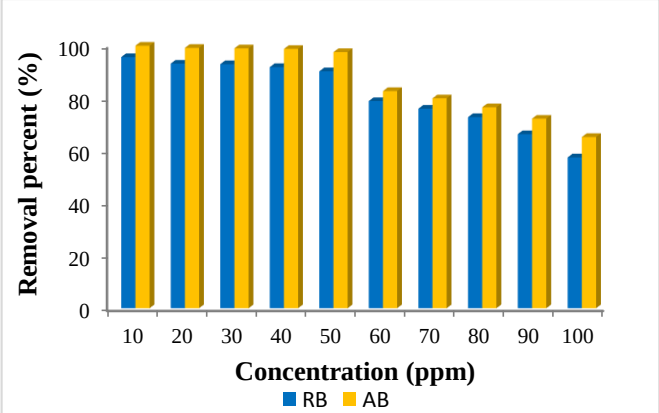

Figure 7. Effect of concentration on removal percent of methylene blue by raw bentonite and activated bentonite

3.4.2 The Effect of Initial Concentration on Dye Removal

Table 4 and Figure 7 shows that the initial dye concentration on the adsorption of raw bentonite and activated bentonite. According to Figure 7, increasing the initial dye concentration lead to a decrease in adsorption capacity of dyes on raw bentonite and activated bentonite. The adsorption capacity of activated bentonite was higher than raw bentonite with initial dye concentrations at 10 ppm to 100 ppm for methylene blue, it was found that the removal percent were nearly between 57 % and 99 %. These indicated that the initial dye concentration played with large effect in the adsorption capacity of organic dyes on activated bentonite.

3.4.3 The Effect of Dosage on Dye Removal

In order to find out the minimum amount of adsorbents required for the removal of organic dye for raw and activated bentonite, the experiments of dosage were conducted. It is evident that for the quantitative removal of 50 ppm dye solutions in 25 ml. Table 5 and Figure 8 show the effect of dosage on removal of organic dyes by raw bentonite and activated bentonite. Maximum dosage of 0.4 g is required in case of raw bentonite and activated bentonite. The data clearly show that the activated bentonite was more effective than raw bentonite. It was observed that by increasing the absorbent dose from 0.1 g to 0.6 g, the removal efficiency increased and attained to equilibrium. The number of available adsorption sites increase by increasing the adsorbent dose and that results in the increase of removal efficiency.

Table 5. The Removal Percent of Methylene Blue at Different Dosages by Raw Bentonite and Activated Bentonite

Volume = 25 mL, Concentration = 50 ppm, Time = 1 h,

Dosage (g)	Removal Percent of Dye (%)	
	RB	AB
0.1	68.4	76.45
0.2	71.4	78.56
0.3	81.7	85.5
0.4	90.1	97.4
0.5	90.7	98.6
0.6	94.2	98.3

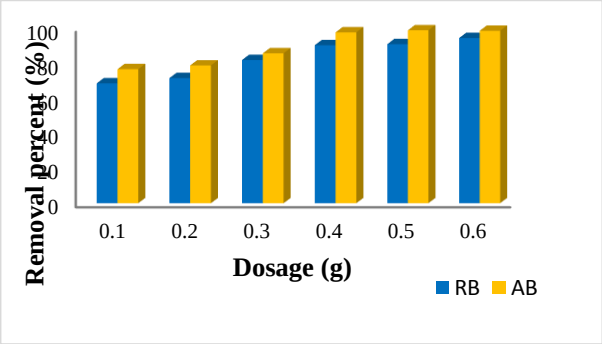

Figure 8. Effect of dosage on removal percent of methylene blue by raw bentonite and activated bentonite

From these results, the concentration of the dye samples can be calculated from the equation. The amount of dye adsorbed per unit weight of an adsorbent, q, was calculated using the following formula.

$$q = (C_o - C_e)\, V / m \quad (1)$$

where, C_o is the initial concentration of dye, (mg L^{-1}); C_e is the equilibrium concentration of dye in solution (mg L^{-1}), m is the mass of the bentoniote (mg) and V is the volume of solution (L).

4. CONCLUSIONS

This study reveals that bentonite and activated bentonite were tested with regards to decolourization nature of methylene blue aqueous solution. The EDXRF spectra shows that both bentonite samples contain iron, silica, aluminium, and calcium in major constituents and potassium, titanium and manganese in minor constituents. The SEM figures indicate that bentonite was found to be sponge like nature and porous structure. To determine the optimum conditions, the effect of contact time, effect of initial dye concentration and effect of dosage of bentonite were also investigated for the removal of dye (methylene blue) on bentonite samples. Activated bentonite sample was found to remove 97.4 % of methylene blue under the optimum conditions of dosage 0.4 g, contact time 1 h and initial concentration of 50 ppm. It was deduced that the percent removal of dye increase with the increasing time. The minimum dosage of bentonite (0.1 g) is required to remove the methylene blue dye. On the context of the resulting data, bentonite can be used as environmental and eco-friendly sorbent material for the removal of organic dyes from wastewater.

ACKNOWLEDGEMENT

The author would like to thank Dr Zaw Naing, Associate Professor, Department of Chemistry, Dagon University, for following to be carry out of this research programmed. The author also gratefully acknowledge the support and help of the Universities' Research Centre (URC) for EDXRF and SEM measurements.

REFERENCES

[1] S. Ozcan and A. Ozcan, "Adsorption of Acid Dyes from Aqueous Solutions onto Acid Activated Bentonite". *Journal of Colloid on Interface Science*, 2004, pp-39-45

[2] N. Nwe Aung, "Study on the Colour Removal of Some Texitle Dyes by Modified Bentonites". Myanmar: PhD Dissertation, University of Yangon, 2011, pp-37-52

[3] M. Waine Sein, "The Study of Bleaching Characteristics of Burmese Bentonite Clay". Burma: B.Sc(IC), Yangon Arts and Science University, 1997, pp-1-103

[4] T. Win Kyaw, "Refining of Used Engine Oil by Using Bentonite Clay to Produce Base Oil". Myanmar: PhD Dissertation, University of Yangon, 2009, pp-35-42

[5] Z. Naing, "Studies on the Uses of Local Unburned Carbon as Environmental Friendly Sorbent Material". Yangon: PhD Dissertation, Department of Chemistry, University of Yangon, 2005, pp-19-23

[6] A. Gurscs., S. Kaaca and R. Bayrak, "Determination of Adsorptive Properties of Clay/water System: Methylene Blue Sorption". *Journal of Colloid on Interface Science*, 2004, pp-310-314

[7] H. Tahir, M. Sultan and Q. Jahanzeb, "Removal of Basic Dye Methylene Blue by Using Bioabsorbents Ulva Lactuca and Sargassum". *African Journal of* Biotechnology, 2008, pp-2649-2655

Assessment of Soil Quality by Supporting with Pe-Bizat, Peanut Husk, Cowdung from Taung Thaman Village, Amarapura Township, Mandalay Region

Pa Pa San[1], Tin Myo Latt[2], Thandar Khaing[3], Nyein Nyein Aye[3], Yi Yi Lwin[3]
[1,2,3]*Department of Chemistry, Yadanabon University, Mandalay, Myanmar*
papasan1771@gmail.com

ABSTRACT : *The aim of this research is to determine the effect of organic fertilizer (Pebizat plant, Peanut husk, Cowdung) application on physicochemical properties of soil collected from Taung Thaman Village, Amarapura Township, Mandalay Region. This determination was carried out on unfertilized soil sample 1 as control and fertilized soil sample 2 and 3 which were prepared by addition of organic fertilizer 10 % of different ratio of sample 2 and 3 to soil. pH, moisture, organic matter, exchangeable cation, texture and electrical conductivity (EC) of these soil samples were determined by their respective methods. The elemental composition of soil samples were measured by applying Energy Dispersive X-ray Fluorescence (EDXRF). The contents of N, P, K nutrients of fertilizer were determined by chemical instrumental methods. Available N and P contents were determined by alkaline permanganate method and Truog's method respectively. Available K of fertilized and unfertilized soil sample was determined by AAS.*

Keywords : pH, electrical conductivity, EDXRF, AAS

1. INTRODUCTION

Soil is an important source of raw materials. Although the concept is quite clear for agriculture where soil is the main raw material from which food is produced. Soil provides raw materials such as clay, sands, minerals and peat which are used for many different industrial applications. As is the case of "more traditional" raw material such as iron ore, oil and natural gas, soil is essentially a non-renewable resource with potentially rapid degradation rates and extremely slow formation and regeneration processes [1]. The use of soil as a source of raw materials is obviously depleting the available soil resources and is considered as a non-sustainable type of soil use. The potential for global warming due to increasing and concentrations of radiatively active gases in the atmosphere is of current concern. Several possible causes of soil degradation are acidification, salinization, and sodification, accumulation of toxic elements depletion of plant nutrients, reduction of soil organic matter content, composition and crusting and water logging, except for rice (Website 1).

Application of organic residues is recommended to compensate the soil organic matter (SOM) decline after the conversion of native soil to agriculture soil. Addition of organic residues and their composts in agriculture to enhance soil fertility results in biological transformations that can have profound effect on chemical process. e.g. acidity and alkalinity can be generated by the mineralization and oxidation of organic N. These changes may lead to the precipitation and dissolution of soil carbonates in calcareous soils in semi-arid and arid regions. Calcareous soils cover more than 47 % of Earth's land area and many properties of these soils depend on the reactivity of the carbonate system [2].

Soil organisms contribute to a wide range of essential ecosystem services, including the maintenance of soil fertility through the decomposition of organic matter (OM), the recycling of carbon and nitrogen and other nutrients, the improvement of soil structure for erosion control, higher water storage and improve water flow [2, 3]. The beneficial effects of increased levels of SOM on chemical, physical and biological soil properties have been widely demonstrated [4].

Soil conservation is the prevention of soil loss from erosion or reduced fertility caused by over usage, acidification, salinization or other chemical soil contamination. Slash and burn and other unsustainable methods of subsistence farming are practiced in some less developed areas (Website 1)

1.1 Aim and Objectives

The aim of this project paper is to investigate the effect of soil quality by using Pe-bizat, Peanut husk, cowdung.

The objectives are

- To collect soil samples
- To prepare collected soil samples for analysis
- To determine particle size of soil samples
- To measure physicochemical properties
- To characterize soil properties of advanced Spectroscopic Techniques such as EDXRF, AAS

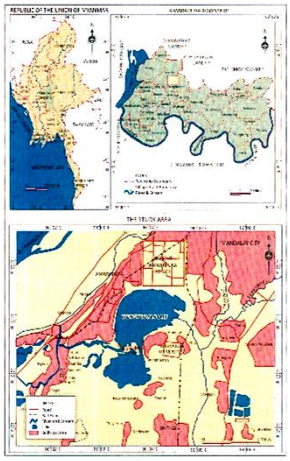

Figure 1. Location map of study area

Soil

Soil plays an important role in the nutritional value of our food. Soil can be defined as a solid material on Earth's surface that results from the interaction of weathering and biological activity on the parent material or underlying hard rock [3].

Sources of Soil Pollution

Sulphurdioxide (SO_2), and $NO_2.SO_2$ present in air undergoes photolytic and catalytic oxidation to form SO_3 which reacts with rainy water or moisture to form acid rain. This acid rain damages the standing crops. Repeated use or excess use of the same fertilizer pollutes the soil. Inadequate damage system in fields is another source of soil pollution. Spraying the vegetable and fruit plants with insecticides and herbicides pollutes the soil [4].

Ion Exchange in Soil

When the loosely held cations or anions on the mineral surfaces are replaced by ions of the same charge (sign and magnitude) in solution. Cation exchange is most common and necessary for soil fertility. As soil weather, they lose cation exchange capacity and lose fertility.

Cation Exchange

Clay minerals have negative charge due to substitution of aluminium or silicon in the crystal lattice. Humus also contributes negative change, due to the presence of dissociated organic acids.

$$\text{humus} - \text{COOH} \longleftrightarrow \text{humus} - \text{COO}^- + \text{H}^+$$

Cations move out of soil solution and adsorb anionic soil colloids (clay or humus), kicking cations that were previously attached back out into the soil solution.

Cation Exchange Capacity (CEC)

The mole of exchangeable positive charge per unit mass 100 g of dry soil (mmole/100 g).

Calcium and magnesium contribute twice as much to the CEC as an equivalent number of sodium and potassium ions because of their 2+ charges (Website 1).

Anion Exchange

The important soil anions, nitrate and phosphate, behave in different ways at exchange sites. Nitrate and chloride are only weakly held at positive sites. Phosphate and sulfate are very strongly bound to the exchange sites. Phosphate can become covalently and irreversibly bound.

Anion Exchange Capacity (AEC)

Anion exchange capacity is a measurement of the positive charges in soils demonstrating the amount of negative charges which a soil can absorb. There are relatively few anions that are restrictive in agriculture but they are important, such as sulfur or phosphorus. The anion lyotrophic series is:

$$H_2PO_4^- > SO_4^{2-} > NO_3^- > Cl^-$$

CEC and AEC will generally increase when pH drops and decrease when pH rises [1].

Plant Nutrients

Plants require 17 elements for normal growth. Carbon, hydrogen and oxygen are found in air and water. Nitrogen, potassium, magnesium, calcium, phosphorous and sulfur are absorbed from soil. The latter six elements are used in relatively large amounts by plants and are called macronutrients. There are eight other elements that are used in much smaller amount, these are called micronutrients or trace elements. The micronutrients include iron, zinc, molybdenum, manganese, boron, copper, cobalt and chlorine [5].

Fertilizer

A fertilizer is a materials supplies nutrients to plants, the technical term "fertilizer" denotes any materials, organic or synthetic applied to the soil or sprayed on plants to add nutrients for plant growth. Fertilizer, organic or inorganic mineral substances occuring in nature or man-made are used as plant nutrients to engender changes in the chemical properties of the soil for plant growth. Chemical salt, which contains plant nutrients were used as fertilizer only during the last 100 years [6].

Fertilizers may be classified as organic fertilizers and inorganic fertilizers or chemical fertilizers. There are two types of organic fertilizers, manure and humus. Manure is obtained by the decomposition of animal dung and urine. Humus comes from plant residues. Chemical fertilizers are an increasingly important factor in prosperous agriculture. Fertilizers are used primarily, to increase the supply of available plant nutrients in the soil and also to balance the plant nutrients ratio [3].

Manures are best used as soil conditioners instead of nutrient suppliers. Horse, cow, pig, chicken, and sheep manures are commonly available. The actual nutrient content varies widely. The highest concentration of nutrients is found when manures are fresh. As it is aged, composted, nutrient content is charged. Even through fresh manures have the highest amount of nutrients, vegetable producers should use composted forms of manure to ensure a lesser amount of salts, thereby reducing the chance of burning plants. Fresh manure should not be used where it will contact tender plant roots [5].

Inorganic Fertilizers

Inorganic fertilizers are now produced in ways which cannot be continued indefinitely. Potassium and phosphorus come from mines (or saline takes such as the Dead Sea) and such resources are limited. Many inorganic fertilizers do not replace trace mineral elements in the soil which become gradually depleted by crops.

Organic Fertilizers

Organic fertilizers provide the best nutrients and minerals for a healthy garden because they are naturally occuring. Naturally occurring organic fertilizers include manure, slurry, worm castings, peat, seaweed, humic acid, and guano. Processed organic fertilizers include compost, blood meal, bone meal, humic acid, amino acids, and seaweed extracts. Other examples are organic enzyme-digested proteins, fish meal, and feather meal. Decomposing crop residue (green manure) from prior years is another source of fertility [6].

2. MATERIALS AND METHODS

2.1 Sample Collection

The soil samples were collected from Taung-Thaman Village, Amarapura Township, Mandalay Region for this research work. The soil samples were dug the depth 18 cm from the earth surface in the study areas and were put in thick plastic bags. The soil samples were allowed to dry in air stones and pieces of micro-organism matter were picked out and the remainders were crushed into fine powder. Large lumps were broken up by hand and then the soils were ground. After grinding, the soils were screened by 2 mm sieve. Soil remaining on the sieve which is greater than 2 mm was not used to analyse. Unfertilized soil was used as control soil sample 1.

Unfertilize Soil

Fertilize Soil

Figure 2. Plant of Pe-bizat

Botanical name	:	*Dolichos biflorus* Linn.
Family name	:	Papilionaceae
English name	:	Horse gram
Myanmar name	:	Pe-bizat

2.2 Preparation of Fertilized Soil Sample

To obtain fertilized samples, the soil was mixed with Pe-bizat, peanut husk, cowdung on a weight per weight (w/w) ratio, at the rate 90 : 10 (90 % soil, 5 % Pe-bizat, 2.5 % peanut husk, 2.5 % cowdung) sample 2, and 90 : 10 (90 % soil, 5 % peanut husk, 2.5 % pe-beizat, 2.5 % cowdung) sample 3 respectively. 500 g of fertilized sample 2 and 3 were placed in the plastic pot and added 105 and 110 cm^3 of water. After composting 2 months, two fertilized samples were air-dried and then used for other chemical analysis.

Sample 2 **Sample 3**

2.3 Analysis of Physicochemical Properties of Soil Sample

The pH of soil sample (1), (2) and (3) were measured by suspension method using pH meter (F-51, HORIBA). In this measurement 1: 2.5 soil : water was used.

Moisture of soil sample (1), (2) and (3) were measured by Gravimetric method using Temperature controlled Oven.

Organic matter of soil sample (1), (2) and (3) were measured by Tyurin's method using Analytical balance.

The electrical conductivity (EC) of soil sample (1), (2) and (3) were measured by saturation extract method using conductivity meter (DS-51, HORIBA).

Total NPK analysis can be measured by Kjeldahl distillation method, Molybivanado phosphoric acid method and Wet digestion with HNO_3 : $HClO_4$ (4:1) using Gerhardt Vapodest 20S, UV Vis spectrophotometer PD-

303 UV and Atomic Absorption Spectrophotometer AA-7000, SHIMADZU respectively.

Soil texture refers to the relative proportions of sand, silt and clay. Texture of unfertilized soil sample (1), fertilized soil sample (2) and (3) were measured by the pipette method using Analytical balance.

Exchangeable cation analysis can be measured by 1N Ammonium acetate extraction method using Atomic absorption spectrophotometer AA-7000 SHIMADZU.

The elemental composition of soil samples 1, 2 and 3 were measured by applying Energy Dispersive X-ray Fluorescence (EDXRF).

3. RESULTS AND DISCUSSION

3.1 Physicochemical Properties of Soil Sample

Table 1. Physicochemical Analysis

Sample	pH	Moisture content (%)	Organic matter (%)	EC (dS/m)
1 (Unfertilize Soil)	7.3	1.8	1.37	0.09
2 (soil + Pe-bizat, Penut husk, Cowdung)	7.5	1.8	2.19	0.38
3 (soil + Penut husk, Pe-bizat, Cowdung)	7.8	2.4	2.94	0.35

Moisture content of soil samples ranged from 1.8 % to 2.4 %. pH value of fertilized samples 2 and 3 (7.5, 7.8) were higher than that of control soil sample 1 (7.3). Increasing pH is clearly evaluable in these soils in terms of improving microelement availability and reducing the solubility of sore toxic elements.

By adding different ratio of Pe-bizat, Penut husk with cowdung, increased soil organic matter were obtained in sample 2 and 3 (2.19 % and 2.94 %) while sample 1 was (1.37 %).

Organic matter plays a major role in moisture retention, helping crops withstand drought contributes to the chemical and biological properties of soil and also a source of and exchange for nutrient, affects the fate of applied pesticides and contributes to the physical properties of the soil. Organic matter provides glue-like substances that act to stick individual particles together to form stable aggregates and good soil structures.

Electrical conductivity (EC) is a measure of the salt concentration in the soil solution. The fertilized soil sample 2 and 3 possed higher EC (0.38 , 0.35 dS/m) than soil sample 1 (0.09 dS/m). Good quality topsoil should have an electrical conductivity value within the range of 100-1500 micro siemens cm^{-1} (μS/cm).

The high EC contents in different ratio of Pe-bizat, Peanut husk, Cowdung with soil were attributed to salt levels of NPK nutrients in fertilized soil samples.

Table 2. Total NPK Analysis

Sample	Total			Available (mg/kg)		
	N (%)	P (%)	K (%)	N	P	K
1	0.15	0.07	0.05	28	1.2	210
2	0.21	0.26	2.26	44	7.0	452
3	0.21	0.11	1.76	48	2.3	494

Manuring is an invaluable way of improving soil water holding capacity and tilth but it could be major pollutant if attention is not paid to how it works in the soil (Banth, 1985). Manure has several effects when added to the soil including manure contains nitrogen (as ammonium), phosphorus, potassium and micro-nutrients that can be used directly by plants. These compounds also trigger-off biological activities which make nutrients in the manure and organic matter available to plant. Total N, total P and total K of fertilized soil samples 2 and 3 were ranged between 0.15 % and 0.21 %, 0.07 % and 0.26 %, 0.05 % and 2.26 % respectively.

In Table (2), by addition of different ratio of Pe-bizat, Penut husk, Cowdung with soil sample 2 and 3 were found to be increased total NPK.

Table 3. Texture Analysis

Sample	Composition			
	Sand (%)	Silt (%)	Clay (%)	Texture
1 (unfertilized soil)	53	16	31	Sandy clay loam
2 (soil + Pe-bizat, Penut husk, Cowdung)	63	11	26	Sandy clay loam
3 (soil + Penut husk, Pe-bizat, Cowdung)	53	21	26	Sandy clay loam

In this research, textural analysis showed all soil samples are in the class of sandy clay loam.

Table 4. Exchangeable Cation Analysis

Sample	$cmol_c/kg$								
	Na^+	Ca^{++}	Mg^{++}	K^+	Al^{+++}	H^+	CEC	ESP	EMgP
1	1.3	19.1	12.2	0.70	ND	ND	33.30	3.90	36.64
2	1.2	27.0	11.4	1.51	ND	ND	41.11	3.60	34.23
3	1.5	24.5	11.4	1.64	ND	ND	39.04	4.50	34.23

Cation exchange capacity (CEC) describes the ability of a soil to retain cations on colloids as a result of negative charges. CEC is important, for retaining nutrients and making them available to plants.

The summation of major exchangeable cations present in a sample of soil gave cation exchange capacity (CEC). Exchangeable sodium percentage (ESP) and exchangeable magnesium percentage (EMgP) were calculated as follows.

$$\mathrm{ESP} = \frac{\mathrm{Na}}{\mathrm{CEC}} \times 100(\mathrm{cmol_C / kg}),\ \mathrm{EMgP} = \frac{\mathrm{Mg}}{\mathrm{CEC}} \times 100(\mathrm{cmol_C / kg})$$

Soil organic matter and clay minerals are the two most important constituents that influence soil CEC. Thus increasing soil organic matter through compose addition is likely to increase CEC. Soil pH can effect CEC by altering the surface change of colloids.

A lower concentration of $[H^+]$ or higher pH will neutralize the positive charge on colloids thereby increasing CEC, that the positive relationship by adding different ratio of Pe-bizat, Penut husk, with Cowdung, increased CEC values were observed in soil sample 2 and 3 (41.11 and 39.04) because there was no significant difference among the pH values of three soil samples. Elemental composition of three soil samples were investigated and presented in Table (5).

Table 5. Elemental Percent Composition (%)

Sample	Al	Si	Fe	Ca	Cl	Cu	Zn
1	3.42	19.93	2.26	0.06	0.37	0.8	1.2
2	5.33	16.23	7.72	0.04	0.24	0.9	2.6
3	2.48	18.87	2.42	0.02	0.31	0.1	1.4

4.CONCLUSION

In this research work, the physicochemical changes by the combination of Pe-bizat, Peanut husk, Cowdung to soil were examined at enhancing properties of soil. The pH of fertilized soil sample 2 (Pe-bizat (5 %) : Peanut husk (2.5 %) : Cowdung (2.5 %)) and 3 (Peanut husk (5 %) : Pe-bizat (2.5 %) : Cowdung (2.5 %)) were higher than unfertilized soil sample 1.

Application of Pe-bizat, Peanut husk, Cowdung to soil resulted the increase of pH and cation exchange capacity (CEC). The positive response was observed between the fertilized soil (application of Pe-bizat, Peanut husk, Cowdung with soil) and the increase of organic matter contents. These can also be seen that slightly higher alkalinity and higher EC in fertilized soils.

Furthermore, total NPK values were found as positive relation with the addition of Pe-bizat, Peanut husk, Cowdung to soil samples. It could be concluded that the individual waste material was applied to prepare the organic fertilizer composts of various common waste materials and animal manure can provide the sufficient amount of nutrients to the soil.

ACKNOWLEDGEMENTS

We would like to express our deep gratitude and sincere thanks to Rector Dr Maung Maung Naing, Prorector Dr Si Si Khin and Dr Tint Moe Thu Zar, Yadanabon University, for their encouragement and permission for this research work. We also wish to express our profound gratitude to Dr Hlaing Hlaing Myat, Professor and Head of Chemistry Department, Yadanabon University, for her help to measure the experimental data.

REFERENCES

[1] Alan Wild. Soil and the environment, (1993)
[2] Dao, T.H., & Covigelli, M.A. "Mineralizable carbon, nitrogen, and water extractable phosphorus release from stockpiled and composted manure and manure amended soils. Agronomy Journal, (2003), 95, 405-413
[3] Hesse, P.R, "A Text Book of Soil Chemistry Analysis", William Clowes and Sons Limited, London, (1971)
[4] Bear, F.R. "Chemistry of the Soil", Rehinhold Pub-crop, New York, (1965), 133-473
[5] F.A.O, "Fertilizer and Plant Nutrition Guide", Food and Agriculture Organization of the United Nations, (1984)
[6] Cunningham, W.P., Environmental Science, McGraw-Hill International Edn., New York, (2008)
[7] Dr Than Nyunt and group, "Determination of the Chemical Constituents of Soil in Some Flooded Areas in Monywa Township, Department of Chemistry, Monywa University, (2016)
[8] Dr Moe Tin Khaing, "The Effects of Poultry Residue on Some Physicochemical and Biological Properties of Soil from Myingyan, Mandalay Region, Department of Chemistry, Yadanabon University, (2016)
[9] Zayar, "Study on the Amount of Primary Nutrients (NPK) In Chemical Fertilization and Prepared Organic Fertilizers, Yadanabon University, (2013)
[10] http://ag.arizona, edu/pubs/garden/mg/Soils/organic.html
[11] http://www.ehow.com/info.11401563.Can.fertilize. Peanut-Shells.htm!

Certificate Index	*Author*
VOL01IS01001	*A NweSoe, Paing Thwe Soe, Theint Theint* *"Impact of Written Exam on Students' Project Performance"*
VOL01IS01002	*Aung San Min, San San Mon, Hla Myat Thandar, Min Min Aye* *"Microcontroller Based Automatic Water Level Controller"*
VOL01IS01003	*Aye Aye Htun* လွွဲပါဘူးသမုဆွေ တေးထပ်ကဗျာလေ့လာချက်
VOL01IS01004	*Aye Aye Khaing, Yu Ya Win* *"Local University-Industry Linkage and Job Perception"*
VOL01IS01005	*Aye Aye Lwin,Thin Thin Soe* *"Assessment of Toe River Water Quality around Maubin Township from Ayeyarwady Region in Myanmar"*
VOL01IS01006	*Aye Myint Sein, Myint Myint Khine, Aye Thida* *"Isolation of Lupeol Compound and Pharmacological Actions of Crataeva nurvala Ham. Bark (Kadet)"*
VOL01IS01007	*Hnin Wuit Yee, Hla Ngwe* *"Physicochemical Characterization of Water Soluble Chitosan and Its Acute Toxicity and Weight Loss Activity"*
VOL01IS01008	*Htay Htay Khaing* *"Preparation of Biodiesel From Waste Fried Palm Oil Using Zeolite Catalyst"*
VOL01IS01009	*Khaing Khin Aye, Thi Thi Swe* မြန်မာ့လုပ်ငန်းသုံးဆိုင်ရာ စကားပုံများ လေ့လာချက်
VOL01IS01010	*Khin Cho Latt, Chaw Ei Su* *"A Study On Some Noticeable Factors In Communicative English for Non-Native Speaker"*
VOL01IS01011	*Khin Cho Thant, Tun Tun Win, Thet Hnin Lwin* *"Effect of Gamma Radiation on Agronomic Characteristics of Maize (Zea Mays L.)"*
VOL01IS01012	*Khin Ma Lay* မဏိကုဏ္ဍလဝတ္ထုမှ ထူးခြားသောစာဟန်
VOL01IS01013	*Khin Moh Moh Thin, Hla Yin Moe, Linn Linn Aye* *" Calculate the Electrical Network by Using Matrices "*
VOL01IS01014	*Khin Myo Kyi* *"Study on Audio Watermarking Based on Arnold Transformation with DWT-DCT"*
VOL01IS01015	*Khin San Win, Ni Ni Aung, Thu Zar Myint, Hlaing Hlaing Myat)* *"Comparative Study on Nutritional Values, Antimicrobial Activities and Antioxidant Activities of Papaya Leaves and Tea Leaves"*
VOL01IS01016	*Khin San Win, Swe Swe Lwin* *"Determination of Antimicrobial and Antioxidant Activities of the Fruits of Momordica charantia L. (Bitter Gourd)"*
VOL01IS01017	*Kyi Kyi Hla* ထားဝယ်ဒေသ(ကျောက်ဆည်)ဒေသိယစကားလေ့လာချက်
VOL01IS01018	*Kyi Kyi Thwin, Nyi Nyi Htway* *"Innovative Strategies to Develop Speaking Performance: A Study of Teachers and Learners at UCS (Taungoo)"*
VOL01IS01019	*Kyi Pyar Moe, Myo Su Su Hlaing* *" Solution and Application of Heat Equation Using Method of Separation of Variables"*

VOL01IS01020 *Kyi Zar Nyunt, Wint Aye Khaing, San San Yu*
"A Survey of Comparison in Decision Tree Algorithms for Classification"

VOL01IS01021 *Lae Lae Khine, Nwe Ni Soe*
"Influence of Dopant Calcium Concentration on Electrical Behavior of $PbTiO_3$ Ceramic Capacitor"

VOL01IS01022 *Lae Lae Oo*
"An Integrated Approach to Teaching Verb (Tenses) for All Students"

VOL01IS01023 *Lwin Ko Oo, Nan Thidar Chit Swe, Than Zaw Oo, Ye Chan*
"Influence of Reducing Agents on the Formation of Reduced Graphene Oxide"

VOL01IS01024 *May Myo Swe,Yi Yi Maw, Su Hlaing Win*
ဦးသုခ၏ အကျော်ဒေးယျဗုဒ္ဓသမီးတော်များ ဝတ္ထုတိုများမှ သရုပ်ဖော်အဖွဲ့များ

VOL01IS01025 *Moe Moe Yee, Kyaw Naing*
"Mineral Elements, Essential Nutritive Elements and Toxic Elements in Some Myanmar Indigenous Medicines Containing Kyauk-thway"

VOL01IS01026 *Moe Sandar Naing, Ju Ju Khin, Kyi Kyi Wai*
"Assessment of Soil Quality in Ywar Thar Gyi Village, Kyaiklat Township, Ayeyarwady Region"

VOL01IS01027 *Mya Mya Sainn*
"Isolation and Characterization of Essential Oils from Houttuyania cordata Thunb.(Fish Mint)"

VOL01IS01028 *Myat Thu Zar, Nang Mwe Seng, Su Mon Thwin*
"Tuning of PID Controller using Ziegler-Nichols Method for Room Temperature Control System"

VOL01IS01029 *Myint Myint Swe, San San Htwe, Sandar Win*
"Design And Construction of Mosfet Inverter"

VOL01IS01030 *Myint Myint Than*
"Audio Watermarking Based on MP3 Encoding Process"

VOL01IS01031 *Nay Nandar Linn*
"Relaxed Web Development System with Advanced Encryption Standard (AES) Algorithm"

VOL01IS01032 *Nilar Tint*
မင်းသုဝဏ်၏ သမိုင်းနောက်ခံ ဇာတ်လမ်းကဗျာ လေ့လာချက်

VOL01IS01033 *Nwe Nwe Aung, Khin Phyo Win*
"Determination of Dyeing Process and Colour Fastness Properties of Natural Dye Extracted from Mango Bark (Mangifera indica L.) on Cotton Cloth"

VOL01IS01034 *Ohnmar Khine, Myo Kay Thwe*
"Appropriateness of Eclectic Approach to English Language Teaching"

VOL01IS01035 *Pa Pa San, Tin Myo Latt, Thandar Khaing, Nyein Nyein Aye, Yi Yi Lwin*
"Assessment of Soil Quality by Supporting With Pe-Bizat, Peanut Husk, Cowdung from TaungThaman Village, Amarapura Township, Mandalay Region"

VOL01IS01036 *Paing Thwe Soe, Nilar Soe, Theint Theint*
"Impact of Teaching Method on Academic Performance: An Experimental Research Study"

VOL01IS01037 *Paing Thwe Soe, Nay Nandar Linn, Thin Thin Htwe*
"The Role of Capacity Assessment in Research Capacity Building Strategy: An Experimental Study"

VOL01IS01038 *Phyo Yatanar Lin, Nilar Thein*
" Teachers' Performance Appraisal by Using Fuzzy Expert System"

VOL01IS01039 *Pyae Sone Aung, Zaw Naing*
"Removal of Organic Dye (Methylene Blue) by Activated Bentonite Clay"

VOL01IS01040 *San San Htwe*
"Numerical Solution to the Laplace Equation for a Magnetostatic Potential"

VOL01IS01041 *San San Yu, Kyi Zar Nyunt*
"Quantitative Association Rule Based on Exam Report System"

VOL01IS01042 *Soe Kyaw Kyaw, Yu Yu Hlaing*
"Evaluation of Quality Control Parameters of Four Different Brands of Paracetamol Tablets"

VOL01IS01043 *Thanda Aung, Phyo Phyo Wai, Wint War Htet Naing, Theint Theint Phyo, Than Than Myint, Ye Myint Aung, Ni Ni Than*
"Phytochemical Investigation and Antioxidant Activities of Three Selected Medicinal Plants from Ayeyarwady Region, Myanmar"

VOL01IS01044 *Thida Tin, Yee Lai Win, Myat Myat Thu*
"Synthesis and Characterization of Silver Nanoparticles Using Three Different Leaves"

VOL01IS01045 *Thinzar Htun*
"Enhancing the Different Types of Writing Skill of the Third Year Students at the University of Computer Studies, Taungoo"

VOL01IS01046 *Thwe Thwe Maw, Yin Yin San*
"Promoting the Students' Speaking Skills Through the Use of Communicative Language Teaching Approach"

VOL01IS01047 *Thwet Hnin Moe, Ye Win*
အင်းဝခေတ်ကျောက်စာ(၁၀)ချပ်လာဝါကျရိုးဖွဲ့ပုံလေ့လာချက်

VOL01IS01048 *Tin Tin Pyone, Wai Lwin Oo*
"Analysis of Elemental Concentrations on the Vegetables"

VOL01IS01049 *Win Cho, Kyi Kyi Khaing*
သော်တာဆွေ၏"ကြိုးခွဲရသည်"ဝတ္ထုတို၌ ဖလေ့သုံးစကားများ ဆန်းစစ်ချက်

VOL01IS01050 *Yi Mon Khine*
"Effective Motivations and Activities to Improve English Skills for University Students"

VOL01IS01051 *Yi Yi Thant*
"The Impact of Integrating Reading and Writing Skills at the Technological University's Students"

VOL01IS01052 *Yin Yin San, Thwe Thwe Maw*
"Using Prewriting Strategies for Promoting EFL Students' Writing Skills and Attitudes"

VOL01IS01053 *Zarchi San, Pan Wint Hmone Htwe, K Khaing Wint*
"Design and Construction of Dual Axis Solar Tracker in Pyay"

VOL01IS01054 *Zaw Min Tun, Aye Myat Mon*
"A Study of Quality Assurance in Universities"

VOL01IS01055 *Zin Nwe Khaing, Hla Yin Moe, San San Nwe*
"Optimization Problem Solving with Graphical and Simplex Method"